OAK RIDGE
NATIONAL LABORATORY
MANAGED BY UT-BATTELLE
FOR THE DEPARTMENT OF ENERGY

ORNL/LTR-2013/334

Design Concept for Rabbit Irradiation in the RB* Position of HFIR

September 2013

Prepared by

Mark Bradisse, Jorge Narvaez, and Kevin R. Robb
Oak Ridge National Laboratory

UT-BATTELLE
ORNL-27 (4-00)

DOCUMENT AVAILABILITY

Reports produced after January 1, 1996, are generally available free via the U.S. Department of Energy (DOE) Information Bridge.

Web site http://www.osti.gov/bridge

Reports produced before January 1, 1996, may be purchased by members of the public from the following source.

National Technical Information Service
5285 Port Royal Road
Springfield, VA 22161
Telephone 703-605-6000 (1-800-553-6847)
TDD 703-487-4639
Fax 703-605-6900
E-mail info@ntis.gov
Web site http://www.ntis.gov/support/ordernowabout.htm

Reports are available to DOE employees, DOE contractors, Energy Technology Data Exchange (ETDE) representatives, and International Nuclear Information System (INIS) representatives from the following source.

Office of Scientific and Technical Information
P.O. Box 62
Oak Ridge, TN 37831
Telephone 865-576-8401
Fax 865-576-5728
E-mail reports@osti.gov
Web site http://www.osti.gov/contact.html

This report was prepared as an account of work sponsored by an agency of the United States Government. Neither the United States Government nor any agency thereof, nor any of their employees, makes any warranty, express or implied, or assumes any legal liability or responsibility for the accuracy, completeness, or usefulness of any information, apparatus, product, or process disclosed, or represents that its use would not infringe privately owned rights. Reference herein to any specific commercial product, process, or service by trade name, trademark, manufacturer, or otherwise, does not necessarily constitute or imply its endorsement, recommendation, or favoring by the United States Government or any agency thereof. The views and opinions of authors expressed herein do not necessarily state or reflect those of the United States Government or any agency thereof.

ORNL/LTR-2013/334

Design Concept for Rabbit Irradiation in the RB* Position of HFIR

Mark Bradisse
Jorge Narvaez
Kevin R. Robb

Date Published: September 2013

Prepared by
OAK RIDGE NATIONAL LABORATORY
Oak Ridge, Tennessee 37831-6283
managed by
UT-BATTELLE, LLC
for the
U.S. DEPARTMENT OF ENERGY
under contract DE-AC05-00OR22725

CONTENTS

Page

CONTENTS IV
LIST OF FIGURES VI
LIST OF TABLES VIII
ACKNOWLEDGEMENTS IX
ABSTRACT 1
1. INTRODUCTION 2
1.1 THE HIGH FLUX ISOTOPE REACTOR 2
1.2 PROBLEM STATEMENT 3
1.3 OVERVIEW OF METHODS 4
2. PRELIMINARY CALCULATIONS 5
2.1 RABBIT 5
2.2 RABBIT THERMAL MODEL DEVELOPMENT 7
2.3 RB* RABBIT BASKET 9
3. MCNP MODEL 14
3.1 MCNP OVERVIEW 14
3.2 EXISTING HFIR CODE AND MODIFICATIONS 14
3.3 EXPERIMENT LOCATION 15
3.4 MCNP CASES RUN FOR THIS PROJECT 15
3.5 GEOMETRY 16
3.6 MATERIALS 19
3.7 TALLIES 20
3.8 MCNP MODE, SOURCE INFORMATION AND K-CODE 23
4. RESULTS 24
4.1 HEAT GENERATION 24
4.2 NEUTRON FLUX 28
4.3 CRITICALITY 33
4.4 RABBIT THERMAL MODEL RESULTS 34
5. SYSTEM VARIATION STUDIES ON STEEL SAMPLE, BOC CASE 37
5.1 VARIATIONS IN HEAT GENERATION RATES 38
5.2 VARIATIONS IN NEUTRON FLUX 39
5.3 VARIATIONS IN CRITICALITY 42
6. FUTURE DESIGN AND ANALYSIS RECOMMENDATIONS 43
6.1 REACTIVITY WORTH OF ASSEMBLY 43
6.2 NEUTRON FLUX AND SPECTRUM 43
6.3 SAMPLE TEMPERATURE DRIFT OVER THE CYCLE 44
7. CONCLUSIONS 45
8. REFERENCES 46
APPENDIX A. MCNP MODEL A-1
A-1 GENERIC MODIFICATIONS A-1

A-2 ADDITIONS TO MODEL EXPERIMENT A-1
A-3 MATERIALS DEFINITION A-5
A-4 TALLIES DEFINITION A-6
APPENDIX B. HEAT GENERATION RATES B-1
B-1 NEUTRON HEAT GENERATION RATES B-1
B-2 PHOTON HEAT GENERATION RATES B-4
B-3 TOTAL HEAT GENERATION RATES B-7
APPENDIX C. NEUTRON FLUX C-1
C-1 GRAPHITE SAMPLES, BEGINNING OF CYCLE C-1
C-2 GRAPHITE SAMPLES, END OF CYCLE C-4
C-3 STEEL SAMPLES, BEGINNING OF CYCLE C-7
C-4 STEEL SAMPLES, END OF CYCLE C-10
C-5 STEEL SAMPLES, BEGINNING OF CYCLE – TWO ASSEMBLIES (3B-7B) C-13
C-6 STEEL SAMPLES, BEGINNING OF CYCLE – TWO ASSEMBLIES (7A-7B) C-18
C-7 STEEL SAMPLES, BEGINNING OF CYCLE – THREE-CHANNEL ASSEMBLY C-23

LIST OF FIGURES

Figure **Page**

FIG. 1. CROSS–SECTIONAL VIEW OF HFIR [1] 2
FIG. 2. RADIAL CROSS SECTION OF THE RABBIT ASSEMBLY, TAKEN AT THE MIDPLANE. THE SAMPLE IS SHOWN IN BLUE, THE VCR4TI4 HOLDER IN GREEN, AND THE AL6061 CAPSULE IN GREY. THE OUTER GAS GAP IS SHOWN IN RED, WHILE THE INNER GAS GAP BETWEEN THE SAMPLE AND HOLDER IS TOO SMALL TO SEE HERE. 6
FIG. 3. AXIAL CROSS SECTION OF THE RABBIT ASSEMBLY. THE SAMPLE IS SHOWN IN BLUE, THE VCR4TI4 HOLDER IN GREEN, AND THE AL6061 CAPSULE IN GREY. 6
FIG. 4. EXAMPLE RADIAL THERMAL PROFILE FOR RABBIT ASSEMBLY (1 KW HEAT GENERATION). 8
FIG. 5. VIEW OF THE EXTRUSION 10
FIG. 6. VIEW OF THE RESTRICTOR 10
FIG. 7. VIEW OF THE ANCHOR 11
FIG. 8. RADIAL CROSS–SECTION OF THE BASKET ASSEMBLY, TAKEN AT THE REACTOR'S MIDPLANE, WITH RABBITS SHOWN FILLING EACH CHANNEL. CHANNELS FOR COOLANT WATER ARE SHOWN IN WHITE; THE EXTRUSION IS SHOWN IN GOLD. 13
FIG. 9. AXIAL CROSS–SECTION OF THE BASKET ASSEMBLY, WITH RABBITS SHOWN IN THEIR NORMAL CONFIGURATION. FROM LEFT TO RIGHT, THE REGIONS AND THEIR LENGTHS ARE: TOP UNFILLED REGION OF RABBIT CHANNELS (6.2595 IN.), ANNULAR RABBIT REGION (18.375 IN.), BOTTOM UNFILLED REGION OF RABBIT CHANNELS (0.5 IN.), RESTRICTOR (0.5 IN.), AND ANCHOR (1.1541 IN.). 13
FIG. 10. MODIFIED MCNP MODEL OF HFIR THAT SHOWS THE EXPERIMENT LOCATION, RB*–7B 15
FIG. 11. AXIAL AND RADIAL CROSS SECTIONS OF A RABBIT MODELED ON MCNP. NOTE THAT THE INNER GAS GAP IS TOO SMALL TO BE SEEN IN THE RADIAL VIEW. 17
FIG. 12. RADIAL CROSS SECTION AT CORE'S MIDPLANE OF RB*–7B SHOWING THE EXTRUSION AND CHANNEL LATTICE. 18
FIG. 13. AXIAL VIEW OF THE RB*–7B POSITION (CENTER) LOADED WITH FORTY–NINE RABBITS CENTERED AT MIDPLANE. ONLY TWENTY–ONE RABBITS ARE VISIBLE IN THIS VIEW. 18
FIG. 14. PLANES SEPARATING THE EXTRUSION INTO DIFFERENT SECTIONS FOR CALCULATING HEAT GENERATION ARE SHOWN HERE, LABELED AS "DTM" FOLLOWED BY A NUMBER. 20
FIG. 15. AXIAL HEAT GENERATION PROFILE FOR SAMPLES LOCATED IN THE CENTER CHANNEL OF THE ASSEMBLY. 25
FIG. 16. AXIAL POWER PROFILE FOR RABBITS LOCATED IN THE CENTER CHANNEL OF THE ASSEMBLY. 25

FIG. 17. AXIAL HEAT GENERATION PROFILE FOR ALL MATERIALS LOCATED IN THE CENTER CHANNEL. IN THIS CASE, THE HOLDER IS LOADED WITH STEEL SAMPLES, AND THE CORE IS AT THE END OF ITS LIFE. 26
FIG. 18. POWER GENERATED IN MIDPLANE RABBITS (STEEL SAMPLES, BOC). THE CHANNEL AT THE "10 O'CLOCK" POSITION IS THE INNER CHANNEL, WHILE THE CHANNEL AT THE "4 O'CLOCK" POSITION IS THE OUTER CHANNEL..... 27
FIG. 19. AXIAL FLUX PROFILE FOR SAMPLES IN THE CENTER CHANNEL. BOTH MATERIALS AND BOTH POINTS IN THE CYCLE ARE SHOWN..... 28
FIG. 20. FLUX THROUGH MIDPLANE RABBITS, IN N/CM^2–S. THE CHANNEL AT 10 O'CLOCK IS THE INNER CHANNEL, WHILE THE CHANNEL AT 4 O'CLOCK IS THE OUTER CHANNEL. 30
FIG. 21. MATERIAL AND TIME DEPENDENCE OF FLUX SPECTRA. FLUX VALUES ARE NORMALIZED BY THE WIDTH OF THEIR LETHARGY BINS. 31
FIG. 22. CORRECTED NEUTRON FLUX SPECTRA FOR VARIOUS REGIONS OF HFIR..... 32
FIG. 23. THERMAL PROFILE OF A RABBIT WITH STAINLESS STEEL SAMPLES..... 34
FIG. 24. THERMAL PROFILE OF A RABBIT WITH GRAPHITE SAMPLES. A GRAPHITE THERMAL CONDUCTIVITY OF 35 W/M–K WAS ASSUMED. 35
FIG. 25. THERMAL PROFILE OF A RABBIT WITH GRAPHITE SAMPLES. A GRAPHITE THERMAL CONDUCTIVITY OF 10 W/M–K WAS ASSUMED. 35
FIG. 26. HFIR CROSS–SECTIONAL VIEW, SHOWING THE RB*–7B, –3B, AND –7A POSITIONS 37
FIG. 27. CROSS–SECTIONAL VIEW OF THREE-CHANNEL RABBIT ASSEMBLY..... 37
FIG. 28. AXIAL HEAT GENERATION PROFILE FOR SAMPLES LOCATED IN THE CENTER CHANNEL OF EACH ASSEMBLY FOR THE SEVEN–CHANNEL, STEEL SAMPLE, BOC CONFIGURATIONS..... 38

LIST OF TABLES

Table **Page**

TABLE 1 – STAINLESS STEEL SAMPLE MATERIAL COMPOSITION 5
TABLE 2 – MASS AND VOLUME CALCULATIONS FOR THE DIFFERENT REGIONS IN A RABBIT AND EXTRUSION 7
TABLE 3 – MULTIPLIERS FOR PHOTON ENERGY DEPOSITION TALLIES 22
TABLE 4 – SAFETY BASIS HEAT GENERATION RATES 24
TABLE 5 – EFFECTS OF RADIAL POSITION ON POWER GENERATED IN MATERIALS AND RABBITS 27
TABLE 6 – MIDPLANE NEUTRON FLUX 29
TABLE 7 – BOC REACTIVITY CHANGES 33
TABLE 8 – HEAT GENERATION RATES FOR MATERIALS IN THREE-CHANNEL ASSEMBLIES 39
TABLE 9 – COMPARISON OF OUTER CHANNEL HEAT GENERATION RATES FOR THREE-CHANNEL AND SEVEN–CHANNEL CASES 39
TABLE 10 – MIDPLANE NEUTRON FLUX FOR SEVEN–CHANNEL ASSEMBLIES 40
TABLE 11 – NEUTRON FLUX FOR THREE-CHANNEL ASSEMBLY 41
TABLE 12 – COMPARISON OF OUTER CHANNEL FLUX VALUES FOR THREE-CHANNEL AND SEVEN–CHANNEL CASES 41
TABLE 13 – BOC STEEL SYSTEM VARIATIONS AND EFFECTS ON CRITICALITY 42

ACKNOWLEDGEMENTS

This work benefited from the support and advice of Joel McDuffee, Dennis Heatherly, Charles Daily, Nesrin Cetiner, Joel Risner, and Graydon Yoder Jr. as well as all of the members of the Thermal Hydraulics and Irradiation Group.

ABSTRACT

The High Isotope Flux Reactor (HFIR) has one of the highest steady–state neutron fluxes in the world, making it a premier facility for material irradiation research. Due to its popularity for studies in this field, and because of its limited experimental space in the flux trap region, HFIR currently has a backlog of experiments that cannot be run at this time. The purpose of this project is to design a system that will increase the capacity of HFIR to house these experiments by taking advantage of the currently available space in the Removable Beryllium (RB*) reflector region. This process included modeling an existing material irradiation capsule (rabbit) as well as designing a holder that would allow several rabbits to be loaded into an RB* position. To determine the feasibility of this system, a model including the holder and forty–nine rabbits was inserted into the RB*–7B position in two pre-existing MCNP computer models of HFIR; one of these models represented the core composition at the beginning of the fuel cycle (BOC), while the other represented the end of the fuel cycle (EOC). For each of these models two scenarios were run: one with graphite samples and the other with steel irradiation samples. The BOC and EOC models were also run with beryllium plugs (blanks) loaded into all of the RB* positions, which served as a standard. Tallies set up in the MCNP code for each case provided outputs of heat generation rates for each material, neutron flux through each sample and reactivity in HFIR. The results of these models showed that a holder loaded with graphite samples decreased initial reactivity by 0.00143 Δk_{eff} when compared to the blank case while stainless steel samples decreased initial reactivity by 0.00165 Δk_{eff}. Material specific peak heat generation rates were between 24–38% of their corresponding values in the flux–trap region, depending on the material. A graphite sample placed in the center of the holder would experience an average neutron flux of 1.88×10^{15} n/cm^2–sec over the life of the core, while a steel sample in the same position would experience a neutron flux of 1.69×10^{15} n/cm^2–sec. These results showed that this design would make irradiation of rabbit capsules in the RB* positions a feasible and worthwhile concept to pursue further with more in–depth analysis.

1. INTRODUCTION

1.1 THE HIGH FLUX ISOTOPE REACTOR

1.1.1 The Reactor Core Region

The High Flux Isotope Reactor (HFIR), located on the Oak Ridge National Laboratory campus, has the highest steady state thermal neutron flux of any reactor in the world, reaching levels as high as 2.3 X 10^{15} n/cm^2–s [1]. This extraordinarily high flux makes HFIR one of the world's premier facilities for conducting research on material irradiation damage, trans–plutonium isotope production, and neutron activation analysis.

A cross section of the core region of HFIR can be seen in Figure 1. HFIR is a flux–trap type reactor, designed with an unfueled cylindrical region located in the center of the core region. The flux trap is surrounded by two annular fuel elements, comprised of U_3O_8–Al fuel which is highly enriched in U–235; the fuel region has an outer diameter of 43.18 cm (17 in.), and a height of 50.8 cm (20 in.).

The fuel is blanketed by three layers of beryllium material: the removable beryllium, semi–permanent beryllium, and permanent beryllium reflectors. These layers are designed to reflect escaping neutrons back into the fuel region.

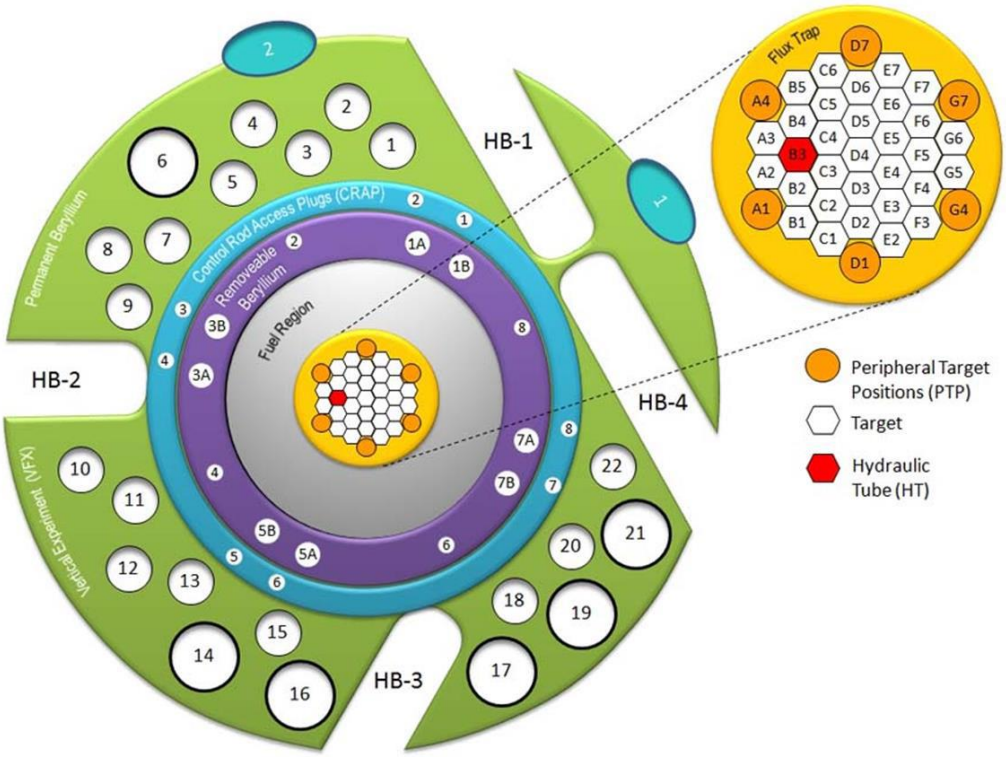

Fig. 1. Cross–sectional view of HFIR [1]

HFIR operates at a power level of 85 MW_t, with a fuel cycle of ~25 days before a new core is loaded into the reactor [1]. It is cooled and moderated by water, with core inlet and outlet temperatures of 322 K

(120°F) and 342 K (156°F), respectively, and inlet and outlet pressures of 3.23 MPa (468 psi) and 2.47 MPa (358 psi), respectively [1].

1.1.2 Rabbit Capsules

A rabbit is a hollow cylindrical aluminum capsule loaded with a sample of a given material and placed in the reactor at an irradiation site. Rabbits are the most cost–effective method of sample irradiation: they are small, relatively simple, and made out of easily accessible materials. They are also designed such that they can be shuttled in and out of the reactor using a hydraulic tube facility (hence the name "rabbit"), allowing them to be irradiated for any amount of time. They can also be used in other flux trap positions, but when used in that configuration, must remain in the reactor for at least a full fuel cycle.

The rabbit design used for this project was the un–finned rabbit shown in HFIR drawing X3E020977A538–Rev 0 [1]. This capsule is 6.668 cm (2.625 in.) long with an outer diameter of 1.097 cm (0.432 in.).

1.1.3 The Flux Trap

The flux trap is the region in the center of the reactor assembly which houses thirty–one target positions. It was designed primarily for use in trans–plutonium isotope production, but the high neutron flux there makes it ideal for radiation damage testing, neutron activation analysis, and other materials experiments as well.

1.1.4 RB* Position

There are eight large and four small spaces for experiments in the removable beryllium reflector region (RB* positions). The locations of these can be seen in Figure 1. This project was concerned with the large RB* positions, and henceforth all instances of RB* in this report will refer to those positions. When not in use, the RB* positions are filled with beryllium plugs; the RB* position is a hole in the removable beryllium reflector that is parallel to the core centerline and runs the height of the core. The hole in the beryllium is lined with an aluminum tube that has an inner diameter of 4.60 cm (1.811 in.), the length of the liner tube assembly is 66.68 cm (26.25 in.), and the radial distance from RB* axis to core axis is 27.31 cm (10.75 in.).

1.2 PROBLEM STATEMENT

When a material is designated for irradiation in HFIR, a small sample is generally irradiated in the flux trap region, where the thermal neutron flux is at its highest. Unfortunately, given the limited space in the flux trap and the high demand for sample irradiation, there is a backlog of irradiation requests that cannot presently be fulfilled.

In order to alleviate this demand, the intent of this project was to design a way for rabbits to be irradiated in the RB* position. Though the neutron flux in this part of the reactor is not as high as in the flux trap, it exceeds values of 10^{15} n/cm^2–s, and therefore is still appropriate for use in experiments that require high neutron flux [1].

1.3 OVERVIEW OF METHODS

This project included the design of a rabbit capsule as well as a holder device to fit into the RB* position.

A preliminary design was created using Excel; this took into account estimates of heat transfer and flow characteristics in the system. This design was then used in an MCNP model of HFIR; several versions of this model were run for different points in the fuel cycle and loading scenarios. Tallies for heat generation rates, neutron flux, and criticality were included in the scripts; the outputs of these analyses provided the data used to evaluate the usefulness of using the RB* position for rabbit irradiation.

2. PRELIMINARY CALCULATIONS

2.1 RABBIT

2.1.1 Sample

For simplicity, the rabbit design selected for analysis was modeled as a cylinder 4.50 cm (1.772 in.) long with a diameter of 0.716 cm (0.282 in). It was assumed that the rabbit specimens were constructed out of either a stainless steel alloy (composition given in Table 1) or graphite; this report contains analyses for both materials.

Table 1 – Stainless Steel Sample Material Composition

Material	Percent by Weight
Iron	89.56%
Chromium	8.00%
Tungsten	2.00%
Vanadium	0.20%
Tantalum	0.04%
Carbon	0.10%
Cobalt	0.10%

2.1.2 Vanadium holder and Inner Gas Gap

The specimens were assumed to be contained inside a holder constructed from a vanadium alloy (V4Cr4Ti) which was chosen for its high melting point and good thermal properties. A gap of 0.00127 cm (0.0005 in.) between the sample and vanadium shell was assumed to be filled with helium gas at room temperature.

The vanadium holder was modeled as an annulus 5.72 cm (2.250 in.) long, with an outer diameter of 0.902 cm (0.355 in.) The end caps, sunk 0.254 cm (0.1 in.) from either end of the annulus, would be 0.533 cm (0.021 in.) thick. The holder wall thickness would vary depending on the desired thermal properties for the given sample. This will be discussed in detail in Section 2.1.6; for preliminary calculations, a thickness of 0.0914 cm (0.036 in.) was used.

2.1.3 Outer Gas Gap

The vanadium holder would be surrounded by helium fill gas. Like the holder walls, the thickness of this gas gap would be chosen based on the required thermal profile. For preliminary calculations, a thickness of 0.0254 cm (0.01 in.) was used.

2.1.4 Aluminum Capsule

The capsule that would serve as the outermost layer of the rabbit was modeled as an annulus 6.67 cm (2.625 in.) long and 0.0724 cm (0.0285 in.) thick, with an outer diameter of 1.097 cm (0.432 in.) The

bottom cap would be flush with the bottom of the annulus, with a thickness of 0.432 cm (0.17 in.) The top cap, sunk 0.0635 cm (0.025 in.) from the top of the annulus, was assumed to be 0.292 cm (0.115 in.) thick. Aluminum alloy 6061 was the optimal choice of material for this piece, given its thermal and neutronic properties and resistance to corrosion.

2.1.5 Assembly

Figure 2 shows a radial cross sectional view of the rabbit assembly, while Figure 3 shows an axial cross section. The volume and mass of each part are given in Table 2.

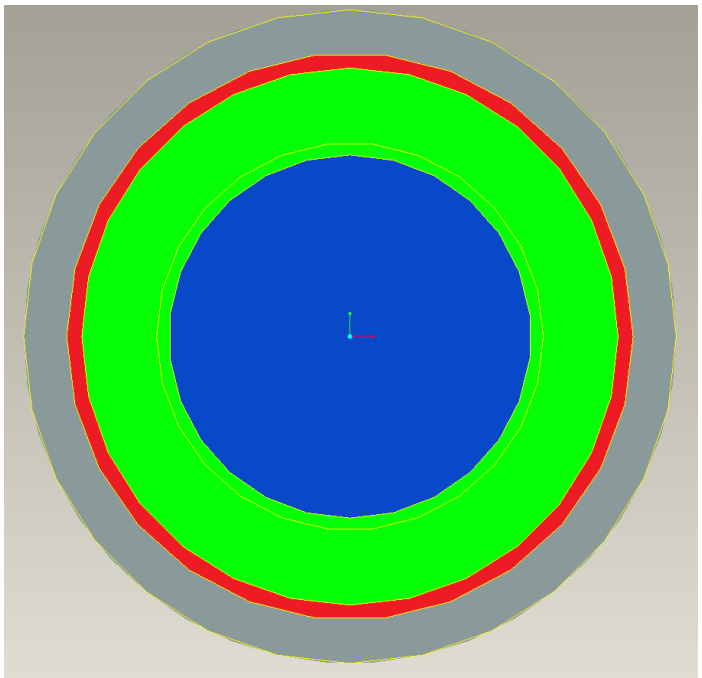

Fig. 2. Radial cross section of the rabbit assembly, taken at the midplane. The sample is shown in blue, the VCr4Ti4 holder in green, and the Al6061 capsule in grey. The outer gas gap is shown in red, while the inner gas gap between the sample and holder is too small to see here.

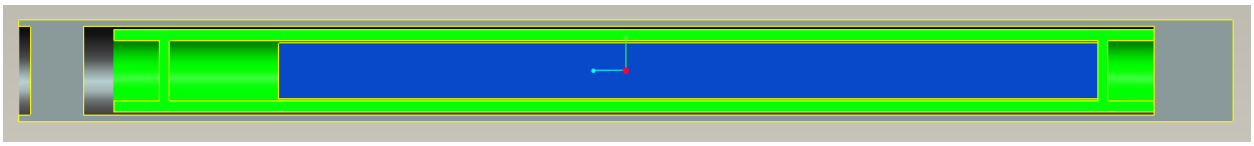

Fig. 3. Axial cross section of the rabbit assembly. The sample is shown in blue, the VCr4Ti4 holder in green, and the Al6061 capsule in grey.

Table 2 – Mass and volume calculations for the different regions in a rabbit and extrusion

Region	Density (g/cm^3)	Volume (cm^3)	Mass (g)
Graphite	1.78	1.814	3.228
Stainless Steel	7.87	1.814	14.273
Inner He Layer	1.64E-04	0.256	4.201E-05
V4Cr4Ti Holder	6.05	1.374	8.310
Outer He Layer	1.64E-04	0.747	1.224E-04
Al6061 Housing	2.7	2.070	5.589

2.2 RABBIT THERMAL MODEL DEVELOPMENT

In order to simplify the heat transfer modeling process, the following assumptions were made:

- All heat is generated in the sample, other components generate no heat
- Thermal expansion was neglected
- Thermal conductivities for the sample and metal components were assumed to be constant (not functions of temperature)
- Convection heat transfer across both gas gaps was assumed to be negligible
- Heat transfer in the axial direction was neglected

The temperature profile across the (stainless steel) sample followed the relationship for heat transfer across a cylindrical element with uniform heat generation [4]:

$$T(r) = \frac{q'''}{4k_s}(R_s^2 - r^2) + T_{s,g1}$$

Here, q_s''' is the volumetric heat generation rate, k_s is the thermal conductivity of the sample, R_s is the radius of the sample, and $T_{s,g1}$ is the temperature at the sample-gas interface and r is the radial position being evaluated.

The temperature differences across the inner gas gap, vanadium holder, and aluminum capsule followed the relationship for heat transfer through annular elements with no heat generation [4]:

$$T_{inner} - T_{outer} = q_s'''V\frac{1}{k}\frac{ln\frac{r_o}{r_i}}{2\pi L}$$

Here, V is the sample volume and L is the axial length being considered.

In order to calculate the temperature profile across the outer gas gap, radiation heat transfer was also considered. This relationship, therefore, includes another term to account for this [3]:

$$q_s'''V = Q_{conduction} + Q_{radiation}$$

$$q_s'''V = \frac{T_i - T_o}{\frac{1}{k}\frac{ln\frac{r_o}{r_i}}{2\pi L}} + \frac{2\pi r_i L\, \sigma F(T_i^4 - T_o^4)}{\frac{1}{\varepsilon_i} + \frac{1-\varepsilon_o}{\varepsilon_o}\frac{r_i}{r_o}}$$

Here, the view factor F was assumed to be equal to 1.0, and the emissivities, ε, of the vanadium and aluminum equal to 0.35 and 0.031, respectively [8]. The Stefan–Boltzmann constant is represented by σ.

Thermal conductivities for the stainless steel sample, vanadium holder, and aluminum capsule were assumed to be 16.3, 30.7, and 180 W/m–K, respectively [8]. Helium, on the other hand, exhibits thermal behavior that is a stronger function of temperature; consequently, the inner and outer gas gaps would require different values of *k*. The inner gap was assumed to have a thermal conductivity of 0.289 W/m–K (corresponding to a temperature of 655 K (720°F)); the outer gap was assumed to have a thermal conductivity of 0.213 W/m–K (corresponding to a temperature of 516 K (470°F)) [4].

An example solution for the radial temperature profile is given in Figure 4 for a sample heat generation rate of 1000 Watts (a specific heat generation rate of 6.74 X 10^8 W/m^3). This profile was derived based on the predicted coolant temperature and coolant heat transfer coefficient discussed in Section 2.3.4.

As was mentioned before, the outer gas gap and vanadium holder thicknesses would be changed to achieve the desired centerline temperature for the sample. Depending on the material and experiment, the centerline temperature could vary from 300K to 1500K.

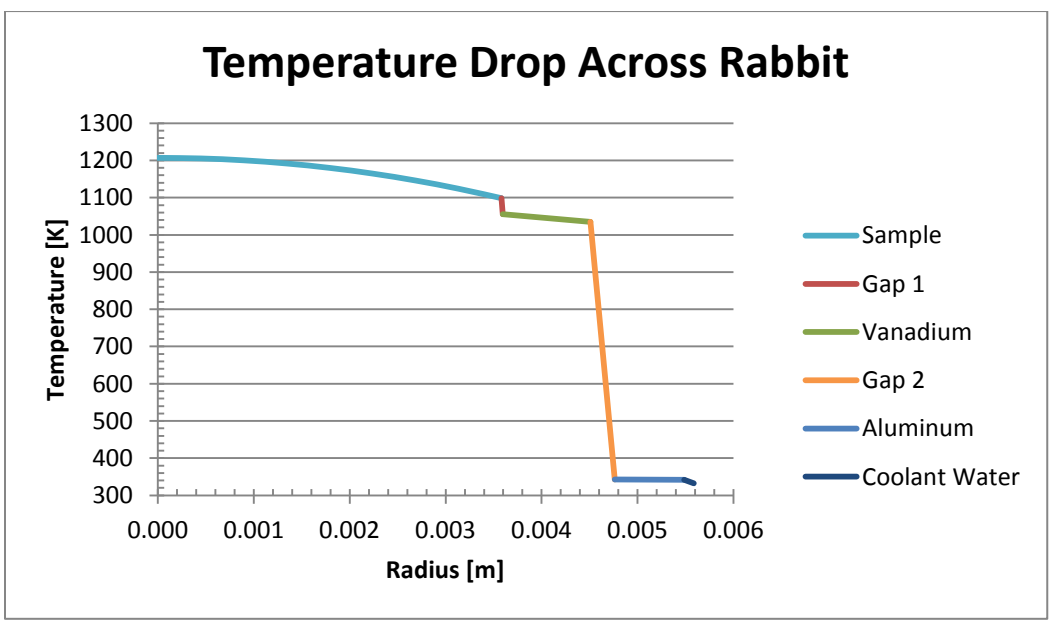

Fig. 4. Example radial thermal profile for rabbit assembly (1 kW heat generation).

2.3 RB* RABBIT BASKET

2.3.1 Extrusion

To place rabbits in the RB* position, a basket must be designed in order to hold the rabbits in the open RB* location. The design for the basket was that of a cylindrical extrusion, dimensioned to fit the RB* position, with space inside to house rabbit capsules. The outer diameter of the extrusion was set to 4.55 cm (1.791 in.), which would fit the inner diameter of the RB* liner tube with a 0.0254 cm (0.01 in.) gap between surfaces; this would serve as a channel for coolant to flow around the extrusion.

Parallel cylindrical channels that run the length of the extrusion create the space to insert the rabbits. Given the dimensions of the rabbit, the basket was designed with seven channels, arranged in a hexagonally–packed fashion, with one in the center and six around the perimeter. Channel centerlines were designed to ensure that webbing thicknesses were the same between each channel.

Extruded channels would be large enough to accommodate the cross section of one rabbit (a circle of diameter 1.097 cm (0.432 in.)) and provide a gap for coolant to flow past; the dimensions for this gap will be discussed in Section 2.3.4.

The channels in the extrusion would be long enough to house seven rabbits, stacked one on top of the other. The bottoms of these channels would include a pin across the diameter; rabbits would simply be dropped into the channels, one on top of the other, with the bottom rabbit resting on this pin. The pin would be positioned such that the midplane of the rabbit in the center of the stack would coincide with the midplane of the core.

The top of the extrusion was designed to extend 2.54 cm (1.0 in.) beyond the top of the liner tube assembly, with a hole of diameter 1.27 cm (0.5 in.) drilled radially through the extrusion, with the center 0.635 cm (0.25 in.) from the top; this would allow for the holder assembly to be easily extracted from the core after irradiation. The proposed length of this piece, taking all of this into account, is 63.842 cm (25.1345 in.); this would also accommodate the restrictor and anchor pieces that will be discussed in the following sections.

A view of the extrusion is shown in Figure 5.

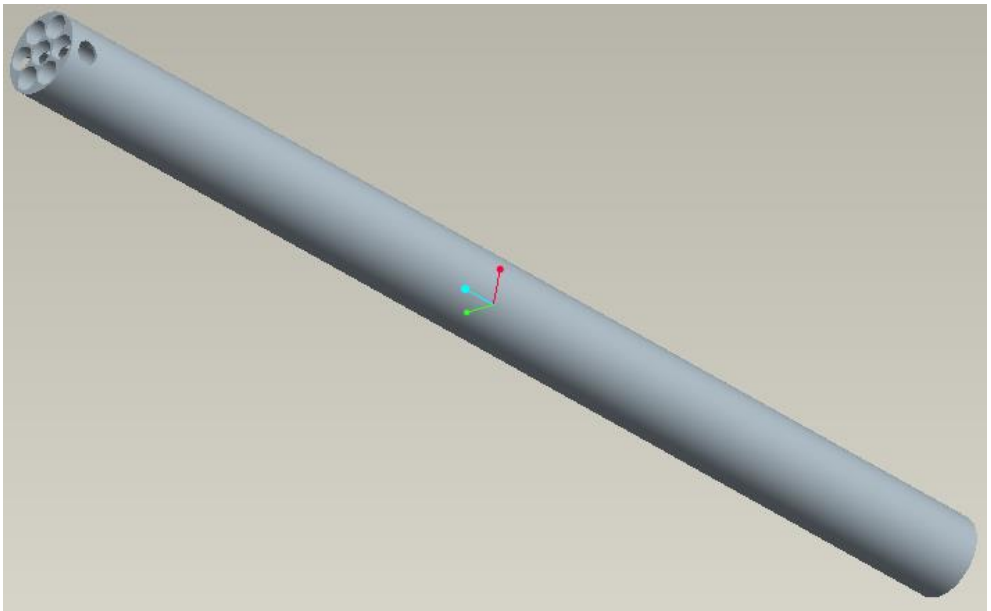

Fig. 5. View of the extrusion

2.3.2 Restrictor

In addition to this primary extrusion, the design of the basket also includes a flow restrictor. The bottom of each channel terminates in a hole of smaller diameter and relatively short length. This orifice will serve as an area of increased pressure drop in the coolant channel, allowing for a reasonable coolant gap while preventing unreasonable flow bypass through the rabbit basket. These restrictor channels are centered within the extruded channels.

The restrictor was designed to be 1.27 cm (0.5 in.) long, and the bottom edge of the lowest rabbit would be located 1.27 cm (0.5 in.) above the top of the restrictor. The diameter of the restrictor channels is discussed in Section 2.3.4

A view of the restrictor is shown in Figure 6.

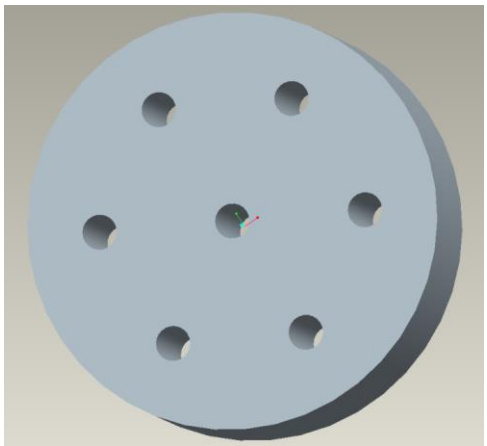

Fig. 6. View of the restrictor

2.3.3 Anchor

The bottom of the RB* liner tube terminates in an angular fitting. In order to ensure that the basket fits snugly into the RB* liner tube, an anchor was designed for the bottom of the basket. This anchor was designed as an annulus of outer diameter 4.55 cm (1.791 in.) and inner diameter 0.751 cm (1.391 in.); this would allow coolant to flow through the center with negligible pressure drop. The bottom face of this piece will be machined with a 30 degree angle to the axis so it would rest in the center of the liner tube.

The length of the anchor was chosen such that the center of the fifth loaded rabbit (from bottom to top) would coincide with the reactor's core axial midplane. The lengths of the "straight" and "angular" regions would be 1.83 cm (0.7211 in.) and 1.10 cm (0.433 in.), respectively. Four holes of diameter 0.635 cm (0.25 in.) would be drilled radially through the annulus at the midplane of the "straight" region to allow coolant to pass through the gap surrounding the basket assembly.

A view of the anchor is shown in Figure 7.

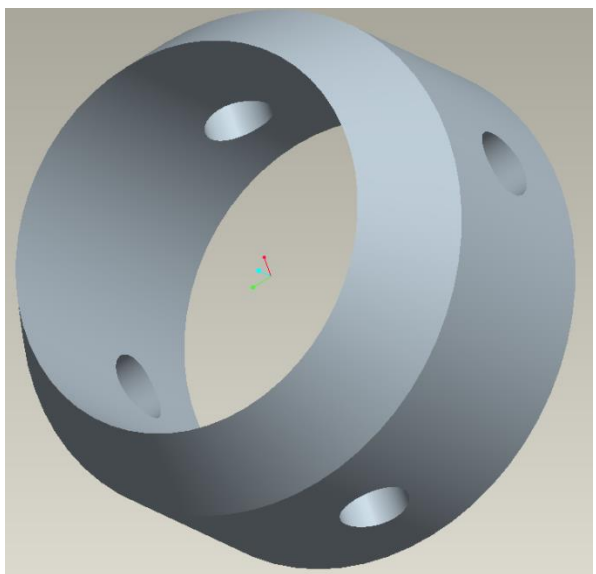

Fig. 7. View of the anchor

2.3.4 Hydraulic Diameter Calculations

The appropriate dimensions of the gap surrounding the rabbits and restrictor hole diameter were found using Excel. Pressure drop across the length of a pipe can be found using the Darcy formula [2]:

$$\Delta p = \frac{\rho v^2}{2}\left(f\frac{L}{D_e} + K_{inlet} + K_{outlet}\right)$$

Here, K represents losses due to changes in channel diameter, f is the Darcy friction factor, L is the channel length, v is the fluid velocity, ρ is the fluid density, and D_e is the equivalent diameter of the channel, which is given by:

$$D_e = 4\frac{Channel\ Area}{Wetted\ Perimeter}$$

OR

$$D_e = 2t_{gap} \quad for\ annular\ channel$$

All properties of water in this section match those for the core inlet conditions of HFIR; 332 K (138 °F) and 3.23 MPa (468 psi).

In the proposed configuration, coolant would enter at the top of the extruded channels, above the stack of rabbits; it would then flow into the annular region surrounding the stack of rabbit capsules, exit this region and enter the circular restrictor channels, exit the restrictor into the large anchor channel, and finally exit through the bottom of the RB* liner tube. Therefore, the full pressure drop equation is given by:

$$\Delta p = \frac{\rho {v_r}^2}{2}\left(f_r\frac{L_r}{D_{e,r}} + K_{in,r} + K_{out,r}\right) + \frac{\rho {v_a}^2}{2}(f_a\frac{L_a}{D_{e,a}} + K_{in,a} + K_{out,a})$$

Here, subscript *a* represents the annular region surrounding the rabbit capsules, and subscript *r* represents the restrictor. The pressure drops in the anchor region and extruded channel regions above the rabbits were assumed to be negligible due to the relatively large diameter.

The Darcy friction factors were found using the Petukhov correlation for a smooth pipe [3]:

$$f = (0.79\ln(Re) - 1.64)^{-2}, \qquad Re = \frac{\rho v D_e}{\mu}$$

Loss factors were assumed to be those associated with sudden channel expansion and contraction between two pipes with a large difference in diameter; these were 0.4 and 1.0 for inlet and outlet regions, respectively [2].

The following constraints were also applied:

- The coolant velocity in the region surrounding the rabbits must be between five and eight meters per second to prevent local hotspots and flow excursion in the channel.
- The mass flow rates in both the restrictor and annular regions must be equal to satisfy the coolant mass balance
- The coolant mass flow rate in each rabbit channel must be above 19.0 L/min (5.0 gal/min)

With these constraints in mind, as well as the total pressure drop requirement of 0.689 MPa (100 psi) (approximate pressure drop across the core region of HFIR), an Excel file was set up to iterate on the equations. After convergence, the results showed that a 0.127 cm (0.050 in.) wide annular coolant gap and a restrictor channel of 0.381 cm (0.15 in.) diameter satisfied the requirements. The flow rate of coolant through one channel would be 19.00 L/min (5.02 gal/min), with a corresponding Reynolds number of 38,080.

Finally, the heat transfer coefficient was calculated for the region surrounding the rabbit using the Dittus–Boelter relation [4]:

$$h = 0.023 \frac{k}{D_e} \left(\frac{\rho v D_e}{\mu} \right)^{0.8} \left(\frac{c_p \mu}{k} \right)^{0.4}$$

The heat transfer coefficient was found to be 45,400 W/m^2–K.

2.3.5 Basket Assembly

Figure 8 shows a radial cross–section of the basket assembly, while Figure 9 shows an axial cross–section.

All parts of the basket would be made from Al–6061 alloy in order to resist corrosion and support a favorable neutron economy.

Given the calculations from Section 2.3.4, the thickness of the aluminum "webbing" between channels would be 0.1238 cm (0.04875 in.); aluminum of this thickness should be able to stand up to the relatively low pressures in this system, and there should not be any concern that this is too thin.

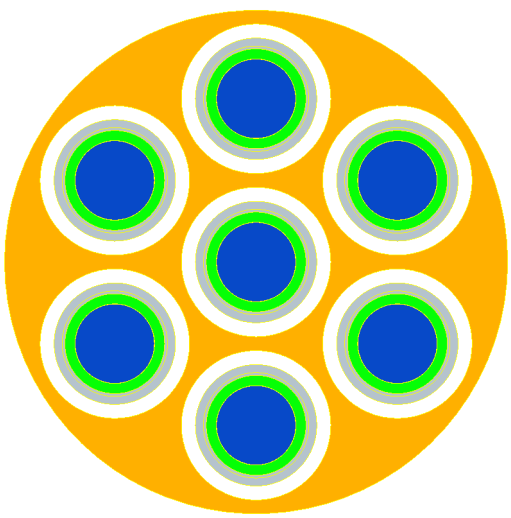

Fig. 8. Radial cross–section of the basket assembly, taken at the reactor's midplane, with rabbits shown filling each channel. Channels for coolant water are shown in white; the extrusion is shown in gold.

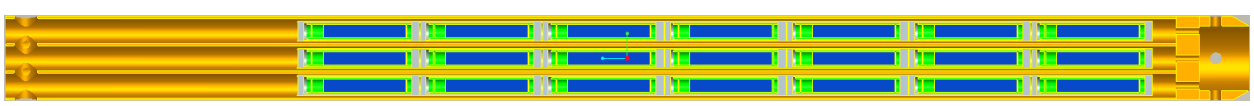

Fig. 9. Axial cross–section of the basket assembly, with rabbits shown in their normal configuration. From left to right, the regions and their lengths are: top unfilled region of rabbit channels (6.2595 in.), annular rabbit region (18.375 in.), bottom unfilled region of rabbit channels (0.5 in.), restrictor (0.5 in.), and anchor (1.1541 in.).

3. MCNP MODEL

3.1 MCNP OVERVIEW

MCNP, which was developed at Los Alamos National Laboratory, is an acronym for Monte Carlo Neutral Particles; it is a popular nuclear engineering computer program used for generating and tracking particles as they move through a system.

The design of the RB* rabbit facility has to be based on knowledge of heat generation rates in the system, neutron flux through the samples, and the effect that the design would have on the criticality of the reactor. MCNP is capable of calculating values for each of these, making it the first step in the design analysis. For this project, MCNP version 5 was used [9].

3.2 EXISTING HFIR CODE AND MODIFICATIONS

An MCNP model of the geometry and neutron sources in HFIR already exists, and can be found on the HFIR website [5]. This model is based on the geometry of HFIR fuel cycle #400, with two versions to account for the differences in material composition at the beginning and end of the cycle. This code required several modifications so that it could be used for this project, including the following:

- All references to xsdir68 (a special user–defined cross section library) were removed. These cross sections were neither relevant nor accessible for this project.
- All instances of ".73c" in cross section and material data were changed to ".70c" for correct cross–section data.
- All instances of ".60t" in cross section and material data were changed to ".10t" for correct cross–section data.
- Calcium "20000.70c" in material card 62 was changed to "20000.66c" for correct cross–section data.
- All instances of Molybdenum "42000.70c" were changed to "42000.66c" for correct–cross section data.
- The Europium liner tube that was located in the RB*–7A position was removed and replaced with Aluminum. Material cards m38 and m39 were deleted.
- The Aluminum plugs located in RB* positions 1B, 3A, 3B, and 7B were removed and replaced with Beryllium plugs.
- The inner and outer diameters of RB* positions 7A, and 7B were changed to match the radius of all the other RB* holes.
- The MCNP mode was changed from "mode n" to "mode n p." All neutron and photon importances were set accordingly.

3.3 EXPERIMENT LOCATION

All of the irradiation cases analyzed for this project with MCNP were loaded into the RB*–7B position. In some special cases, an additional extrusion assembly was loaded into positions 3B (radially opposite to position 7B) and position 7A (next to position 7B). These cases can be found in Section 5.

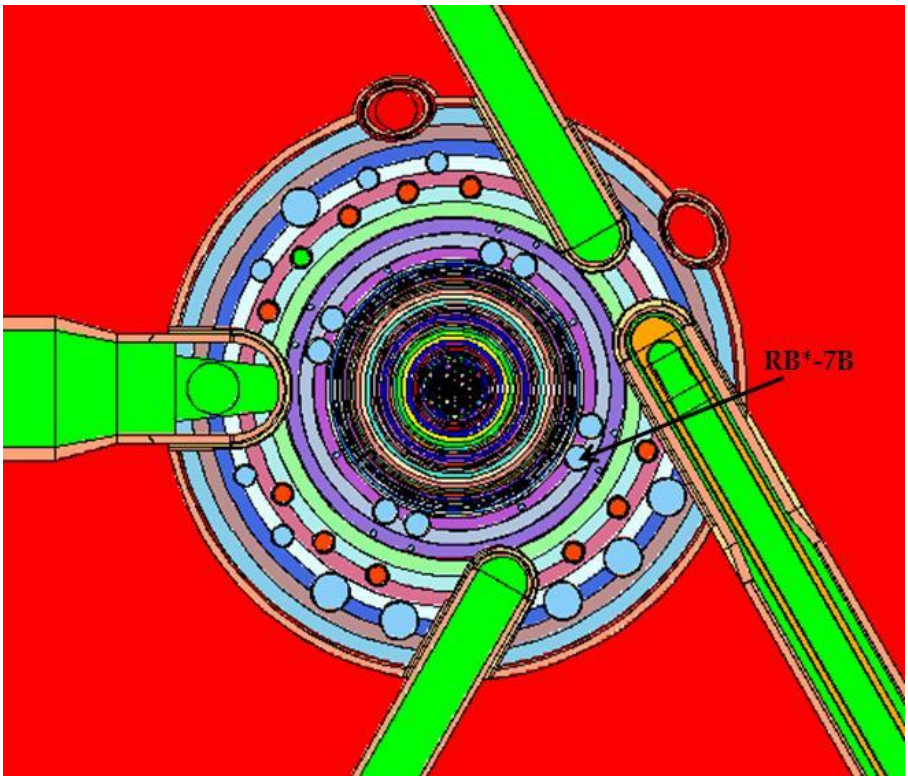

Fig. 10. Modified MCNP model of HFIR that shows the experiment location, RB*–7B

3.4 MCNP CASES RUN FOR THIS PROJECT

Several versions of the HFIR MCNP model were run for this project. These cases are listed here:

- Beginning of Cycle, 49 rabbits with graphite samples
- Beginning of Cycle, 49 rabbits with stainless steel samples
- Beginning of Cycle, beryllium plug “blank”
- End of Cycle, 49 rabbits with graphite samples
- End of Cycle, 49 rabbits with stainless steel samples
- End of Cycle, beryllium plug “blank”

3.5 GEOMETRY

The basket that was modeled in MCNP was a simplified version of Figure 9. The primary design changes were the omissions of the flow restrictor, anchor, and hole at the top of the extrusion. The geometry used within MCNP is illustrated in Figures 11–13.

3.5.1 Rabbit Geometry

Each rabbit was modeled based on the specifications listed in Section 2.1. Right Circular Cylinder (RCC) surface cards were used to reduce the number of lines of code needed to define the geometry of one rabbit.

An MCNP script was created to compare the masses and volumes calculated by MCNP with the masses and volumes found on Table 2. The cell and surfaces cards for this script are shown below:

```
c Cell Cards
50 901 -7.87    -69500              u=1 imp:n,p=1   $ Sample (Stainless Steel) Volume
51 902 -1.64e-4 -69501 69500                u=1 imp:n,p=1   $ He Gas Layer 1 Volume
52 903 -6.05    69500 69501 -69502:(-69503 69504):(-69505 69506) u=1 imp:n,p=1 $ V Vol
53 902 -1.64e-4 -69507 #52 #51 #50   u=1 imp:n,p=1   $ He Gas Layer 2 Volume
54 900 -2.70    -69508 69507:(-69509 69510)       u=1 imp:n,p=1   $ Al Volume

c Surface Cards
c        Vx        Vy        Vz       Hx Hy Hz      r
69500 rcc 23.765062 -13.445625 -2.250440 0  0  4.50088 0.35814  $ Sample Surface
69501 rcc 23.765062 -13.445625 -2.250440 0  0  5.10032 0.35941  $ Gas Layer 1 Surface
69502 rcc 23.765062 -13.445625 -2.303780 0  0  5.20700 0.46228  $ Vanadium Surface
69503 rcc 23.765062 -13.445625  2.903220 0  0  0.25400 0.46228  $ V Top Flange Outer
69504 rcc 23.765062 -13.445625  2.903320 0  0  0.25400 0.35941  $ V Top Flange Inner
69505 rcc 23.765062 -13.445625 -2.557780 0  0  0.25400 0.46228  $ V Bottom FlangeOuter
69506 rcc 23.765062 -13.445625 -2.557780 0  0  0.25400 0.35941  $ V Bottom FlangeInner
69507 rcc 23.765062 -13.445625 -2.557780 0  0  5.88010 0.48768  $ Gas Layer 2 Surface
69508 rcc 23.765062 -13.445625 -2.989580 0  0  6.60400 0.56007  $ Al Layer
69509 rcc 23.765062 -13.445625  3.614420 0  0  0.06350 0.56007  $ Al Flange Outer
69510 rcc 23.765062 -13.445625  3.614420 0  0  0.06350 0.48768  $ Al Flange Inner
```

Note that the script centers the rabbit at (23.765062, -13.445625, 0) which is the center of the RB*–7B hole as shown on the existing MCNP HFIR code (transformation card 33, tr33)

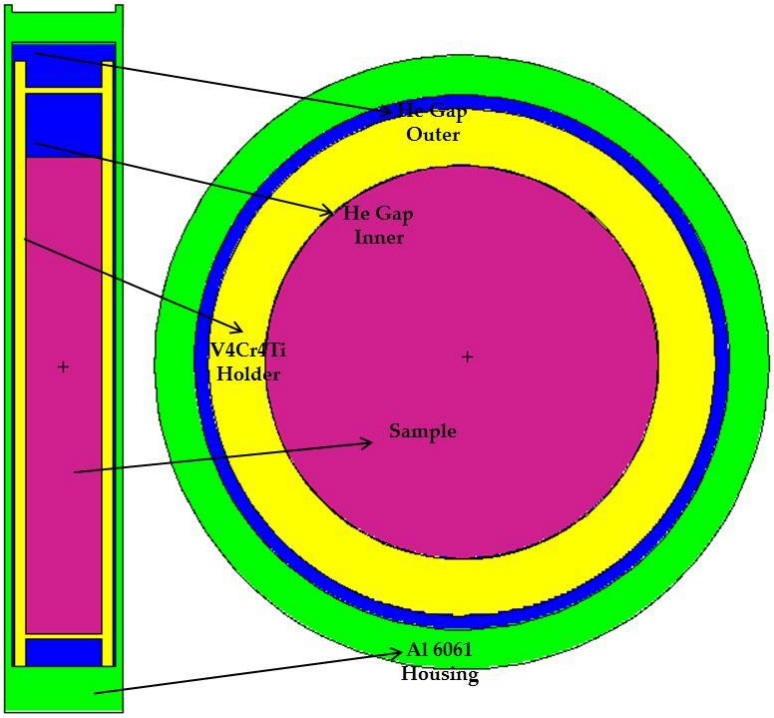

Fig. 11. Axial and radial cross sections of a rabbit modeled on MCNP. Note that the inner gas gap is too small to be seen in the radial view.

3.5.2 Extrusion Geometry

The next step after creating a single rabbit was to create a channel that could be used to load 7 rabbits vertically. The following code places the extrusion at the center of RB*–7B with a single channel at its center and one rabbit centered at the core's axial midplane:

```
c Cell Cards
c ********************************** Begin Extrusion *************************
1  900 -2.70    -1 #10                  vol= 363.0705     imp:n,p=1   $ Extrusion grid
10 900 -2.70    -2            fill= 1                    imp:n,p=1   $ Center Channel
2    9 -0.98465 #54 69508   u=1 vol= 266.8334     imp:n,p=1   $ Coolant Region
c ********************************** End Extrusion *************************

c Surface Cards
c ********************************** Begin Extrusion *************************
1 rcc 23.765062 -13.445625 -29.21  0 0 58.42  2.27457  $ Extrusion(L= 23", r= 0.8955")
2 rcc 23.765062 -13.445625 -29.21  0 0 58.42  0.67564  $ Coolant  (L= 23", r= 0.2660")
c ********************************** End Extrusion *************************
```

In order to create the extrusion grid with seven channels, TRCL cards were used, the following was added to the cell cards:

```
c ******************************************************************************
c The following creates a hexagonal lattice based upon the center channel universe
c ******************************************************************************
c ———————————————————————— Begin Lattice ————————————————————————
11 like 10 but trcl ( 1.277478  0.737552 0)                    $ Holder at  30°
12 like 10 but trcl ( 0         1.475105 0)                $ Holder at  90°
13 like 10 but trcl (-1.277478  0.737552 0)                $ Holder at 150°
14 like 10 but trcl (-1.277478 -0.737552 0)                    $ Holder at 210°
```

```
15 like 10 but trcl ( 0          -1.475105 0)          $ Holder at 270°
16 like 10 but trcl ( 1.277478 -0.737552 0)            $ Holder at 330°
c ———————————————————————————— End Lattice ————————————————————————
```

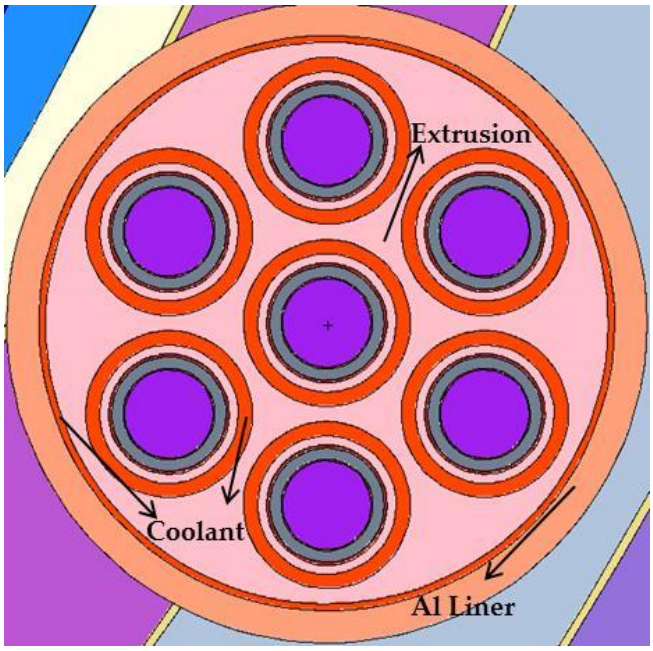

Fig. 12. Radial cross section at core's midplane of RB*–7B showing the extrusion and channel lattice.

Finally, surface and cell cards were added for 6 more rabbits that would yield a total of 49 rabbits inside the extrusion. The final script is shown in Appendix A.

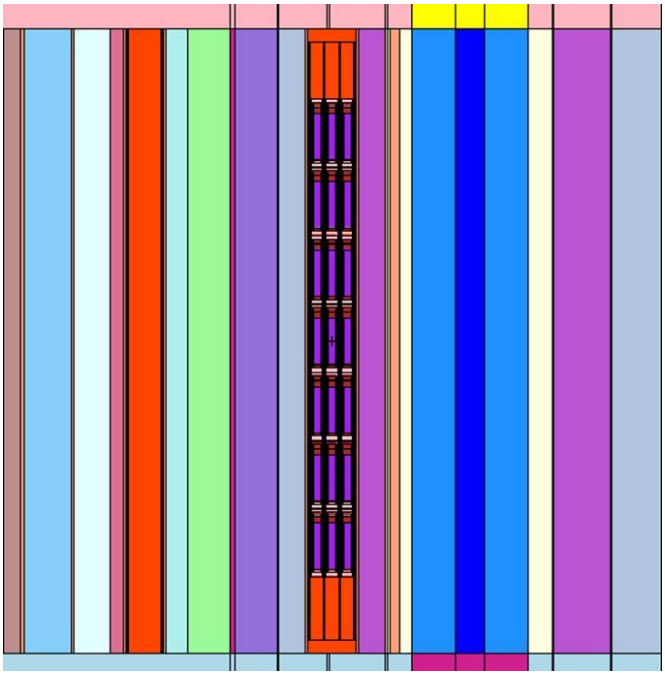

Fig. 13. Axial view of the RB*–7B position (center) loaded with forty–nine rabbits centered at midplane. Only twenty–one rabbits are visible in this view.

3.6 MATERIALS

This project required the addition of five new materials to the script: graphite, stainless steel, Al–6061 alloy, helium gas, and V4Cr4Ti alloy. The compositions for each material were taken from a report on a similar design project for the flux–trap region [6].

The MCNP code for these materials is given here:

```
c $ Al6061 Housing Material, density= 2.7 g/cm³
m900  13027     -0.9758          $ Al
     14000     -0.006            $ Si
     26000     -0.007            $ Fe
     29000     -0.00275     $ Cu
     25055     -0.0015           $ Mn
     12000     -0.001            $ Mg
     24000     -0.00195     $ Cr
     30000     -0.0025      $ Zn
     22000     -0.0015           $ Ti
c
c $ Graphite Sample, density = 1.78 g/cm³
m901  06000      1          $ C
c
c $ Natural Helium Gas, density = 1.64e-4 g/cm³
m902  02003.70c  -1.37000e-6    $ He-3
     02004.70c  -0.99999863    $ He-4
c
c $ V4Cr4Ti Holder Material, density = 6.05 g/cm³
m903  23000     -0.905            $ V
     22000     -0.047            $ Ti
     24000     -0.042            $ Cr
     26000     -0.002            $ Fe
     14000     -0.004            $ Si
c
c $ Stainless Steel Sample, density = 7.87 g/cm³
m904  26000     -0.8956      $ Fe
     24000     -0.08     $ Cr
     74000     -0.02     $ W
     23000     -0.002            $ V
     73181     -0.0004      $ Ta
     06000     -0.001            $ C
     27059     -0.001            $ Co
```

3.7 TALLIES

3.7.1 Heat Generation Rates

One of the primary concerns in this project was the heat generation rate in each rabbit capsule, as well as in the basket and coolant water itself. In the preliminary design, only heat generation in the sample was accounted for; in reality, though, all materials in the assembly generate heat due to neutron scattering and absorption as well as photon energy deposition.

3.7.1.1 Rabbit locations used for tallies

For these tallies, only a few chosen rabbits were used to show the relationship between position in the assembly and internal heat generation rates. By choosing rabbits appropriately, computation time could be kept low while still giving an accurate picture of heat generation in the assembly.

All seven rabbits in the center channel were included in the tallies, as neutron and gamma fluxes in the reactor are strong functions of axial position; data from this set of rabbits would provide a good axial heat generation profile.

Since particle flux in the reflector region is also a function of radial position, more rabbits were selected to gauge this dependence. Therefore, in addition to the rabbit positions discussed above, the top, midplane, and bottom rabbits from the channels closest and farthest from the core were also included in the heat generation tallies. These rabbits would provide reasonable data for a radial heat generation profile.

3.7.1.2 Extrusion and water sections used for tallies

Because heat generation in the RB* position is such a strong function of axial location, the extrusion and coolant water regions in the assembly were divided into nine sections for internal heat generation calculations. These regions were defined by the same cross–sectional planes that defined rabbit positions, which can be seen in Figure 14.

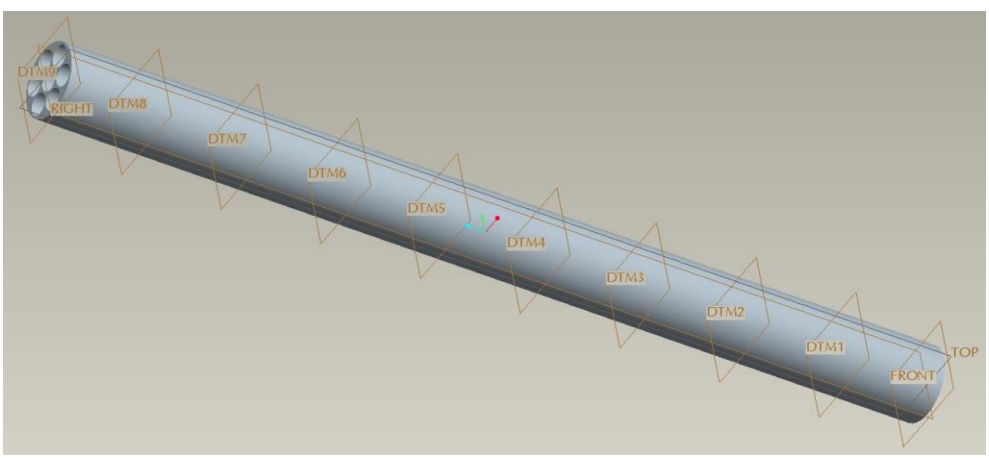

Fig. 14. Planes separating the extrusion into different sections for calculating heat generation are shown here, labeled as "DTM" followed by a number.

These regions were used to obtain the necessary tallies to plot axial heat generation rates for both water and the Al6061 extrusion. In total, a set of eight new planes were added at the end of the MCNP surface cards in order to split the water and extrusion cells into bins; these planes surface cards are shown below:

```
c ———————————— Tally Surfaces for water and extrusion only ————————————
10000 pz -23.33625
10001 pz -16.66875
10002 pz -10.00125
10003 pz -3.333750
10004 pz  3.333750
10005 pz  10.00125
10006 pz  16.66875
10007 pz  23.33625
c ————————————————————————————————————————————————————————————————————————
```

In order to calculate heat generation rates, an energy deposition tally was used. In this tally, the cell to be split was specified and the above surfaces were used to store the output in the generated bins. The masses of the nine sections were calculated by hand and entered into the code at the end of the tally section. An example of this is shown below:

```
c ———————————— Neutron and Photon Energy Deposition Tallies – Water ——————
fc66 NEUTRON ENERGY DEPOSITION IN WATER
f66:n 2                                                    $ Cell 2 corresponds to water
fs66 -10000 6i -10007                                      $ Tally split into 9 bins
fm66 1.0291E+06                                            $ Neutron Multiplier
sd66 56.155 23.918 23.918 23.918 23.918 23.918 23.918 23.918 56.155    $ Bin Mass
c
c
fc76 PHOTON ENERGY DEPOSITION IN WATER
f76:p 2                                                    $ Cell 2 corresponds to water
fs76 -10000 6i -10007                                      $ Tally split into 9 bins
fm76 1.610129E+06                                                $ Photon Multiplier
sd76 56.155 23.918 23.918 23.918 23.918 23.918 23.918 23.918 56.155    $ Bin Mass
c ————————————————————————————————————————————————————————————————————————
```

3.7.1.3 Rabbit materials selected for tallies

Heat generation rates were calculated for the stainless steel and graphite samples, V4Cr4Ti holders, Al6061 housing capsules, coolant water in annular regions of the extrusion, and Al6061 extrusion.

Heat generation in both helium gaps was ignored because, although neutron scattering results in a large specific heat generation rate, the mass of helium in each rabbit is so small that the total heat generated would be negligible.

3.7.1.4 Neutron energy deposition tallies

Each cell mentioned above would require a tally tracking energy deposition from neutrons. An example of one of these tallies is shown here:

```
fc6 NEUTRON ENERGY DEPOSITION IN GRAPHITE SAMPLES
f6:n  (20 30 40 50 60 70 80 < 10)
    (20 50 80 < 13)
    (20 50 80 < 16)
fm6 1.0291E+06  $  6.4234E+18 * 1.602E-13
```

The multiplier is necessary because MCNP normalizes all tallies to one source particle. This would be applied to the MCNP output to obtain heat generation in W/g:

$$Heat\ Generation\ \left[\frac{W}{g}\right] = 6.4234e18\ \left[\frac{neutrons}{s}\right] * 1.602e-13\ \left[\frac{J}{MeV}\right] * Output\ \left[\frac{MeV}{g-neutron}\right]$$

This calculation takes into account conversion factors as well as the strength of the HFIR neutron source [6].

3.7.1.5 Photon energy deposition tallies

Each cell mentioned above would require a tally tracking energy deposition from neutrons. An example of one of these tallies is shown here:

```
fc36 PHOTON ENERGY DEPOSITION IN GRAPHITE SAMPLES
f36:p (20 30 40 50 60 70 80 < 10)
    (20 50 80 < 13)
    (20 50 80 < 16)
fm36 1.587489E+06  $  6.4234E+18 * 1.602E-13 * 1.5426
```

Like the neutron tallies, MCNP normalizes all tallies to one source particle, and therefore requires a multiplier to produce a meaningful output. Unlike the neutron tallies, however, these outputs required a second multiplier. MCNP only tracks photons produced in fission events, and therefore the program does not account for the significant heat generation caused by photons resulting from fission product decay.

Values for the second multiplier were based on data from J. McDuffee's report on a similar design project for the flux–trap region [6]. Assuming that the ratio of heating from fission photons to fission product photons is uniform throughout the core, multipliers were calculated such that, when applied to the MCNP output, the results would show the heat generation from all photon types. These values are given in Table 3.

Table 3 – Multipliers for photon energy deposition tallies

Material	Multiplier
Graphite	1.5426
Al6061	1.6087
V4Cr4Ti	2.0706
Stainless Steel	1.5120
Water	1.5640

These multipliers also account for activation of materials, and subsequent decay and local energy deposition. Though this effect is accounted for in all materials, the only one for which there is a significant contribution is the vanadium alloy, because of the reaction:

$$^{51}_{23}V\ (n,\gamma)\ ^{52}_{23}V \rightarrow\ ^{52}_{24}Cr + \beta^-$$

This results in a high energy β–particle (3.975 MeV) which deposits most of its energy in the immediate vicinity, and explains why the multiplier for the vanadium alloy is significantly higher than for the other materials.

3.7.2 Neutron Flux Tallies

The only values of neutron flux that were of interest for this project were those inside the samples; tallies were included in the MCNP script to find the flux in each of the sample locations discussed in section 3.6.1.1.

The neutron flux was separated into 44 energy bins, with energy bin delimiters based on J. McDuffee's report [6]. A representative flux tally is reproduced here:

```
c NEUTRON FLUX TALLY
fc4 NEUTRON FLUX TALLY IN GRAPHITE SAMPLES
f4:n      (20 30 40 50 60 70 80 < 10)
          (20 50 80 < 13)
          (20 50 80 < 16)          $ Middle Rabbits, Inner Rabbits, Outer Rabbits
fm4 6.4234E+18                     $ Multiplier
c 44-group Energy Spectrum (in MeV)
e4        3.0000E-09  7.5000E-09  1.0000E-08  2.5300E-08  3.0000E-08  4.0000E-08  5.0000E-08  7.0000E-08  1.0000E-07
          1.5000E-07  2.0000E-07  2.2500E-07  2.5000E-07  2.7500E-07  3.3500E-07  3.5000E-07  3.7500E-07  4.0000E-07
          6.2500E-07  1.0000E-06  1.7700E-06  3.0000E-06  4.7500E-06  6.0000E-06  8.1000E-06  1.0000E-05  3.0000E-05
          1.0000E-04  5.5000E-04  3.0000E-03
          1.7000E-02  2.5000E-02  1.0000E-01  4.0000E-01  9.0000E-01  1.4000E+00  1.8500E+00  2.3500E+00  2.4790E+00
          3.0000E+00  4.8000E+00  6.4340E+00  8.1873E+00  2.0000E+01
```

Again, the multiplier accounts for the fact that MCNP normalizes all tallies to the flux per source particle.

3.8 MCNP MODE, SOURCE INFORMATION AND K–CODE

As mentioned in Section 3.2, each scenario was run on neutron and photon mode (mode n p). The source cards were kept the same as the ones found in the public HFIR models. The effective reactivity (k_{eff}) of the model was computed for each different scenario discussed in Section 3.4. To obtain good statistics for both k_{eff} and all proposed tallies, 100,000 neutron histories were run during each cycle. Data collection began after skipping 500 cycles, for a total of 10,500 cycles run during the completion of the script. The mode, k–code and source commands, which were the same for all cases, are shown here:

```
mode n p
kcode 100000 1.00 500 10500 350000
sdef erg=d1 axs=0 0 1 rad=d2 ext=d3
sp1 -3 0.988 2.249
si2 0 51
si3 -3 31
```

4. RESULTS

4.1 HEAT GENERATION

4.1.1 Safety Basis Heat Generation

Table 4 contains the highest heat generation rates for each material across all loading schemes and points in the fuel cycle, as well as their relationships to corresponding materials located in the flux trap. Heat generation values in the flux trap can be found in a report by J. McDuffee [6].

Table 4 – Safety Basis Heat Generation Rates

	Maximum Heat Generation Rate in RB* Position [W/g]	Maximum Heat Generation Rate in Flux Trap [W/g] [6]	RB*/Flux Trap
Steel	16.7	44.2	38%
Graphite	12.9	39.0	33%
Vanadium	20.4	56.1	36%
Aluminum	13.2	38.0	35%
Water	18.6	76.2	24%

Heat generation rates are lower in the RB* position given that this position is farther away from the flux trap, with a ratio of about 1:3 from RB* to flux trap region.

The vanadium holder experiences the highest heat generation because of the large contribution of local decay products, while water experiences the second highest, because of the neutron scattering that takes place there.

4.1.2 Design Basis Heat Generation Information

Due to the amount of information in this category, heat generation rate data for all materials, loading schemes, and points in the fuel cycle can be found in Appendix B.

4.1.3 Axial Power Dependence

Figure 15 shows the axial heat generation profile for samples in the center channel of the assembly. Both sample types, as well as both points in the cycle, are included.

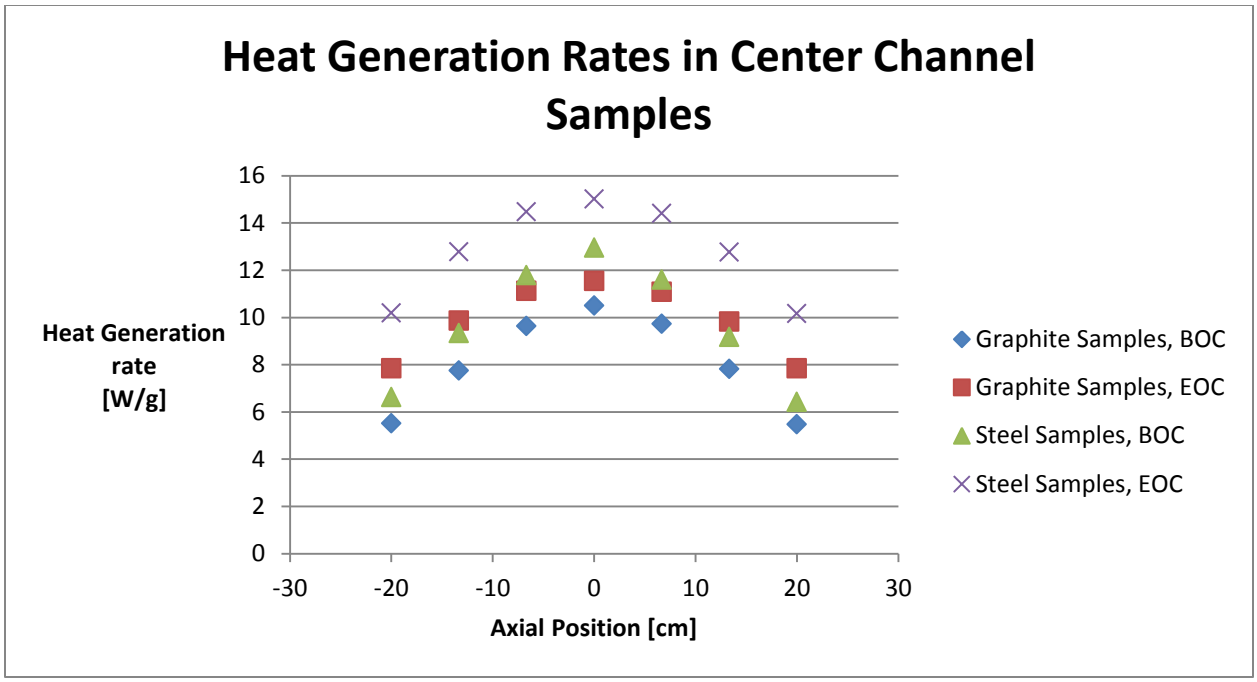

Fig. 15. Axial heat generation profile for samples located in the center channel of the assembly.

The axial profile of total rabbit power produced for capsules in the center channel can be found in Figure 16. It is worth noting that even peak power values are much less than values in the flux trap region; preliminary analysis for this project assumed that each rabbit would produce 1000 watts of heat, while these results show that even the most energetic rabbit in the RB*–7B position does not produce even half of that.

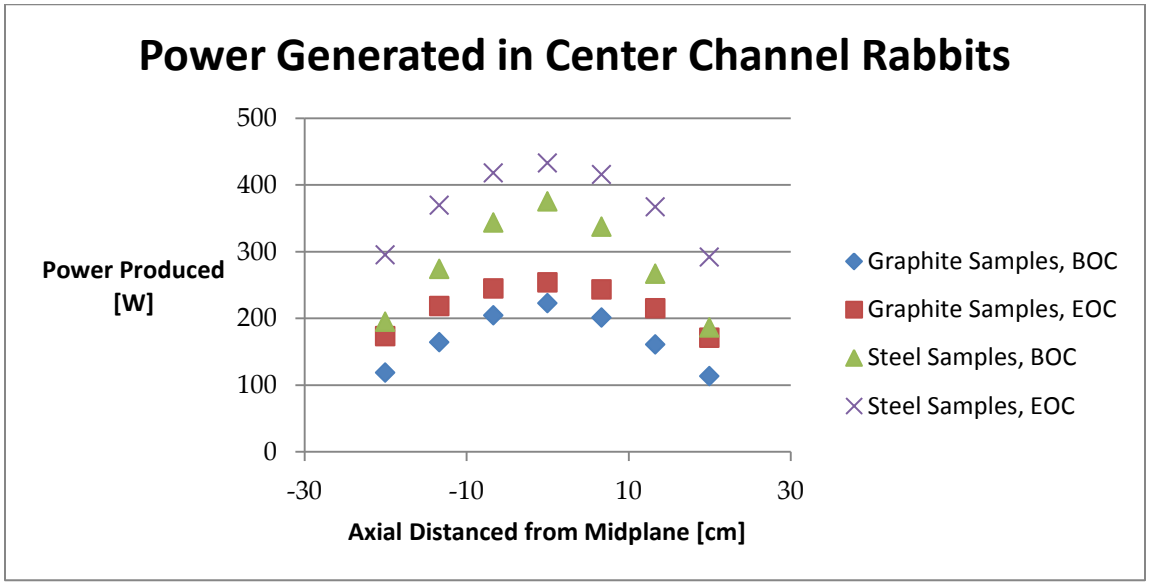

Fig. 16. Axial power profile for rabbits located in the center channel of the assembly.

Finally, as a representative plot to show general heat generation trends, Figure 17 depicts the axial profile of heat generation in all materials in the center channel, with steel samples at the end of the fuel cycle.

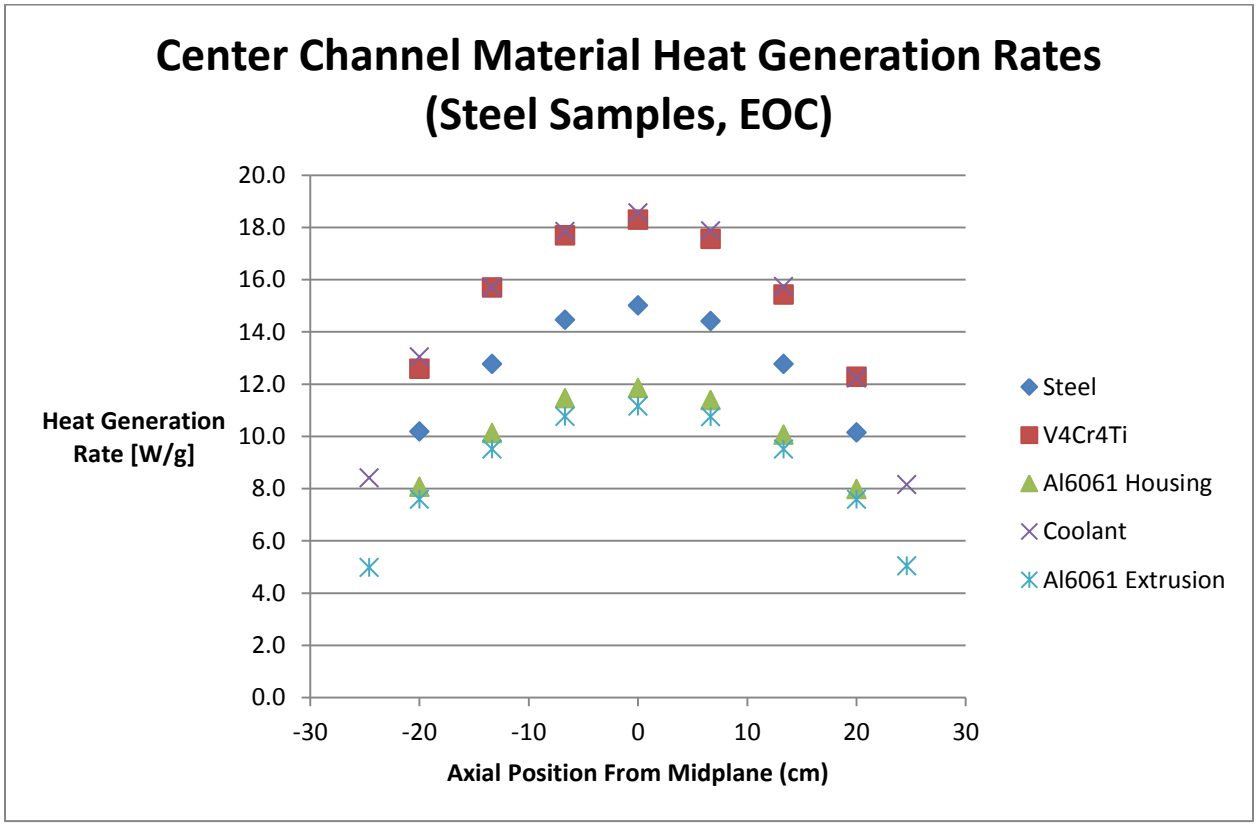

Fig. 17. Axial heat generation profile for all materials located in the center channel. In this case, the holder is loaded with steel samples, and the core is at the end of its life.

4.1.4 Radial Power Dependence

The effect of radial position on power generation can be seen in Table 5. The rabbits used to create this table were those on the core midplane.

Table 5 – Effects of Radial Position on Power Generated in Materials and Rabbits

	Rabbits with Steel Samples				Rabbits with Graphite Samples			
	Inner Channel – BOC	**Outer Channel – BOC**	**Inner Channel – EOC**	**Outer Channel – EOC**	**Inner Channel – BOC**	**Outer Channel – BOC**	**Inner Channel – EOC**	**Outer Channel – EOC**
Sample [W/g]	14.5	11.1	16.7	13	12.2	8.8	12.9	9.8
Vanadium [W/g]	17.8	13.8	20.4	16.1	17.7	14	20.2	16.3
Aluminum [W/g]	12	8.8	13.2	10	11.6	8.7	12.8	9.9
TOTAL [W]	**422**	**322**	**482**	**375**	**251**	**193**	**281**	**222**

For a better visual representation of power as a function of position, Figure 18 overlays a cross section of the midplane rabbits (with steel samples at the beginning of the cycle) with the total power that those rabbits produce.

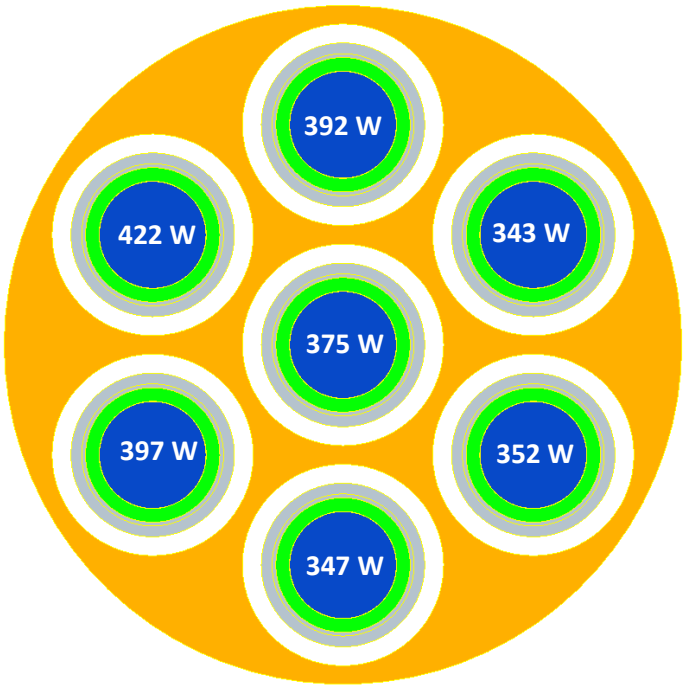

Fig. 18. Power generated in midplane rabbits (steel samples, BOC). The channel at the "10 o'clock" position is the inner channel, while the channel at the "4 o'clock" position is the outer channel.

4.2 NEUTRON FLUX

4.2.1 Axial Dependence of Total Flux Levels

Figure 19 shows the relationship of axial position to neutron flux in samples in the center channel.

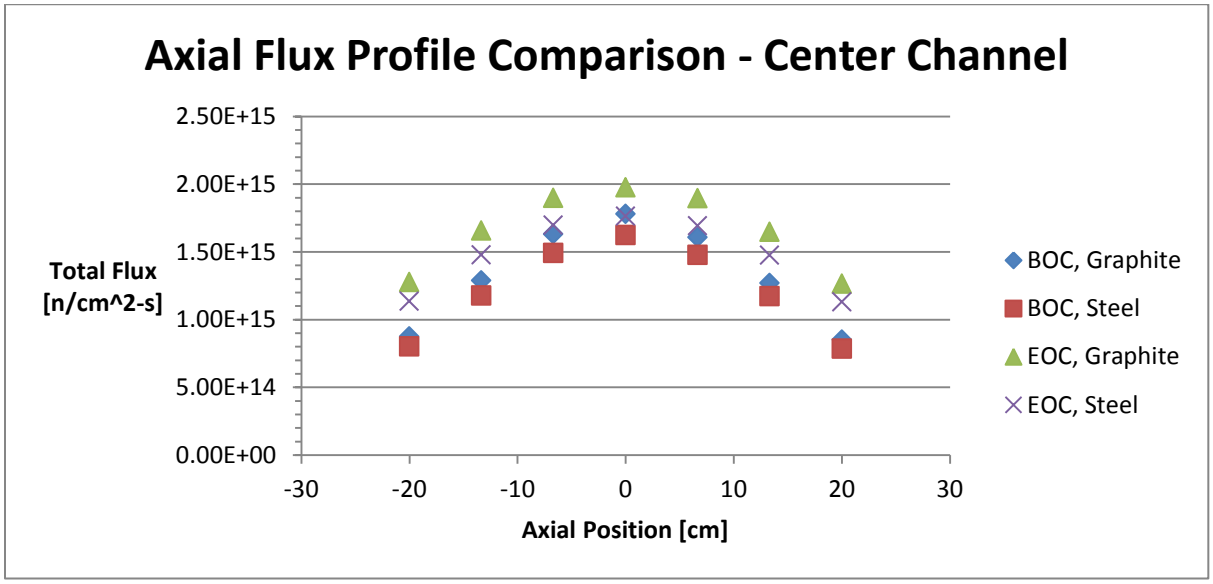

Fig. 19. Axial flux profile for samples in the center channel. Both materials and both points in the cycle are shown.

For both sample materials, the profile rises and flattens during the course of the cycle, just like the heat generation rates given in Figures 15 and 16. This is expected in any reactor; as fissile material burns up in the core, flux must increase to maintain a constant power level. Figure 19 also shows that the flux through the graphite samples is generally higher than through steel samples. This is also to be expected, as steel has a much higher neutron absorption cross section than graphite, removing more neutrons from the vicinity.

The peak neutron flux shown here (for the EOC case with graphite samples) is 1.98×10^{15}, which is just under half of the peak value in the flux trap region [1].

4.2.2 Total, Fast, and Thermal Flux Levels

Table 6 contains data for total, fast, and thermal flux tallies for the samples at the midplane. Thermal neutrons are defined as those having energies less than 0.625 eV, and fast neutrons are defined as those having energies greater than 0.1 MeV.

Table 6 – Midplane Neutron Flux

	Inner Channel Flux			Center Channel Flux			Outer Channel Flux		
	Total	**Fast**	**Thermal**	**Total**	**Fast**	**Thermal**	**Total**	**Fast**	**Thermal**
BOC Graphite	1.96E+15	6.32E+14	6.74E+14	1.78E+15	5.11E+14	6.84E+14	1.66E+15	4.22E+14	7.15E+14
EOC Graphite	2.18E+15	6.06E+14	9.17E+14	1.98E+15	4.91E+14	8.94E+14	1.85E+15	4.08E+14	9.17E+14
BOC Steel	1.83E+15	6.30E+14	5.55E+14	1.62E+15	5.10E+14	5.45E+14	1.51E+15	4.21E+14	5.85E+14
EOC Steel	2.00E+15	6.03E+14	7.49E+14	1.76E+15	4.88E+14	7.06E+14	1.65E+15	4.05E+14	7.38E+14

Table 6 shows that graphite samples result in a higher neutron flux than steel samples, particularly in the thermal spectrum; this agrees with the data in Figure 19. Thermal flux values also increase in time, due to the withdrawal of the control blades, but fast flux is generally unaffected by sample material or point in cycle. Due to the constant power level, the number of fissions in the core is also constant; since fission produces (overall) a constant number of fast neutrons, and since the moderating capabilities of the reactor are not transient, fast flux values are relatively stable in time.

4.2.3 Flux and Spatial Dependence

For a better visual representation of neutron flux as a function of position, Figure 20 overlays a cross section of midplane rabbits (with steel samples at the beginning of the cycle) with the total neutron flux through those rabbits.

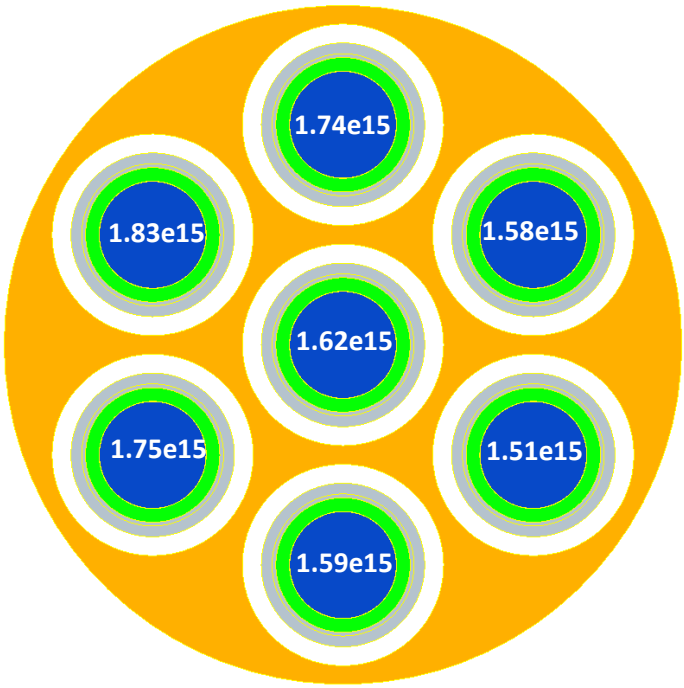

Fig. 20. Flux through midplane rabbits, in n/cm^2–s. The channel at 10 o'clock is the inner channel, while the channel at 4 o'clock is the outer channel.

4.2.4 Flux Spectra and Material and Time Dependence

Figure 21 shows the relationship between sample materials, point in core life, and neutron energy spectrum for center channel samples at the core midplane.

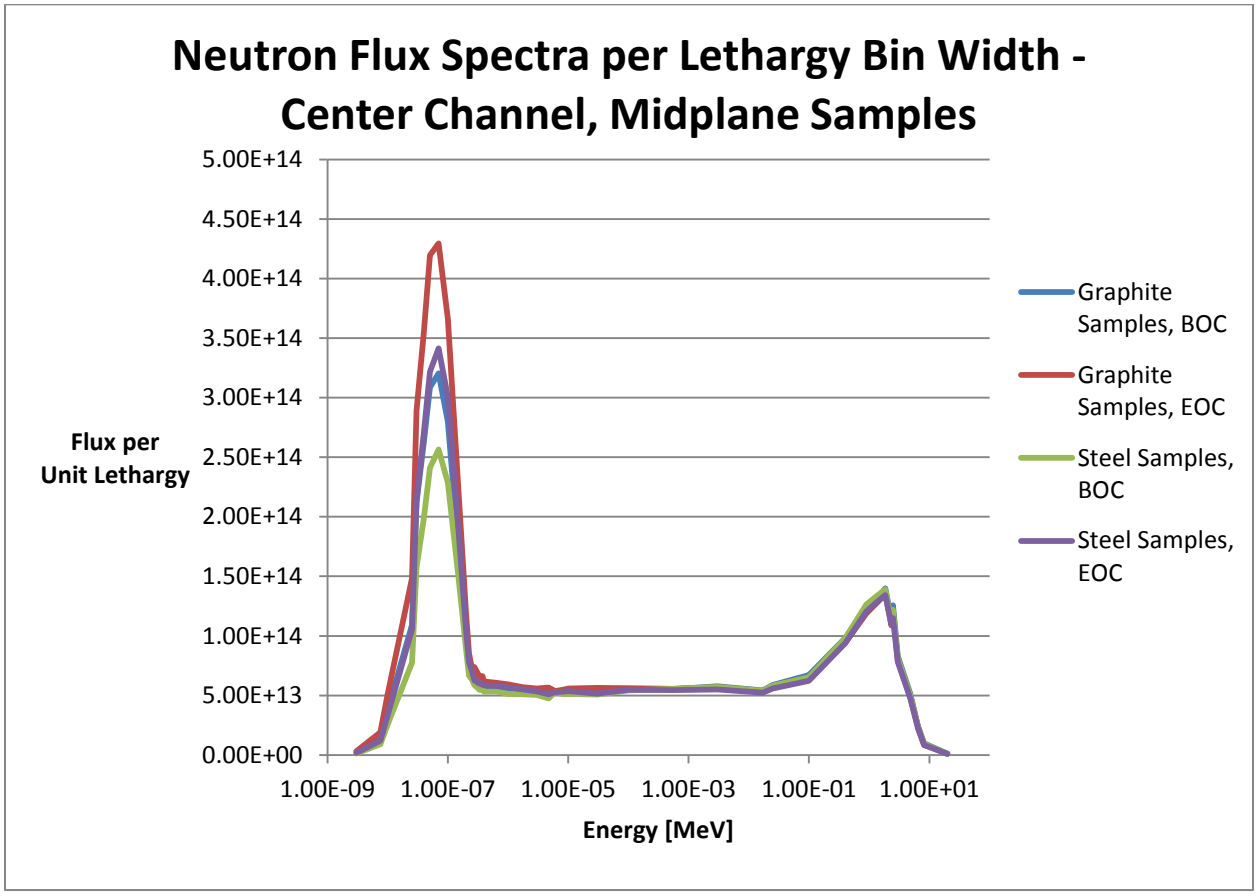

Fig. 21. Material and time dependence of flux spectra. Flux values are normalized by the width of their lethargy bins.

This plot shows that thermal flux values are particularly affected by the choice of sample (steel will remove many thermal neutrons from the system, while graphite will remove few), while fast and epithermal flux values are rather unaffected; this agrees with the data in Table 6, which was discussed earlier.

4.2.5 Comparison of Flux Spectra from Different Regions of HFIR

Finally, Figure 22 compares the corrected flux spectrum for the center channel midplane rabbit with flux spectra from the peripheral target positions (PTP), target rod rabbit holders (TRRH), and hydraulic tube (HT). All cases of flux shown in Figure 22 are for the beginning of the cycle, with steel samples and vanadium holder. Flux data for the flux trap regions was taken from J. McDuffee's report [6].

Figure 22 shows that the neutron flux in the RB* position is roughly half of that in the peripheral tube positions, and roughly one third of that in the hydraulic tube.

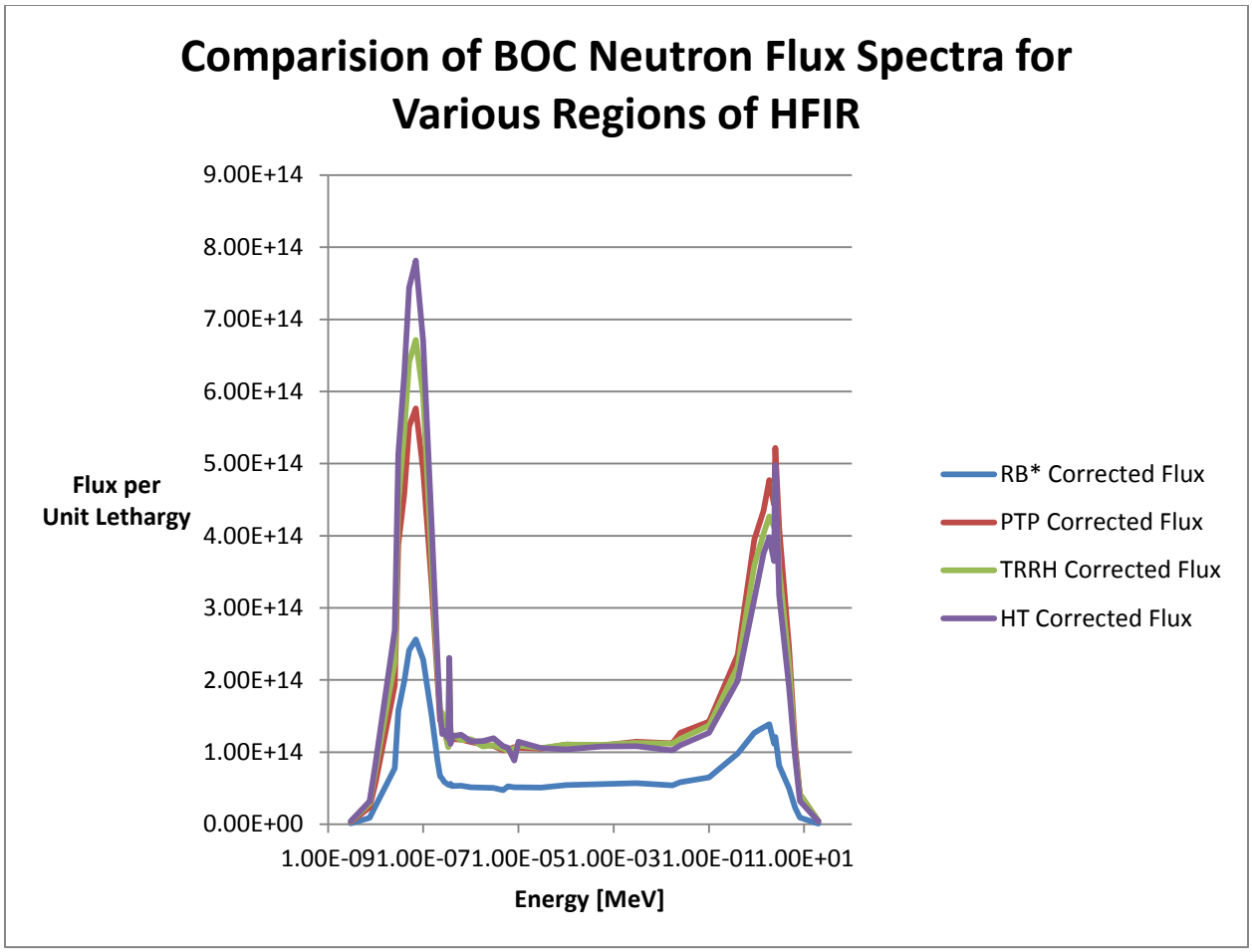

Fig. 22. Corrected neutron flux spectra for various regions of HFIR

Complete tables of neutron flux levels for the RB* position, for all loading schemes and points in the cycle, can be found in Appendix C.

4.3 CRITICALITY

Table 7 contains information on the change in beginning of cycle core reactivity that comes with loading one of these assemblies into the RB* position, as compared to the standard loading of a beryllium plug.

Table 7 – BOC Reactivity Changes

Case	Reactivity k_{eff}			Δk_{eff}			$\Delta\rho$ (cents) (if β = 0.0076)
Graphite	1.01628	±	0.00003	0.00143	±	4.2E-05	18.19
Empty (Be Plug)	1.01771	±	0.00003				
Steel	1.01606	±	0.00003	0.00165	±	4.2E-05	21.00
Empty (Be Plug)	1.01771	±	0.00003				

An assembly loaded with graphite samples decreases reactivity less than an assembly with steel samples; this occurs because the neutron absorption capabilities of graphite are much less than those of steel. Both sample materials, however, lower reactivity by some amount, as the assemblies contain a large volume of aluminum in the extrusion and housing capsules regardless of sample material. Aluminum has a higher neutron absorption cross section than beryllium.

Lower reactivity after the completion of a cycle translates into a shorter core lifetime. There is enough evidence to believe, however, that the reduction in core lifetime due to these assemblies is small. Given that differential control blade worth in HFIR is somewhere in the range of 15.55 – 70.9 cents per inch depending on blade location and point in the cycle, inserting the designed assembly of rabbits into the RB* position would have a small effect on core reactivity [7].

4.4 RABBIT THERMAL MODEL RESULTS

New information on heat generation rates made it possible to create a more accurate model of the temperature profile across the rabbit.

To simplify analysis, all heat was once again assumed to be generated in the sample. To find the value of the effective rabbit power, heat generation rates in the capsules were calculated only for the sections bounded by the same planes as the sample: that is, the capsules were modeled as annuli that were the same height as the sample. Heat generation rates were taken for rabbits in the inner channel at the core midplane, for both sample materials and both times in the fuel cycle. These cases are reproduced in Figures 23–25.

Thermal conductivities of the helium gaps were updated to more accurate temperature-dependent values, to reflect the more accurate heat generation rates, but all other assumptions discussed in Section 2.1.6 were kept for this model.

In these plots, the green line represents the vanadium holder, while the blue line represents the aluminum capsule. Inner and outer gas gaps are red and gold, respectively.

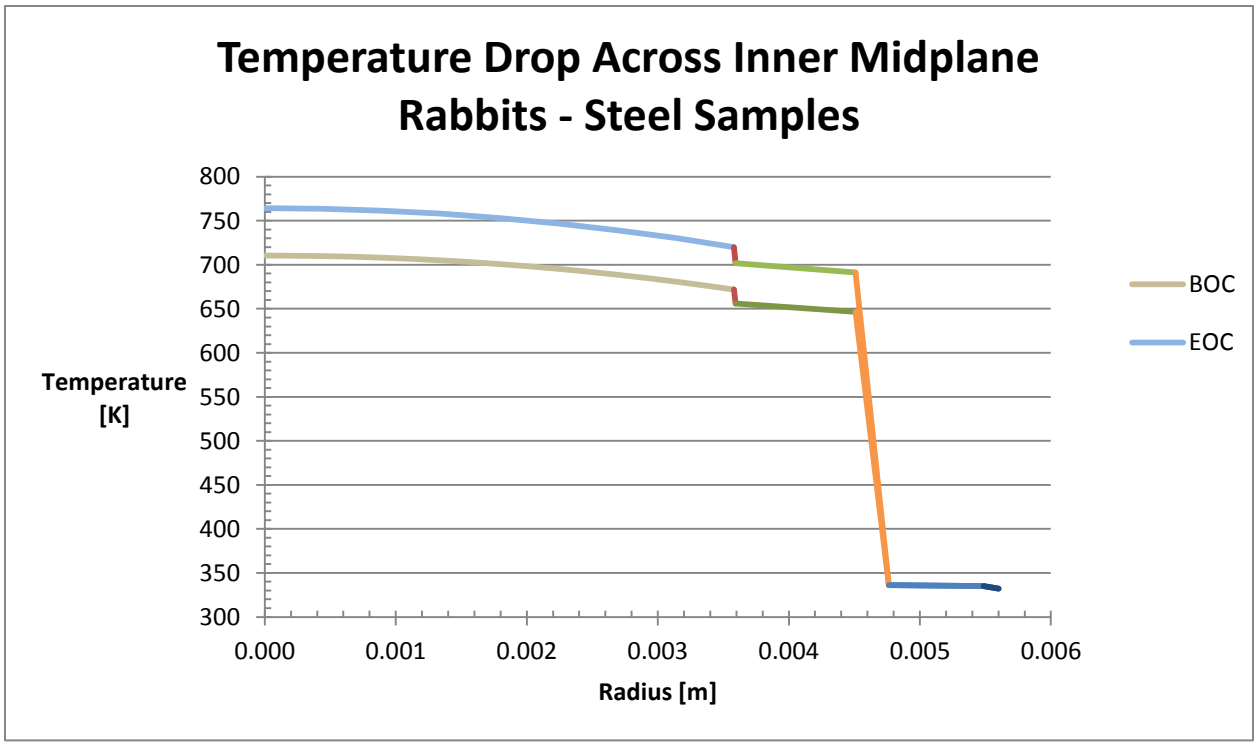

Fig. 23. Thermal profile of a rabbit with stainless steel samples

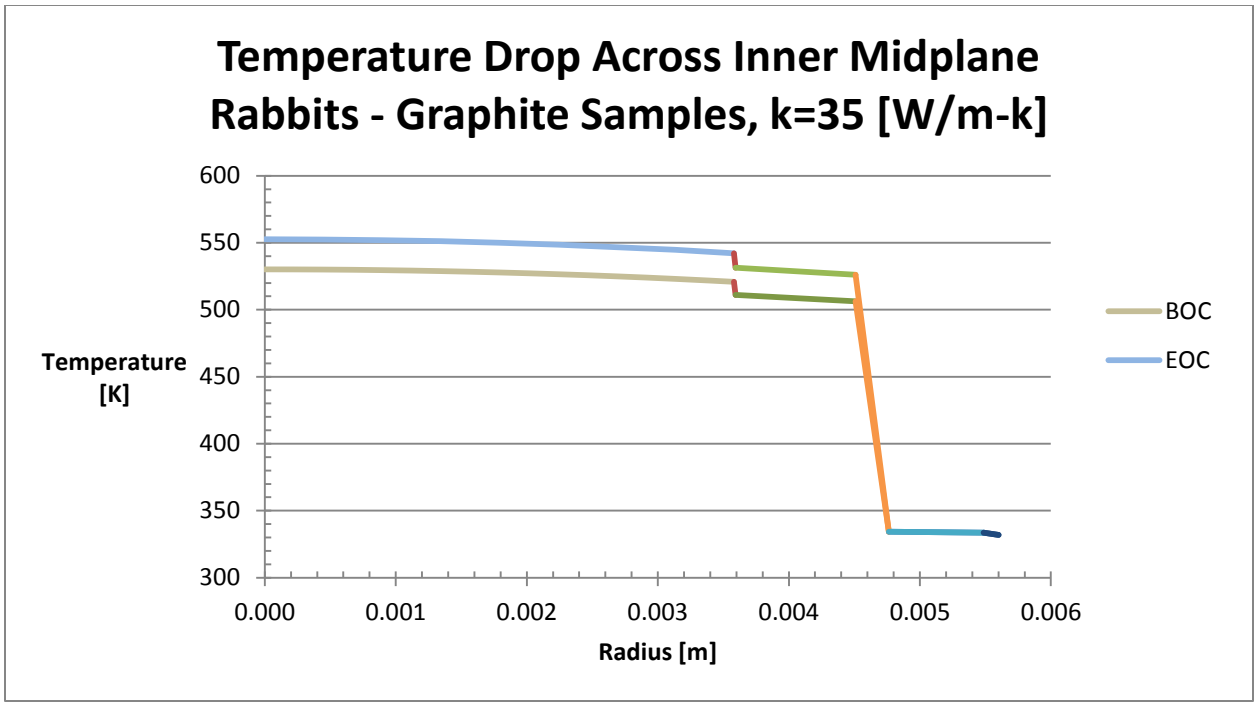

Fig. 24. Thermal profile of a rabbit with graphite samples. A graphite thermal conductivity of 35 W/m–K was assumed.

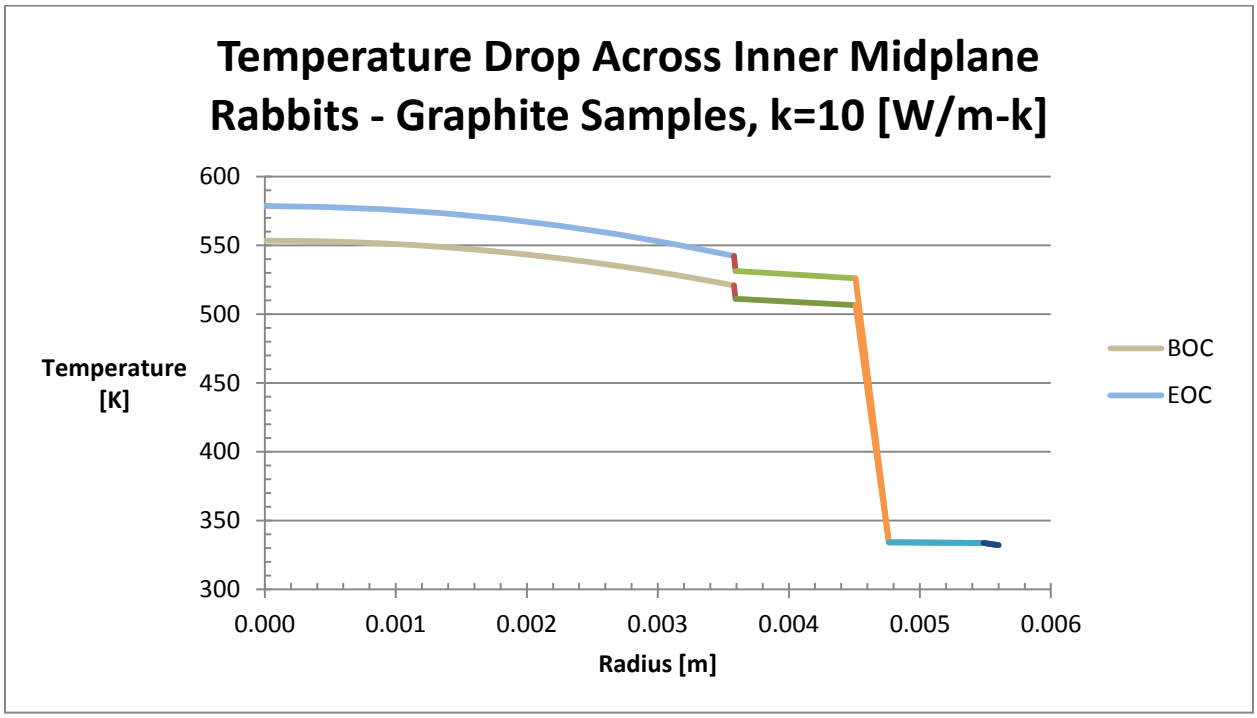

Fig. 25. Thermal profile of a rabbit with graphite samples. A graphite thermal conductivity of 10 W/m–K was assumed.

These temperature profiles show that a rabbit with graphite samples will experience a centerline temperature drift of about 10K – 25 K during the course of the cycle, while a steel sample will experience a drift of approximately 50 K.

Recognizing that the thermal conductivities of the capsule materials are high, and that the capsules themselves are thin, the thermal profiles across both aluminum and vanadium are likely flat, even when considering their internal heat generation; therefore, this model should still give a reasonably accurate centerline temperature.

It is important to note that, because of the lower heat generation rate than the model given in Section 2.2, the centerline temperature is also correspondingly lower. Additionally, these heat generation rates were taken for the hottest rabbit in the assembly; for other rabbits, the centerline temperature will be correspondingly lower (see Table 5).

5. SYSTEM VARIATION STUDIES ON STEEL SAMPLE, BOC CASE

After varying sample material and point in cycle, variations on system geometry were conducted. Using the BOC steel sample model as a starting point, the following variations were explored:

- Two extrusion assemblies, placed in the RB*–3B and RB*–7B positions (opposite positions, see Figure 26)
- Two extrusion assemblies, placed in the RB*–7A and RB*–7B positions (adjacent positions, see Figure 26)
- One extrusion assembly, placed in the RB*–7B position, with four rabbit channels removed (assembly diagram shown in Figure 27)

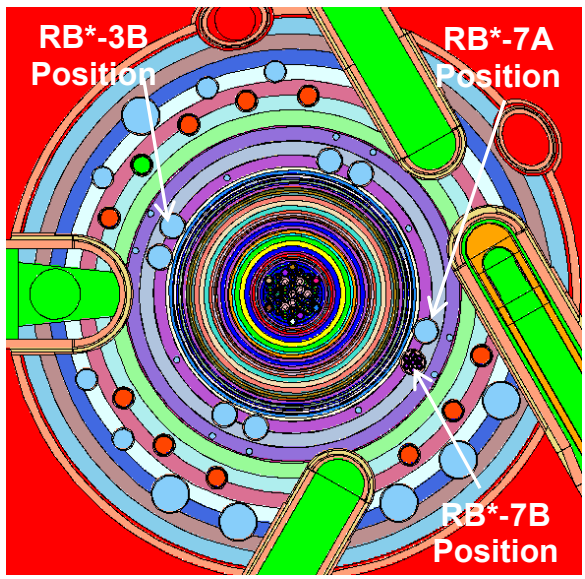

Fig. 26. HFIR cross–sectional view, showing the RB*–7B, –3B, and –7A positions

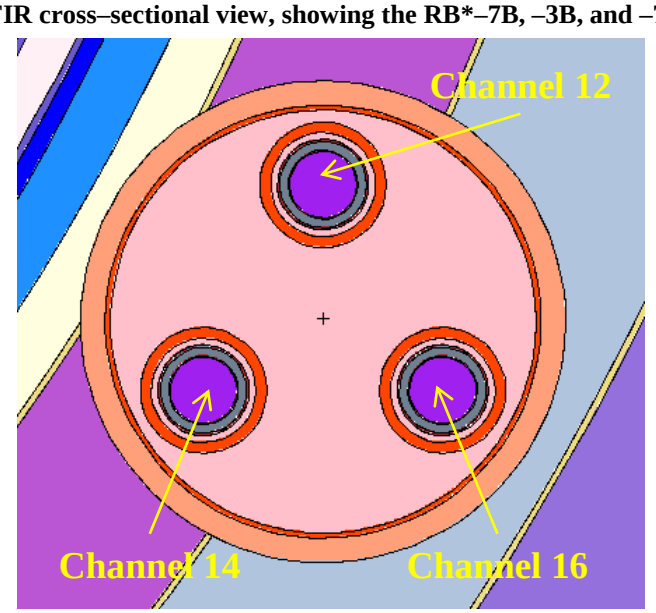

Fig. 27. Cross–sectional view of three-channel rabbit assembly

5.1 VARIATIONS IN HEAT GENERATION RATES

5.1.1 Seven–Channel Cases

Figure 28 shows the heat generation rate in samples in the center channels of each assembly for each configuration discussed above.

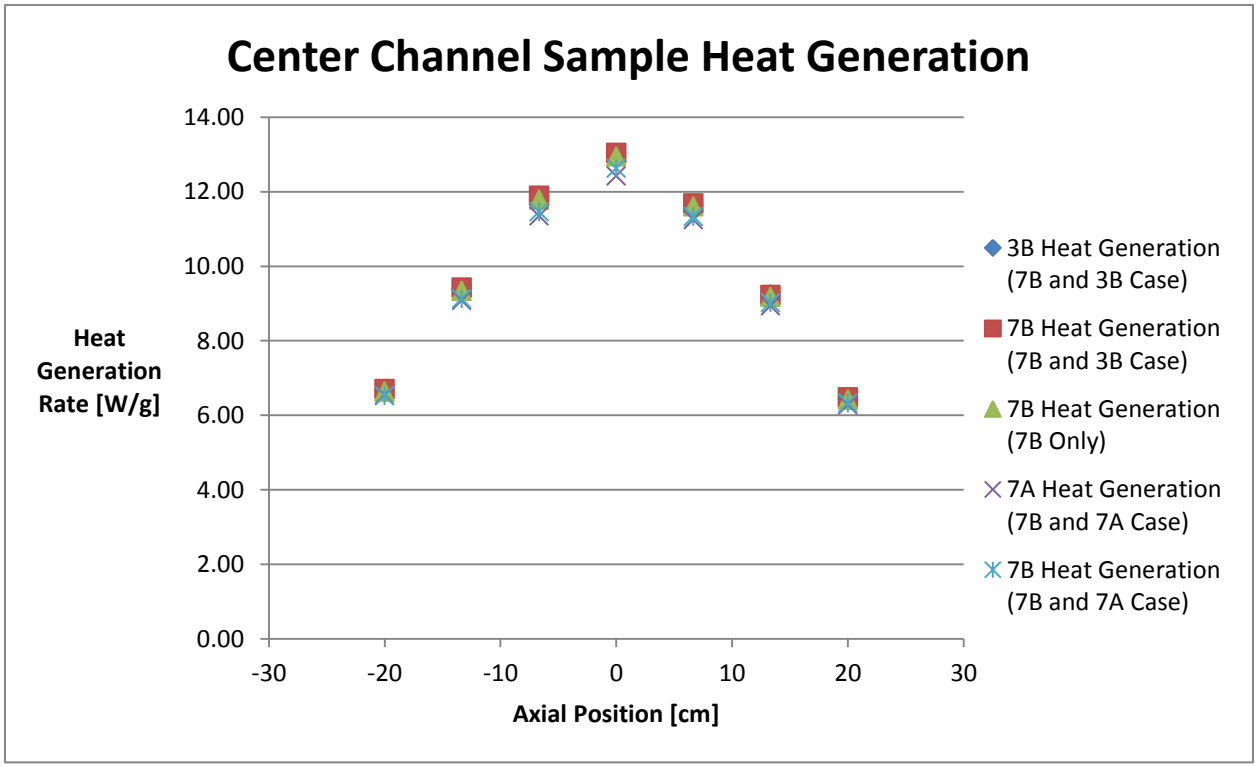

Fig. 28. Axial heat generation profile for samples located in the center channel of each assembly for the seven–channel, steel sample, BOC configurations

This data shows that the placement of a second assembly determines the effect on heat generation rates. When two assemblies are placed in opposite positions, heat generation rates hardly differ from the case of a single assembly; when two assemblies are placed in adjacent positions, however, there is a slight (4% at most) decrease in heat generation rates in corresponding sample positions.

As will be shown in Sections 5.2.1 and 5.3, the number and position of assemblies has a more significant effect on both neutron flux and criticality values, making changes in heat generation a small concern by comparison.

5.1.2 Three-Channel Case

Table 8 shows data for the heat generation rates for each material in the center channel of the three-assembly case.

Table 8 – Heat Generation Rates for Materials in Three-Channel Assemblies

Axial Position [cm]	Channel 12 Heat Generation Rates [W/g]			Channel 14 Heat Generation Rates [W/g]			Channel 16 Heat Generation Rates [W/g]			Assembly Heat Generation Rates [W/g]	
	Steel	V4Cr4Ti	Al6061 Housing	Steel	V4Cr4Ti	Al6061 Housing	Steel	V4Cr4Ti	Al6061 Housing	Water	Al6061 Extrusion
-24.61										6.30	3.26
-20.00	6.68	8.37	5.45	6.73	8.45	5.51	5.85	7.37	4.56	9.82	4.93
-13.34	9.36	11.71	7.68	9.37	11.75	7.70	8.06	10.07	6.27	13.07	6.88
-6.67	11.77	14.63	9.53	11.95	14.77	9.63	9.98	12.35	7.67	16.27	8.56
0.00	13.10	16.09	10.44	13.19	16.24	10.50	10.87	13.33	8.26	17.74	9.38
6.67	11.73	14.36	9.57	11.76	14.45	9.63	9.85	12.06	7.62	16.56	8.67
13.34	9.28	11.32	7.68	9.33	11.39	7.68	7.95	9.68	6.17	13.55	6.98
20.00	6.52	7.93	5.38	6.50	7.99	5.42	5.68	6.99	4.47	9.63	4.99
24.61										6.37	3.31

Channel 16 is in the same location as the outer channel of the seven–channel case, making direct comparison possible; values of heat generation rates for this channel in both the three-channel and seven–channel cases are given in Table 9.

Table 9 – Comparison of Outer Channel Heat Generation Rates for Three-Channel and Seven–Channel Cases

	Steel Heat Generation Rates [W/g]		V4Cr4Ti Heat Generation Rates [W/g]		Al6061 Heat Generation Rates [W/g]	
Axial Position [cm]	**Seven–Channel Case**	**Three-Channel Case**	**Seven–Channel Case**	**Three-Channel Case**	**Seven–Channel Case**	**Three-Channel Case**
-20.0025	6.06	5.85	7.62	7.37	4.83	4.56
0	11.14	10.87	13.75	13.33	8.79	8.26
20.0025	5.91	5.68	7.24	6.99	4.68	4.47

5.2 VARIATIONS IN NEUTRON FLUX

5.2.1 Seven–Channel Cases

Table 10 contains midplane flux data for the cases with two seven–channel assemblies; for comparison, the data for the BOC steel sample model (with one assembly) is also provided.

This data shows that the placement of a second assembly determines the effect on neutron flux through samples. When two assemblies are placed in opposite positions, flux values hardly differ from the case of a single assembly; when two assemblies are placed in adjacent positions, however, there is a slight (8%) decrease in neutron flux through corresponding sample positions. Opposite placement of two assemblies is therefore optimal if high neutron flux is the primary objective.

Table 10 – Midplane Neutron Flux for Seven–Channel Assemblies

		Inner Channel			Center Channel			Outer Channel		
Case	Position	**Total**	**Fast**	**Thermal**	**Total**	**Fast**	**Thermal**	**Total**	**Fast**	**Thermal**
7B Only	7B	1.83E+15	6.30E+14	5.55E+14	1.62E+15	5.10E+14	5.45E+14	1.51E+15	4.21E+14	5.85E+14
3B and 7B	7B	1.84E+15	6.37E+14	5.59E+14	1.63E+15	5.12E+14	5.49E+14	1.53E+15	4.24E+14	5.90E+14
	3B	1.84E+15	6.37E+14	5.57E+14	1.64E+15	5.14E+14	5.48E+14	1.53E+15	4.23E+14	5.91E+14
7A and 7B	7B	1.74E+15	6.15E+14	5.10E+14	1.54E+15	4.97E+14	5.01E+14	1.44E+15	4.09E+14	5.41E+14
	7A	1.73E+15	6.14E+14	5.01E+14	1.53E+15	4.95E+14	4.87E+14	1.41E+15	4.09E+14	5.20E+14

Additionally, the RB*–7A position experiences neutron flux lower than that in the RB*–7B position, particularly in the thermal spectrum; this is most likely due to its closer proximity to a beam–line tube, which would draw thermal neutrons away rather than reflect them back (as beryllium would in its place).

5.2.2 Three-Channel Case

Table 11 shows the data for the neutron flux through each rabbit for the three-channel case.

Table 11 – Neutron Flux for Three-Channel Assembly

	Channel 12			Channel 14			Channel 16		
Axial Position [cm]	**Total**	**Fast**	**Thermal**	**Total**	**Fast**	**Thermal**	**Total**	**Fast**	**Thermal**
-20.0025	8.91E+14	3.04E+14	2.86E+14	8.96E+14	3.03E+14	2.89E+14	8.37E+14	2.35E+14	3.22E+14
-13.335	1.32E+15	4.42E+14	4.33E+14	1.33E+15	4.40E+14	4.37E+14	1.21E+15	3.40E+14	4.62E+14
-6.6675	1.67E+15	5.47E+14	5.63E+14	1.68E+15	5.48E+14	5.71E+14	1.51E+15	4.19E+14	5.86E+14
0	1.83E+15	5.95E+14	6.14E+14	1.83E+15	5.95E+14	6.21E+14	1.63E+15	4.54E+14	6.29E+14
6.6675	1.64E+15	5.58E+14	5.25E+14	1.65E+15	5.60E+14	5.31E+14	1.50E+15	4.29E+14	5.61E+14
13.335	1.30E+15	4.60E+14	3.85E+14	1.31E+15	4.65E+14	3.90E+14	1.20E+15	3.56E+14	4.24E+14
20.0025	8.62E+14	3.24E+14	2.30E+14	8.64E+14	3.25E+14	2.31E+14	8.15E+14	2.53E+14	2.77E+14

Channel 16 is in the same location as the outer channel of the seven–channel case, making direct comparison possible; this is given in Table 12.

Table 12 – Comparison of Outer Channel Flux Values for Three-Channel and Seven–Channel Cases

	Total Flux		Fast Flux		Thermal Flux	
Axial Position [cm]	**Seven–Channel Case**	**Three-Channel Case**	**Seven–Channel Case**	**Three-Channel Case**	**Seven–Channel Case**	**Three-Channel Case**
-20.0025	7.82 E+14	8.37E+14	2.16E+14	2.35E+14	3.10E+14	3.22E+14
0	1.51E+15	1.63E+15	4.21E+14	4.54E+14	5.85E+14	6.29E+14
20.0025	7.74E+14	8.15E+14	2.32E+14	2.53E+14	2.76E+14	2.77E+14

The data in Table 12 shows that flux is higher in the three-channel case than the seven channel case. Fast flux is about 8% higher in all three-channel assembly positions. Additionally, the three-channel case thermal flux profile has a larger axial peaking factor than the seven–channel case.

5.3 VARIATIONS IN CRITICALITY

Table 12 shows a comparison between each BOC steel sample case with the standard case of a beryllium plug.

Table 13 – BOC Steel System Variations and Effects on Criticality

Case	Reactivity k_{eff}			Δk_{eff}			$\Delta\rho$ (cents) (if β = 0.0076)
Steel, 7B Only	1.01606	±	0.00003	0.00165	±	4.2E-05	21.00
Empty (Be Plug)	1.01771	±	0.00003				
Steel, 3B and 7B	1.01446	±	0.00003	0.00325	±	4.2E-05	41.42
Empty (Be Plug)	1.01771	±	0.00003				
Steel, 7A–7B	1.01468	±	0.00003	0.00303	±	4.2E-05	38.61
Empty (Be Plug)	1.01771	±	0.00003				
Steel, 7B, Three Channel	1.01643	±	0.00003	0.00128	±	4.2E-05	16.28
Empty (Be Plug)	1.01771	±	0.00003				

The data above shows that the location of a second assembly changes the effect that it would have on reactivity. Loading a second assembly opposite the first shows a linear decrease in reactivity; loading a second assembly adjacent the first shows a slightly sub–linear decrease in reactivity. Adjacent placement of two assemblies is therefore optimal if longer cycle time is the primary objective.

It is also clear that decreasing the number of samples will also extend cycle time, but the effect is not linear in the number of samples. This is most likely because the samples are being replaced with aluminum, and not beryllium, which is the predominant material in the empty case.

6. FUTURE DESIGN AND ANALYSIS RECOMMENDATIONS

The following refinements are suggested to improve either the analysis or the design of the irradiation concept.

6.1 REACTIVITY WORTH OF ASSEMBLY

The worth of one assembly of rabbits (49) in the RB* position at BOC was determined to be -21.0 cents for steel samples and -18.2 cents for graphite samples. The reduction is due to the substitution of the beryllium plug that is normally in the RB* position with the aluminum basket and rabbits. The influence of the rabbits is shown in Section 5.3 by comparing the cases of 3 vs. 7 channels for rabbits (21 vs. 49 rabbits). Reducing the number of rabbits by more than half only reduced the worth by 22.5%. An estimate of the reactivity worth of the holder in lieu of the beryllium plug can be made by extrapolating the two cases analyzed (7 channels and 3 channels) to the case of 0 channels. In doing so, the worth of the aluminum basket, in lieu of the beryllium plug, is approximately -12.7 cents.

A few options have been identified for possible future exploration as means to reduce the impact of the test setup on the core reactivity.

- The holder could be made of a different material.
    - If the holder was instead made of beryllium, one could expect the impact on reactivity to be reduced by nearly 12.7 cents. The holder could be made of an aluminum–beryllium alloy. An alloy of 62% Be and 38% Al, such as that manufactured by Materion, could possibly reduce the impact on reactivity by approximately 7.9 cents.
    - To avoid using Beryllium, the channels for the rabbits could be made of an array of tubes welded together. This would substitute much of the aluminum basket for water. A new design would need to be developed to limit the flow of primary water.
- Rods of material could be inserted into empty channels in the aluminum basket.
    - Beryllium could be inserted into some of the channels. If Be (or Be alloy) rod stock could be used, this could avoid purchasing a uniquely machined Be (or Be alloy) holder. Placing Be rods into 4 of the channels, leaving 3 channels for rabbits (21 rabbits) could reduce the worth of the assembly to roughly -12 cents (for BOC steel).
    - Alternatively, the primary water could fill the channels. This could require different orificing of the channels to limit the flow through the empty channels.

6.2 NEUTRON FLUX AND SPECTRUM

The possible system configuration changes noted above may have minor impacts on the neutron flux as well as the neutron energy spectrum in the rabbits. Including more moderating materials around the

samples (Be, water) may slightly alter the fast flux to thermal flux ratio in the sample. Having less neutron absorbing material around the samples may slightly increase the total flux.

6.3 SAMPLE TEMPERATURE DRIFT OVER THE CYCLE

Heating due to energy deposition from gammas and neutrons increase over the cycle, resulting in higher sample temperatures towards the end of cycle. For the central stainless steel sample, the BOC and EOC predicted sample centerline temperatures were 710 K and 764 K, respectively. This is a 7.6% increase in material temperature over the course of the cycle (12.4% if units of Celsius are used).

The thermal analysis presented in Section 4.4 used constant material properties for Helium. However, the thermal conductivity of He increases with temperature (as well as for steel, vanadium, and aluminum; whereas, the thermal conductivity decreases with temperature for graphite). The increase in He thermal conductivity with temperature helps limit the temperature drift over the cycle.

Three additional phenomena were also not accounted for in the analyses in Section 4.4. First, the dose to the materials decreases the thermal conductivity of the solid materials. This would tend to increase sample temperatures over the cycle. Thermal expansion of the materials would impact the gas gap size. As the gas gap largely determines the sample temperature, changes to the gap size over the cycle has an important impact on the sample temperature. Finally, thermal radiation across the gas gap was neglected. The increase in sample temperature over the cycle length would be slightly mitigated by an increase in thermal radiation heat transfer across the gap.

An additional analysis was performed that took into account the thermal conductivity variation in temperature for the stainless steel sample and the helium as well as the thermal radiation heat transport across the gap. For the central stainless steel sample, the BOC and EOC predicted sample centerline temperatures were 722 K and 769 K, respectively. This is a 6.5% increase in material temperature over the course of the cycle (compared to 7.6% increase for the analyses presented in Section 4.4). Additional analyses are recommended that account for thermal expansion and thermal radiation and use more accurate thermo–physical properties.

The thermal analysis in Section 4.4 also utilized multipliers to account for fission product photon energy deposition in the samples as described in Section 3.7.1.5. More accurate modeling and determination of the energy deposition rates in the samples due to photons could be pursued.

7. CONCLUSIONS

Analysis of the data gathered from these models supports further exploration into the idea of irradiating rabbits in the RB* positions of HFIR. Heat generation rates for all materials are in line with what was expected, approximately a third of those in the flux trap. Neutron flux is still very high in this region; a graphite sample placed in the center of the holder would experience an average neutron flux of 1.88×10^{15} n/cm^2–sec over the life of the core, while a steel sample in the same position would experience a neutron flux of 1.69×10^{15} n/cm^2–sec. The overall effect on core reactivity from the insertion of one of these assemblies is small, and would not significantly impact core lifetime.

Before an assembly is built, however, it is recommended that the assumptions made in this study be verified through more accurate models. In particular, this study recommends that the assumption of similar ratios of gamma heating by fission photons and fission product photons between flux trap and reflector regions be verified by implementing a SCALE model. While this seems to be a reasonable assumption to make, further study in this area would be useful. In addition, additional areas for design and analysis refinement were identified. These should be considered in the future development of this concept.

8. REFERENCES

1. Oak Ridge National Laboratory. *High Flux Isotope Reactor User Guide*. Oak Ridge, TN, May 2011.

2. White, Frank M. *Fluid Mechanics, 5th Edition*. McGraw–Hill: 2002.

3. Incropera and DeWitt. *Fundamentals of Heat and Mass Transfer, 5th Edition.* Wiley: 2001.

4. El–Wakil, M. M. *Nuclear Heat Transport*. American Nuclear Society: 1981.

5. Xoubi, N and Primm, T. *HFIR Model version 4.0 (HFV4.0+).* Retrieved from http://neutrons.ornl.gov/facilities/HFIR/data/, June 2013.

6. McDuffee, Joel. *Heat Generation Rates for Various Rabbit Materials in the Flux Trap of HFIR.* Thermal Hydraulics and Irradiation Group, 2012.

7. Primm, R. T. *Reactor Physics Studies of Reduced–Tantalum–Content Control and Safety Elements for the High Flux Isotope Reactor*. Oak Ridge National Laboratory, 2004.

8. Matweb. *Material Properties.* Retrieved from http://www.matweb.com.

9. MCNP, version 5. Los Alamos National Laboratory, 2003.

APPENDIX A. MCNP MODEL

A–1 GENERIC MODIFICATIONS

```
c ==========================================================================================
c
c (1) Removed reference to xsdir68, used default cross section libraries
c (2) Changed mode and correspondent importances from 'mode n' to 'mode n p'
c (3) Changed definition of RB* liners 7A and 7B to match the radii of all other RB*
c      Liner outer diameter, OD = 5.1816cm,  OD = 2.040"
c      Liner inner diameter, ID = 4.65836cm, OD = 1.834"
c (4) Removed Eu plugs from RB* 7A and 7B, deleted Eu material cards m38 and m39
c (5) Filled all RB* positions with Be plugs (m33), except when rabbits where loaded
c     in RB*-7B
c
c ==========================================================================================

c          RB-7A
6900 32    cz   2.59080    $ liner OD
6901 32    cz   2.32918    $ liner ID

c          RB-7B
6950 33    cz   2.59080    $ liner OD
6951 33    cz   2.32918    $ liner ID
```

A–2 ADDITIONS TO MODEL EXPERIMENT

```
c ******************************************************************************************
c ******************************************************************************************
c ************************************** Begin Extrusion ******************************
c
1  900 -2.70    -1 #10 #11 #12 #13 #14 #15 #16     vol= 363.07 imp:n,p=1   $ Extrusion
10 900 -2.70    -2                          fill= 1     imp:n,p=1  $ Center Channel
2    9 -0.98465 #24 69208 #34 69308 #44 69408 #54 69508
            #64 69608 #74 69708 #84 69808 u=1 vol= 279.73 imp:n,p=1 $ Coolant
c
c ******************************************************************************************
c     The following creates a hexagonal lattice based upon the center channel window
c ******************************************************************************************
c ------------------------------------ Begin Lattice --------------------------------
11 like 10 but trcl ( 1.277478  0.737552 0)                                    $ Holder at  30°
12 like 10 but trcl ( 0         1.475105 0)                              $ Holder at  90°
13 like 10 but trcl (-1.277478  0.737552 0)                                  $ Holder at 150°
14 like 10 but trcl (-1.277478 -0.737552 0)                                     $ Holder at 210°
15 like 10 but trcl ( 0                -1.475105 0)                                $ Holder at 270°
16 like 10 but trcl ( 1.277478 -0.737552 0)                                    $ Holder at 330°
c ------------------------------------ End Lattice ----------------------------------
c
c
c ******************************************************************************************
c  Seven rabbits are defined below that reproduce a total of 49 rabbits. The cells are
c  numbered from bottom to top starting from cells 20 to 80, where cell 50 corresponds
c  to the rabbit centered at mid-core height.
c ******************************************************************************************
c ------------------------------ Start of (20 level) rabbit -------------------------
20 901 -7.87    -69200              u=1 imp:n,p=1   $ Sample (Stainless Steel) Volume
21 902 -1.64e-4 -69201 69200        u=1 imp:n,p=1   $ He Gas Layer 1 Volume
22 903 -6.05     69200 69201 -69202 :(-69203 69204):(-69205 69206) u=1 imp:n,p=1   $ V
```

```
23 902 -1.64e-4 -69207 #22 #21 #20   u=1 imp:n,p=1   $ He Gas Layer 2 Volume
24 900 -2.70    -69208 69207 : (-69209 69210)            u=1 imp:n,p=1   $ Al Volume
c -------------------------------- End of (20 level) rabbit -------------------------
c
c ------------------------------ Start of (30 level) rabbit -------------------------
30 901 -7.87    -69300              u=1 imp:n,p=1   $ Sample (Stainless Steel) Volume
31 902 -1.64e-4 -69301 69300        u=1 imp:n,p=1   $ He Gas Layer 1 Volume
32 903 -6.05     69300 69301 -69302 :(-69303 69304):(-69305 69306) u=1 imp:n,p=1   $ V
33 902 -1.64e-4 -69307 #32 #31 #30   u=1 imp:n,p=1   $ He Gas Layer 2 Volume
34 900 -2.70    -69308 69307 : (-69309 69310)            u=1 imp:n,p=1   $ Al Volume
c -------------------------------- End of (30 level) rabbit -------------------------
c
c ------------------------------ Start of (40 level) rabbit -------------------------
40 901 -7.87    -69400              u=1 imp:n,p=1   $ Sample (Stainless Steel) Volume
41 902 -1.64e-4 -69401 69400        u=1 imp:n,p=1   $ He Gas Layer 1 Volume
42 903 -6.05     69400 69401 -69402 :(-69403 69404):(-69405 69406) u=1 imp:n,p=1   $ V
43 902 -1.64e-4 -69407 #42 #41 #40  u=1 imp:n,p=1   $ He Gas Layer 2 Volume
44 900 -2.70    -69408 69407 : (-69409 69410)                        u=1 imp:n,p=1   $ Al
c -------------------------------- End of (40 level) rabbit -------------------------
c
c ============================== Start of (50 level) rabbit ==========================
50 901 -7.87    -69500              u=1 imp:n,p=1   $ Sample (Stainless Steel) Volume
61 902 -1.64e-4 -69501 69500        u=1 imp:n,p=1   $ He Gas Layer 1 Volume
62 903 -6.05     69500 69501 -69502 :(-69503 69504):(-69505 69506) u=1 imp:n,p=1   $ V
63 902 -1.64e-4 -69507 #52 #51 #50  u=1 imp:n,p=1   $ He Gas Layer 2 Volume
64 900 -2.70    -69508 69507 : (-69509 69510)                        u=1 imp:n,p=1   $ Al
c ================================ End of (50 level) rabbit ==========================
c
c ------------------------------ Start of (60 level) rabbit -------------------------
60 901 -7.87    -69600              u=1 imp:n,p=1   $ Sample (Stainless Steel) Volume
61 902 -1.64e-4 -69601 69600        u=1 imp:n,p=1   $ He Gas Layer 1 Volume
62 903 -6.05     69600 69601 -69602 :(-69603 69604):(-69605 69606) u=1 imp:n,p=1   $ V
63 902 -1.64e-4 -69607 #62 #61 #60  u=1 imp:n,p=1   $ He Gas Layer 2 Volume
64 900 -2.70    -69608 69607 : (-69609 69610)                        u=1 imp:n,p=1   $ Al
c -------------------------------- End of (60 level) rabbit -------------------------
c
c ------------------------------ Start of (70 level) rabbit -------------------------
70 901 -7.87    -69700              u=1 imp:n,p=1   $ Sample (Stainless Steel) Volume
71 902 -1.64e-4 -69701 69700        u=1 imp:n,p=1   $ He Gas Layer 1 Volume
72 903 -6.05     69700 69701 -69702 :(-69703 69704):(-69705 69706) u=1 imp:n,p=1   $ V
73 902 -1.64e-4 -69707 #72 #71 #70  u=1 imp:n,p=1   $ He Gas Layer 2 Volume
74 900 -2.70    -69708 69707 : (-69709 69710)                        u=1 imp:n,p=1   $ Al
c -------------------------------- End of (70 level) rabbit -------------------------
c
c ------------------------------ Start of (80 level) rabbit -------------------------
80 901 -7.87    -69800              u=1 imp:n,p=1   $ Sample (Stainless Steel) Volume
81 902 -1.64e-4 -69801 69800        u=1 imp:n,p=1   $ He Gas Layer 1 Volume
82 903 -6.05     69800 69801 -69802 :(-69803 69804):(-69805 69806) u=1 imp:n,p=1   $ V
83 902 -1.64e-4 -69807 #82 #81 #80  u=1 imp:n,p=1   $ He Gas Layer 2 Volume
84 900 -2.70    -69808 69807 : (-69809 69810)                        u=1 imp:n,p=1   $ Al
c -------------------------------- End of (80 level) rabbit -------------------------
c
c
c ************************************* End Extrusion ********************************
c ****************************************************************************************
c ****************************************************************************************
c

c Surface Cards
c ****************************************************************************************
c ****************************************************************************************
c ********************************** Begin Extrusion ************************************
```

```
1 rcc 23.765062 -13.445625 -29.21  0 0 58.42  2.27457  $ Extrusion(L= 23", r= 0.8955")
2 rcc 23.765062 -13.445625 -29.21  0 0 58.42  0.67564  $ Coolant  (L= 23", r= 0.2660")
c ********************************** End Extrusion **********************************

c ******************************************************************************************
c    Seven rabbits are defined below. The surfaces are numbered from bottom to top
c    starting from cells 69200 to 69800, where level 69500 corresponds to the rabbit
c    centered at the origin. All rabbits have the same geometry, they only differ in
c    their location about the axial (z-axis)
c ******************************************************************************************
c
c ----------------------------- Start of (200 level) rabbit -------------------------
69200 rcc 23.765062 -13.445625 -22.25294 0 0 4.50088 0.35814  $ Sample Surface
69201 rcc 23.765062 -13.445625 -22.25294 0 0 5.10032 0.37084  $ Gas Layer 1 Surface
69202 rcc 23.765062 -13.445625 -22.30628 0 0 5.20700 0.46228  $ Vanadium Surface
69203 rcc 23.765062 -13.445625 -17.09928 0 0 0.25400 0.46228  $ V Top Flange Outer
69204 rcc 23.765062 -13.445625 -17.09928 0 0 0.25400 0.37084  $ V Top Flange Inner
69205 rcc 23.765062 -13.445625 -22.56028 0 0 0.25400 0.46228  $ V Botom Flange Outer
69206 rcc 23.765062 -13.445625 -22.56028 0 0 0.25400 0.37084  $ V Botom Flange Inner
69207 rcc 23.765062 -13.445625 -22.56028 0 0 5.88010 0.48768  $ Gas Layer 2 Surface
69208 rcc 23.765062 -13.445625 -22.99208 0 0 6.60400 0.56007  $ Al Layer (R = 0.2205")
69209 rcc 23.765062 -13.445625 -16.38808 0 0 0.06350 0.56007  $ Al Flange Outer
69210 rcc 23.765062 -13.445625 -16.38808 0 0 0.06350 0.48768  $ Al Flange Inner
c ---------------------------------- End of (200 level) rabbit -----------------------
c
c ------------------------------- Start of (300 level) rabbit -----------------------
69300 rcc 23.765062 -13.445625 -15.58544 0 0 4.50088 0.35814  $ Sample Surface
69301 rcc 23.765062 -13.445625 -15.58544 0 0 5.10032 0.37084  $ Gas Layer 1 Surface
69302 rcc 23.765062 -13.445625 -15.63878 0 0 5.20700 0.46228  $ Vanadium Surface
69303 rcc 23.765062 -13.445625 -10.43178 0 0 0.25400 0.46228  $ V Top Flange Outer
69304 rcc 23.765062 -13.445625 -10.43178 0 0 0.25400 0.37084  $ V Top Flange Inner
69305 rcc 23.765062 -13.445625 -15.89278 0 0 0.25400 0.46228  $ V Botom Flange Outer
69306 rcc 23.765062 -13.445625 -15.89278 0 0 0.25400 0.37084  $ V Botom Flange Inner
69307 rcc 23.765062 -13.445625 -15.89278 0 0 5.88010 0.48768  $ Gas Layer 2 Surface
69308 rcc 23.765062 -13.445625 -16.32458 0 0 6.60400 0.56007  $ Al Layer (R = 0.2205")
69309 rcc 23.765062 -13.445625 -9.720580 0 0 0.06350 0.56007  $ Al Flange Outer
69310 rcc 23.765062 -13.445625 -9.720580 0 0 0.06350 0.48768  $ Al Flange Inner
c ---------------------------------- End of (300 level) rabbit -----------------------
c
c ------------------------------- Start of (400 level) rabbit -----------------------
69400 rcc 23.765062 -13.445625 -8.917940 0 0 4.50088 0.35814  $ Sample Surface
69401 rcc 23.765062 -13.445625 -8.917940 0 0 5.10032 0.37084  $ Gas Layer 1 Surface
69402 rcc 23.765062 -13.445625 -8.971280 0 0 5.20700 0.46228  $ Vanadium Surface
69403 rcc 23.765062 -13.445625 -3.764280 0 0 0.25400 0.46228  $ V Top Flange Outer
69404 rcc 23.765062 -13.445625 -3.764280 0 0 0.25400 0.37084  $ V Top Flange Inner
69405 rcc 23.765062 -13.445625 -9.225280 0 0 0.25400 0.46228  $ V Botom Flange Outer
69406 rcc 23.765062 -13.445625 -9.225280 0 0 0.25400 0.37084  $ V Botom Flange Inner
69407 rcc 23.765062 -13.445625 -9.225280 0 0 5.88010 0.48768  $ Gas Layer 2 Surface
69408 rcc 23.765062 -13.445625 -9.657080 0 0 6.60400 0.56007  $ Al Layer (R = 0.2205")
69409 rcc 23.765062 -13.445625 -3.053080 0 0 0.06350 0.56007  $ Al Flange Outer
69410 rcc 23.765062 -13.445625 -3.053080 0 0 0.06350 0.48768  $ Al Flange Inner
c ---------------------------------- End of (400 level) rabbit -----------------------
c
c ============================= Start of (500 level) rabbit =========================
69500 rcc 23.765062 -13.445625 -2.250440 0 0 4.50088 0.35814  $ Sample Surface
69501 rcc 23.765062 -13.445625 -2.250440 0 0 5.10032 0.37084  $ Gas Layer 1 Surface
69502 rcc 23.765062 -13.445625 -2.303780 0 0 5.20700 0.46228  $ Vanadium Surface
69503 rcc 23.765062 -13.445625  2.903220 0 0 0.25400 0.46228  $ V Top Flange Outer
69504 rcc 23.765062 -13.445625  2.903320 0 0 0.25400 0.37084  $ V Top Flange Inner
69505 rcc 23.765062 -13.445625 -2.557780 0 0 0.25400 0.46228  $ V Botom Flange Outer
69506 rcc 23.765062 -13.445625 -2.557780 0 0 0.25400 0.37084  $ V Botom Flange Inner
69507 rcc 23.765062 -13.445625 -2.557780 0 0 5.88010 0.48768  $ Gas Layer 2 Surface
```

```
69508 rcc 23.765062 -13.445625 -2.989580 0 0 6.60400 0.56007  $ Al Layer (R = 0.2205")
69509 rcc 23.765062 -13.445625  3.614420 0 0 0.06350 0.56007  $ Al Flange Outer
69510 rcc 23.765062 -13.445625  3.614420 0 0 0.06350 0.48768  $ Al Flange Inner
c ================================ End of (500 level) rabbit ==========================
c
c ------------------------------- Start of (600 level) rabbit -----------------------
69600 rcc 23.765062 -13.445625  4.417060 0 0 4.50088 0.35814  $ Sample Surface
69601 rcc 23.765062 -13.445625  4.417060 0 0 5.10032 0.37084  $ Gas Layer 1 Surface
69602 rcc 23.765062 -13.445625  4.363720 0 0 5.20700 0.46228  $ Vanadium Surface
69603 rcc 23.765062 -13.445625  9.570720 0 0 0.25400 0.46228  $ V Top Flange Outer
69604 rcc 23.765062 -13.445625  9.570720 0 0 0.25400 0.37084  $ V Top Flange Inner
69605 rcc 23.765062 -13.445625  4.109720 0 0 0.25400 0.46228  $ V Botom Flange Outer
69606 rcc 23.765062 -13.445625  4.109720 0 0 0.25400 0.37084  $ V Botom Flange Inner
69607 rcc 23.765062 -13.445625  4.109720 0 0 5.88010 0.48768  $ Gas Layer 2 Surface
69608 rcc 23.765062 -13.445625  3.677920 0 0 6.60400 0.56007  $ Al Layer (R = 0.2205")
69609 rcc 23.765062 -13.445625  10.28190 0 0 0.06350 0.56007  $ Al Flange Outer
69610 rcc 23.765062 -13.445625  10.28190 0 0 0.06350 0.48768  $ Al Flange Inner
c ---------------------------------- End of (600 level) rabbit -----------------------
c
c ------------------------------- Start of (700 level) rabbit -----------------------
69700 rcc 23.765062 -13.445625 11.084560 0 0 4.50088 0.35814  $ Sample Surface
69701 rcc 23.765062 -13.445625 11.084560 0 0 5.10032 0.37084  $ Gas Layer 1 Surface
69702 rcc 23.765062 -13.445625 11.031220 0 0 5.20700 0.46228  $ Vanadium Surface
69703 rcc 23.765062 -13.445625 16.238220 0 0 0.25400 0.46228  $ V Top Flange Outer
69704 rcc 23.765062 -13.445625 16.238220 0 0 0.25400 0.37084  $ V Top Flange Inner
69705 rcc 23.765062 -13.445625 10.777220 0 0 0.25400 0.46228  $ V Botom Flange Outer
69706 rcc 23.765062 -13.445625 10.777220 0 0 0.25400 0.37084  $ V Botom Flange Inner
69707 rcc 23.765062 -13.445625 10.777220 0 0 5.88010 0.48768  $ Gas Layer 2 Surface
69708 rcc 23.765062 -13.445625 10.345420 0 0 6.60400 0.56007  $ Al Layer (R = 0.2205")
69709 rcc 23.765062 -13.445625 16.949420 0 0 0.06350 0.56007  $ Al Flange Outer
69710 rcc 23.765062 -13.445625 16.949420 0 0 0.06350 0.48768  $ Al Flange Inner
c ---------------------------------- End of (700 level) rabbit -----------------------
c
c ------------------------------- Start of (800 level) rabbit -----------------------
69800 rcc 23.765062 -13.445625 17.752060 0 0 4.50088 0.35814  $ Sample Surface
69801 rcc 23.765062 -13.445625 17.752060 0 0 5.10032 0.37084  $ Gas Layer 1 Surface
69802 rcc 23.765062 -13.445625 17.698720 0 0 5.20700 0.46228  $ Vanadium Surface
69803 rcc 23.765062 -13.445625 22.905720 0 0 0.25400 0.46228  $ V Top Flange Outer
69804 rcc 23.765062 -13.445625 22.905720 0 0 0.25400 0.37084  $ V Top Flange Inner
69805 rcc 23.765062 -13.445625 17.444720 0 0 0.25400 0.46228  $ V Botom Flange Outer
69806 rcc 23.765062 -13.445625 17.444720 0 0 0.25400 0.37084  $ V Botom Flange Inner
69807 rcc 23.765062 -13.445625 17.444720 0 0 5.88010 0.48768  $ Gas Layer 2 Surface
69808 rcc 23.765062 -13.445625 17.012920 0 0 6.60400 0.56007  $ Al Layer (R = 0.2205")
69809 rcc 23.765062 -13.445625 23.616920 0 0 0.06350 0.56007  $ Al Flange Outer
69810 rcc 23.765062 -13.445625 23.616920 0 0 0.06350 0.48768  $ Al Flange Inner
c ---------------------------------- End of (800 level) rabbit -----------------------
c
c ************************************** End Extrusion ********************************
c ******************************************************************************************
c ******************************************************************************************
c
```

A–3 MATERIALS DEFINITION

```
c ******************************************************************************
c ************************ New Materials Added (In Region 7B) ************************
c
c $ Al6061 Housing Material, density= 2.7 g/cm³
m900  13027 -0.9758            $ Al
     14000 -0.006      $ Si
     26000 -0.007     $ Fe
     29000 -0.00275 $ Cu
     25055 -0.0015   $ Mn
     12000 -0.001     $ Mg
     24000 -0.00195               $ Cr
     30000 -0.0025   $ Zn
     22000 -0.0015   $ Ti
c
c $ Graphite Sample, density= 1.78 g/cm³
m901  06000  1          $ C
c
c $ Natural Helium Gas, density= 1.64e-4 g/cm³
m902  02003.70c  -1.37000e-6    $ He-3
     02004.70c  -0.99999863    $ He-4
c
c $ V4Cr4Ti Holder Material, density= 6.05 g/cm³
m903  23000  -0.905             $ V
     22000  -0.047    $ Ti
     24000  -0.042    $ Cr
     26000  -0.002    $ Fe
     14000  -0.004    $ Si
c ******************************************************************************
c ******************************************************************************
```

In the case of Stainless Steel samples, material card m901 was changed to the following:

```
c $ Stainless Steel Sample, density= 7.87 g/cm³
m901  26000  -0.8956    $ Fe
     24000  -0.08      $ Cr
     74000  -0.02      $ W
     23000  -0.002     $ V
     73181  -0.0004    $ Ta
      6000  -0.001     $ C
     27059  -0.001     $ Co
```

A–4 TALLIES DEFINITION

```
c ---------------------------- Neutron Flux Tally -----------------------------------
fc4 NEUTRON TALLY FLUX IN STEEL
f4:n (20 30 40 50 60 70 80 < 10)
    (20 50 80 < 13)
    (20 50 80 < 16)      $ Center Rabbits, Lower Inner Rabbits, Upper Outer Rabbits
fm4 6.4234E+18          $ Multiplier
c
e4   3.0000E-09  7.5000E-09  1.0000E-08  2.5300E-08  3.0000E-08  4.0000E-08
    5.0000E-08  7.0000E-08  1.0000E-07  1.5000E-07  2.0000E-07  2.2500E-07
    2.5000E-07  2.7500E-07  3.3500E-07  3.5000E-07  3.7500E-07  4.0000E-07
    6.2500E-07  1.0000E-06  1.7700E-06  3.0000E-06  4.7500E-06  6.0000E-06
    8.1000E-06  1.0000E-05  3.0000E-05  1.0000E-04  5.5000E-04  3.0000E-03
    1.7000E-02  2.5000E-02  1.0000E-01  4.0000E-01  9.0000E-01  1.4000E+00
    1.8500E+00  2.3500E+00  2.4790E+00  3.0000E+00  4.8000E+00  6.4340E+00
    8.1873E+00  2.0000E+01                                          $ Energy Spectrum
c ---------------------------------------------------------------------------------
c
c
c ---------------------------------------------------------------------------------
c -------------------- Neutron Energy Deposition Tallies - Rabbit --------------------
fc6 NEUTRON ENERGY DEPOSITION IN GRAPHITE SAMPLES
f6:n  (20 30 40 50 60 70 80 < 10)
     (20 50 80 < 13)
     (20 50 80 < 16)  $ Center Rabbits, Lower Inner Rabbits, Upper Outer Rabbits fm6 1.0291E+06  $ 6.4234E+18 nf/sec *
1.6021E-13 J/MeV = 1.0291E+06 J*nf/(MeV*sec)
c
c
c
fc16 NEUTRON ENERGY DEPOSITION IN VANADIUM
f16:n (22 32 42 52 62 72 82 < 10)
     (22 52 82 < 13)
     (22 52 82 < 16) $ Center Rabbits, Lower Inner Rabbits, Upper Outer Rabbits
fm16 1.0291E+06          $ 6.4234E+18 * 1.6021E-13 = 1.0291E+06 J*nf/(MeV*sec)
c
c
fc26 NEUTRON ENERGY DEPOSITION IN ALUMINUM
f26:n (24 34 44 54 64 74 84 < 10)
     (24 54 84 < 13)
     (24 54 84 < 16) $ Center Rabbits, Lower Inner Rabbits, Upper Outer Rabbits
fm26 1.0291E+06        $ 6.4234E+18 * 1.6021E-13 = 1.0291E+06 J*nf/(MeV*sec)
c ---------------------------------------------------------------------------------
c ---------------------------------------------------------------------------------
c
c
c ---------------------------------------------------------------------------------
c ------------------- Photon Energy Deposition Tallies - Rabbit ----------------------
fc36 PHOTON ENERGY DEPOSITION IN GRAPHITE SAMPLES
f36:p (20 30 40 50 60 70 80 < 10)
     (20 50 80 < 13)
     (20 50 80 < 16) $ Center Rabbits, Lower Inner Rabbits, Upper Outer Rabbits
fm36 1.58749E+06              $ 6.4234E+18 * 1.6021E-13 * 1.5426
c
c
fc46 PHOTON ENERGY DEPOSITION IN VANADIUM
f46:p (22 32 42 52 62 72 82 < 10)
     (22 52 82 < 13)
     (22 52 82 < 16) $ Center Rabbits, Lower Inner Rabbits, Upper Outer Rabbits
fm46 2.130854E+06                        $ 6.4234E+18 * 1.6021E-13 * 2.0706
c
c
```

```
fc56 PHOTON ENERGY DEPOSITION IN ALUMINUM
f56:p (24 34 44 54 64 74 84 < 10)
     (24 54 84 < 13)
     (24 54 84 < 16) $ Center Rabbits, Lower Inner Rabbits, Upper Outer Rabbits
fm56 1.655513E+06                    $ 6.4234E+18 * 1.6021E-13 * 1.5120
c ------------------------------------------------------------------------------
c ------------------------------------------------------------------------------
c
c
c ------------------------------------------------------------------------------
c -------------- Neutron and Photon Energy Deposition Tallies - Water ----------------
fc66 NEUTRON ENERGY DEPOSITION IN WATER
f66:n 2
fs66 -10000 6i -10007                                        $ Tally split into 9 bins
fm66 1.0291E+06                                              $ 6.4234E+18 * 1.6021E-13
sd66 56.155 23.92 23.92 23.92 23.92 23.92 23.92 23.92 56.155 $ Mass
c
c
fc76 PHOTON ENERGY DEPOSITION IN WATER
f76:p 2
fs76 -10000 6i -10007                                        $ Tally split into 9 bins
fm76 1.609512E+06                                        $ 6.4234E+18 * 1.6021E-13 * 1.5640
sd76 56.155 23.92 23.92 23.92 23.92 23.92 23.92 23.92 56.155 $ Mass
c
c
c ------------------------------------------------------------------------------
c -------------- Neutron and Photon Energy Deposition Tallies - Extrusion ------------
fc86 NEUTRON ENERGY DEPOSITION IN EXTRUSION
f86:n 1
fs86 -10000 6i -10007                                        $ Tally split into 9 bins
fm86 1.0291E+06                                              $ 6.4234E+18 * 1.6021E-13
sd86 98.5613 111.8804 111.8804 111.8804 111.8804 111.8804 111.8804 111.8804 98.5613
c
c
fc96 PHOTON ENERGY DEPOSITION IN EXTRUSION
f96:p 1
fs96 -10000 6i -10007                                        $ Tally split into 9 bins
fm96 1.655513E+06                                        $ 6.4234E+18 * 1.6021E-13 * 1.6087
sd86 98.5613 111.8804 111.8804 111.8804 111.8804 111.8804 111.8804 111.8804 98.5613
c ------------------------------------------------------------------------------
c ------------------------------------------------------------------------------
c
c ******************************************************************************************
c ********************************** End Tallies ************************************
```

In the case of stainless steel samples, the neutron and photon tallies were defined as follows:

```
c -------------------- Neutron Energy Deposition Tallies - Rabbit --------------------
fc6 NEUTRON ENERGY DEPOSITION IN STAINLESS STEEL SAMPLES
f6:n  (20 30 40 50 60 70 80 < 10)
     (20 50 80 < 13)
     (20 50 80 < 16)  $ Center Rabbits, Lower Inner Rabbits, Upper Outer Rabbits fm6 1.0291E+06  $ 6.4234E+18 nf/sec *
1.6021E-13 J/MeV = 1.0291E+06 J*nf/(MeV*sec)
c
fc36 PHOTON ENERGY DEPOSITION IN STAINLESS STEEL SAMPLES
f36:p (20 30 40 50 60 70 80 < 10)
     (20 50 80 < 13)
     (20 50 80 < 16) $ Center Rabbits, Lower Inner Rabbits, Upper Outer Rabbits
fm36 1.555999E+06                    $ 6.4234E+18 * 1.60
```

APPENDIX B. HEAT GENERATION RATES

B–1 NEUTRON HEAT GENERATION RATES

B–1.1 Axial Heat Generation Rate Profiles

	Neutron Heat Generation Rate (W/g) (Graphite, 7B Only)									
Axial Position	BOC					EOC				
(cm)	Graphite	V4Cr4Ti	Al6061 Housing	Water	Al6061 Extrusion	Graphite	V4Cr4Ti	Al6061 Housing	Water	Al6061 Extrusion
-24.61				2.657	0.08				3.290	0.11
-20.00	0.60	0.05	0.15	4.772	0.15	0.72	0.00	0.00	5.718	0.18
-13.34	0.88	0.08	0.21	6.523	0.21	0.97	0.08	0.24	7.167	0.24
-6.67	1.09	0.09	0.26	8.111	0.27	1.10	0.09	0.27	8.191	0.28
0.00	1.18	0.10	0.28	8.837	0.29	1.14	0.10	0.28	8.516	0.29
6.67	1.12	0.09	0.26	8.319	0.27	1.10	0.09	0.27	8.180	0.28
13.34	0.92	0.08	0.22	6.893	0.22	0.96	0.08	0.24	7.177	0.24
20.00	0.65	0.05	0.15	4.871	0.16	0.73	0.06	0.18	5.405	0.18
24.61				2.798	0.09				3.979	0.11

	Neutron Heat Generation Rate (W/g) (Steel, 7B Only)									
Axial Position	BOC					EOC				
(cm)	Steel	V4Cr4Ti	Al6061 Housing	Water	Al6061 Extrusion	Steel	V4Cr4Ti	Al6061 Housing	Water	Al6061 Extrusion
-24.61				2.656	0.08				3.262	0.11
-20.00	0.04	0.05	0.14	4.764	0.15	0.04	0.06	0.18	5.671	0.18
-13.34	0.05	0.07	0.21	6.503	0.21	0.06	0.08	0.23	7.108	0.24
-6.67	0.07	0.09	0.26	8.090	0.26	0.07	0.09	0.27	8.126	0.27
0.00	0.07	0.10	0.28	8.804	0.29	0.07	0.10	0.27	8.455	0.28
6.67	0.07	0.09	0.26	8.307	0.27	0.07	0.09	0.26	8.145	0.27
13.34	0.06	0.08	0.21	6.854	0.22	0.06	0.08	0.23	7.135	0.24
20.00	0.04	0.05	0.15	4.841	0.15	0.04	0.06	0.17	5.349	0.18
24.61				2.794	0.09				3.151	0.11

	Neutron Heat Generation Rate (W/g) (Steel, Assemblies in 3B and 7B)									
Axial Position	3B					7B				
(cm)	Steel	V4Cr4Ti	Al6061 Housing	Water	Al6061 Extrusion	Steel	V4Cr4Ti	Al6061 Housing	Water	Al6061 Extrusion
-24.61				2.680	0.082				2.670	0.082
-20.00	0.037	0.052	0.146	4.807	0.147	0.037	0.052	0.144	4.785	0.146
-13.34	0.054	0.075	0.210	6.565	0.213	0.054	0.075	0.210	6.554	0.212
-6.67	0.067	0.092	0.258	8.147	0.265	0.067	0.093	0.258	8.153	0.264
0.00	0.073	0.100	0.280	8.860	0.288	0.073	0.100	0.280	8.877	0.288
6.67	0.069	0.093	0.262	8.352	0.269	0.068	0.093	0.262	8.362	0.269
13.34	0.057	0.077	0.215	6.918	0.221	0.056	0.077	0.214	6.912	0.221
20.00	0.040	0.053	0.151	4.894	0.156	0.040	0.054	0.150	4.886	0.155
24.61				2.807	0.088				2.816	0.088

	Neutron Heat Generation Rate (W/g) (Steel, Assemblies in 7A and 7B)									
Axial Position	7A					7B				
(cm)	Steel	V4Cr4Ti	Al6061 Housing	Water	Al6061 Extrusion	Steel	V4Cr4Ti	Al6061 Housing	Water	Al6061 Extrusion
-24.61				2.606	0.080				2.594	0.079
-20.00	0.037	0.051	0.142	4.685	0.142	0.036	0.051	0.140	4.677	0.142
-13.34	0.053	0.073	0.203	6.378	0.206	0.053	0.073	0.203	6.383	0.206
-6.67	0.065	0.090	0.250	7.919	0.256	0.065	0.090	0.250	7.912	0.256
0.00	0.071	0.097	0.272	8.599	0.278	0.071	0.097	0.270	8.611	0.278
6.67	0.067	0.090	0.254	8.126	0.260	0.067	0.091	0.255	8.122	0.261
13.34	0.055	0.075	0.208	6.730	0.214	0.055	0.074	0.209	6.726	0.214
20.00	0.039	0.052	0.146	4.758	0.151	0.039	0.052	0.145	4.756	0.151
24.61				2.735	0.085				2.736	0.085

B–1.2 Radial Heat Generation Rate Profiles

			Neutron Heat Generation Rate (W/g) (Graphite, 7B Only)					
ROW	Channel Position		BOC			EOC		
	Radial (cm)	Axial (cm)	Graphite	V4Cr4Ti	Al6061 Housing	Graphite	V4Cr4Ti	Al6061 Housing
LOWER	22.49	-20.00	0.765	0.065	0.178	0.922	0.079	0.224
	23.77	-20.00	0.601	0.052	0.146	0.722	0.063	0.181
	25.04	-20.00	0.491	0.043	0.123	0.573	0.051	0.151
MID	22.49	0.00	1.517	0.127	0.353	1.461	0.123	0.347
	23.77	0.00	1.182	0.100	0.283	1.137	0.097	0.281
	25.04	0.00	0.943	0.081	0.233	0.909	0.079	0.234
UPPER	22.49	20.00	0.827	0.067	0.186	0.927	0.077	0.220
	23.77	20.00	0.653	0.054	0.151	0.728	0.061	0.178
	25.04	20.00	0.526	0.044	0.127	0.577	0.049	0.147

			Neutron Heat Generation Rate (W/g) (Steel, 7B Only)					
ROW	Channel Position		BOC			EOC		
	Radial (cm)	Axial (cm)	Steel	V4Cr4Ti	Al6061 Housing	Steel	V4Cr4Ti	Al6061 Housing
LOWER	22.49	-20.00	0.046	0.065	0.177	0.057	0.079	0.220
	23.77	-20.00	0.037	0.052	0.144	0.044	0.061	0.176
	25.04	-20.00	0.030	0.042	0.119	0.035	0.049	0.145
MID	22.49	0.00	0.093	0.127	0.348	0.089	0.121	0.343
	23.77	0.00	0.073	0.100	0.278	0.069	0.096	0.275
	25.04	0.00	0.058	0.081	0.228	0.055	0.077	0.227
UPPER	22.49	20.00	0.051	0.067	0.183	0.057	0.076	0.215
	23.77	20.00	0.039	0.053	0.149	0.044	0.060	0.173
	25.04	20.00	0.032	0.043	0.124	0.035	0.048	0.143

B–2 PHOTON HEAT GENERATION RATES

B–2.1 Axial Heat Generation Rate Profiles

	Photon Heat Generation Rate (W/g) (Graphite, 7B Only)									
Axial Position	BOC					EOC				
(cm)	Graphite	V4Cr4Ti	Al6061 Housing	Water	Al6061 Extrusion	Graphite	V4Cr4Ti	Al6061 Housing	Water	Al6061 Extrusion
-24.61				3.481	3.28				5.189	4.93
-20.00	4.91	8.37	5.31	4.980	5.04	7.12	12.57	7.71	7.169	7.27
-13.34	6.87	11.54	7.39	6.490	7.02	8.89	15.69	9.62	8.302	9.07
-6.67	8.55	14.37	9.19	8.108	8.76	10.02	17.55	10.78	9.364	10.23
0.00	9.32	15.69	9.97	8.864	9.58	10.40	18.23	11.20	9.751	10.64
6.67	8.61	14.01	9.12	8.205	8.85	9.99	17.45	10.78	9.387	10.23
13.34	6.90	11.16	7.32	6.602	7.11	8.86	15.39	9.51	8.327	9.07
20.00	4.83	7.86	5.15	4.678	5.06	7.12	12.19	7.58	6.682	7.28
24.61				3.422	3.36				5.049	4.98

	Photon Heat Generation Rate (W/g) (Steel, 7B Only)									
Axial Position	BOC					EOC				
(cm)	Steel	V4Cr4Ti	Al6061 Housing	Water	Al6061 Extrusion	Steel	V4Cr4Ti	Al6061 Housing	Water	Al6061 Extrusion
-24.61				3.455	3.27				5.148	4.88
-20.00	6.59	8.27	5.40	5.078	5.10	10.14	12.53	7.89	7.374	7.42
-13.34	9.29	11.59	7.60	6.661	7.16	12.72	15.63	9.89	8.598	9.28
-6.67	11.72	14.45	9.44	8.329	8.92	14.40	17.60	11.20	9.716	10.49
0.00	12.88	15.73	10.21	9.106	9.78	14.95	18.20	11.58	10.099	10.87
6.67	11.54	14.09	9.37	8.418	9.00	14.35	17.48	11.13	9.727	10.48
13.34	9.12	11.11	7.44	6.737	7.21	12.71	15.35	9.83	8.608	9.28
20.00	6.38	7.73	5.19	4.726	5.08	10.11	12.22	7.81	6.889	7.42
24.61				3.401	3.33				5.006	4.93

	Photon Heat Generation Rate (W/g) (Steel, Assemblies in 3B and 7B)									
Axial Position	3B					7B				
(cm)	Steel	V4Cr4Ti	Al6061 Housing	Water	Al6061 Extrusion	Steel	V4Cr4Ti	Al6061 Housing	Water	Al6061 Extrusion
-24.61				3.474	3.280				3.472	3.279
-20.00	6.650	8.345	5.414	5.096	5.126	6.663	8.310	5.407	5.090	5.118
-13.34	9.332	11.580	7.612	6.687	7.181	9.370	11.651	7.625	6.713	7.201
-6.67	11.744	14.529	9.472	8.376	8.977	11.823	14.541	9.504	8.401	8.993
0.00	12.965	15.803	10.294	9.132	9.791	12.973	15.815	10.290	9.170	9.838
6.67	11.576	14.145	9.419	8.456	9.040	11.612	14.171	9.440	8.468	9.056
13.34	9.178	11.188	7.495	6.764	7.238	9.171	11.199	7.512	6.774	7.250
20.00	6.392	7.830	5.239	4.753	5.107	6.442	7.811	5.247	4.763	5.115
24.61				3.416	3.340				3.421	3.352

	Photon Heat Generation Rate (W/g) (Steel, Assemblies in 7A and 7B)									
Axial Position	7A					7B				
(cm)	Steel	V4Cr4Ti	Al6061 Housing	Water	Al6061 Extrusion	Steel	V4Cr4Ti	Al6061 Housing	Water	Al6061 Extrusion
-24.61				6.07870	3.349				6.0723	3.347
-20.00	6.548	8.191	5.473	9.736	5.223	6.523	8.156	5.467	9.715	5.209
-13.34	9.081	11.273	7.643	12.950	7.269	9.125	11.404	7.667	12.993	7.303
-6.67	11.346	14.048	9.471	16.100	9.036	11.459	14.143	9.541	16.150	9.095
0.00	12.425	15.211	10.268	17.521	9.867	12.631	15.379	10.381	17.600	9.941
6.67	11.248	13.712	9.405	16.380	9.102	11.332	13.858	9.481	16.443	9.173
13.34	8.934	10.878	7.512	13.377	7.334	9.024	10.963	7.580	13.401	7.360
20.00	6.278	7.660	5.320	9.473	5.217	6.329	7.723	5.352	9.477	5.231
24.61				6.151	3.418				6.151	3.422

B–2.2 Radial Heat Generation Rate Profiles

			Photon Heat Generation Rate (W/g) (Graphite, 7B Only)					
ROW	Channel Position		BOC			EOC		
	Radial (cm)	Axial (cm)	Graphite	V4Cr4Ti	Al6061 Housing	Graphite	V4Cr4Ti	Al6061 Housing
LOWER	22.49	-20.00	5.31	8.87	5.76	7.86	13.80	8.47
	23.77	-20.00	4.91	8.37	5.31	7.12	12.57	7.71
	25.04	-20.00	4.27	7.72	4.68	6.10	11.30	6.66
MID	22.49	0.00	10.66	17.59	11.29	11.48	20.11	12.40
	23.77	0.00	9.32	15.69	9.97	10.40	18.23	11.20
	25.04	0.00	7.88	13.89	8.51	8.85	16.22	9.65
UPPER	22.49	20.00	5.32	8.35	5.65	7.82	13.38	8.33
	23.77	20.00	4.83	7.86	5.15	7.12	12.19	7.58
	25.04	20.00	4.26	7.37	4.58	6.09	11.00	6.58

			Photon Heat Generation Rate (W/g) (Steel, 7B Only)					
ROW	Position		BOC			EOC		
	Radial (cm)	Axial (cm)	Steel	V4Cr4Ti	Al6061 Housing	Steel	V4Cr4Ti	Al6061 Housing
LOWER	22.49	-20.00	7.03	8.81	5.89	11.17	13.85	8.74
	23.77	-20.00	6.59	8.27	5.40	10.14	12.53	7.89
	25.04	-20.00	6.03	7.58	4.71	8.92	11.16	6.76
MID	22.49	0.00	14.44	17.71	11.61	16.57	20.29	12.84
	23.77	0.00	12.88	15.73	10.21	14.95	18.20	11.58
	25.04	0.00	11.09	13.67	8.57	12.98	16.01	9.80
UPPER	22.49	20.00	6.78	8.25	5.71	11.09	13.46	8.58
	23.77	20.00	6.38	7.73	5.19	10.11	12.22	7.81
	25.04	20.00	5.88	7.20	4.56	8.88	10.82	6.66

B–3 TOTAL HEAT GENERATION RATES

B–3.1 Axial Heat Generation Rate Profiles

	Total Axial Heat Generation Rate Profiles (W/g) (Graphite, 7B Only)									
Axial Position	BOC					EOC				
(cm)	Graphite	V4Cr4Ti	Al6061 Housing	Water	Al6061 Extrusion	Graphite	V4Cr4Ti	Al6061 Housing	Water	Al6061 Extrusion
-24.61				6.1	3.37				8.5	5.04
-20.00	5.51	8.43	5.46	9.8	5.19	7.84	12.58	7.71	12.9	7.45
-13.34	7.75	11.61	7.60	13.0	7.23	9.86	15.77	9.86	15.5	9.32
-6.67	9.64	14.46	9.45	16.2	9.02	11.12	17.64	11.06	17.6	10.50
0.00	10.50	15.79	10.25	17.7	9.87	11.54	18.32	11.48	18.3	10.93
6.67	9.73	14.10	9.39	16.5	9.12	11.08	17.54	11.05	17.6	10.51
13.34	7.82	11.23	7.54	13.5	7.34	9.82	15.48	9.74	15.5	9.31
20.00	5.48	7.92	5.30	9.5	5.22	7.85	12.25	7.76	12.1	7.46
24.61				6.2	3.44				9.0	5.09

	Total Axial Heat Generation Rate Profiles (W/g) (Steel, 7B Only)									
Axial Position	BOC					EOC				
(cm)	Steel	V4Cr4Ti	Al6061 Housing	Water	Al6061 Extrusion	Steel	V4Cr4Ti	Al6061 Housing	Water	Al6061 Extrusion
-24.61				6.1	3.35				8.4	4.99
-20.00	6.63	8.32	5.54	9.8	5.25	10.19	12.59	8.07	13.0	7.60
-13.34	9.34	11.67	7.80	13.2	7.37	12.78	15.71	10.12	15.7	9.52
-6.67	11.79	14.54	9.70	16.4	9.18	14.47	17.69	11.47	17.8	10.76
0.00	12.95	15.83	10.49	17.9	10.06	15.02	18.30	11.85	18.6	11.16
6.67	11.60	14.18	9.63	16.7	9.27	14.41	17.57	11.40	17.9	10.75
13.34	9.18	11.19	7.66	13.6	7.42	12.77	15.43	10.07	15.7	9.52
20.00	6.42	7.78	5.34	9.6	5.24	10.16	12.28	7.98	12.2	7.60
24.61				6.2	3.42				8.2	5.04

	Total Heat Generation Rate (W/g) (Steel, Assemblies in 3B and 7B)									
Axial Position	3B					7B				
(cm)	Steel	V4Cr4Ti	Al6061 Housing	Water	Al6061 Extrusion	Steel	V4Cr4Ti	Al6061 Housing	Water	Al6061 Extrusion
-24.61				6.154	3.363				6.142	3.361
-20.00	6.687	8.398	5.559	9.902	5.272	6.700	8.362	5.551	9.875	5.264
-13.34	9.386	11.655	7.822	13.252	7.393	9.424	11.726	7.834	13.267	7.413
-6.67	11.811	14.621	9.730	16.522	9.242	11.890	14.634	9.763	16.554	9.257
0.00	13.039	15.903	10.574	17.991	10.078	13.045	15.915	10.570	18.048	10.127
6.67	11.645	14.238	9.680	16.808	9.310	11.680	14.265	9.701	16.831	9.325
13.34	9.235	11.264	7.710	13.682	7.459	9.227	11.276	7.726	13.685	7.471
20.00	6.432	7.884	5.390	9.647	5.263	6.482	7.864	5.396	9.649	5.270
24.61				6.223	3.427				6.237	3.440

	Total Heat Generation Rate (W/g) (Steel, Assemblies in 7A and 7B)									
Axial Position	7A					7B				
(cm)	Steel	V4Cr4Ti	Al6061 Housing	Water	Al6061 Extrusion	Steel	V4Cr4Ti	Al6061 Housing	Water	Al6061 Extrusion
-24.61				6.0788	3.349				6.0723	3.347
-20.00	6.548	8.191	5.473	9.736	5.223	6.523	8.156	5.467	9.715	5.209
-13.34	9.081	11.273	7.643	12.950	7.269	9.125	11.404	7.667	12.993	7.303
-6.67	11.346	14.048	9.471	16.100	9.036	11.459	14.143	9.541	16.150	9.095
0.00	12.425	15.211	10.268	17.521	9.867	12.631	15.379	10.381	17.600	9.941
6.67	11.248	13.712	9.405	16.380	9.102	11.332	13.858	9.481	16.443	9.173
13.34	8.934	10.878	7.512	13.377	7.334	9.024	10.963	7.580	13.401	7.360
20.00	6.278	7.660	5.320	9.473	5.217	6.329	7.723	5.352	9.477	5.231
24.61				6.151	3.418				6.151	3.422

B–3.2 Radial Heat Generation Rate Profiles

			Total Heat Generation Rate (W/g) (Graphite, 7B Only)					
ROW	Channel Position Radial (cm)	Axial (cm)	BOC Graphite	BOC V4Cr4Ti	BOC Al6061 Housing	EOC Graphite	EOC V4Cr4Ti	EOC Al6061 Housing
LOWER	22.49	-20.00	6.07	8.94	5.93	8.78	13.88	8.70
	23.77	-20.00	5.51	8.43	5.46	7.84	12.64	7.89
	25.04	-20.00	4.76	7.77	4.80	6.67	11.35	6.81
MID	22.49	0.00	12.17	17.72	11.64	12.94	20.23	12.75
	23.77	0.00	10.50	15.79	10.25	11.54	18.32	11.48
	25.04	0.00	8.82	13.97	8.74	9.76	16.30	9.89
UPPER	22.49	20.00	6.15	8.42	5.83	8.75	13.45	8.55
	23.77	20.00	5.48	7.92	5.30	7.85	12.25	7.76
	25.04	20.00	4.79	7.41	4.71	6.67	11.05	6.73

			Total Heat Generation Rate (W/g) (Steel, 7B Only)					
ROW	Position Radial (cm)	Axial (cm)	BOC Steel	BOC V4Cr4Ti	BOC Al6061 Housing	EOC Steel	EOC V4Cr4Ti	EOC Al6061 Housing
LOWER	22.49	-20.00	7.07	8.88	6.06	11.23	13.93	8.96
	23.77	-20.00	6.63	8.32	5.54	10.19	12.59	8.07
	25.04	-20.00	6.06	7.62	4.83	8.95	11.21	6.90
MID	22.49	0.00	14.54	17.84	11.96	16.66	20.41	13.18
	23.77	0.00	12.95	15.83	10.49	15.02	18.30	11.85
	25.04	0.00	11.14	13.75	8.79	13.04	16.09	10.03
UPPER	22.49	20.00	6.83	8.32	5.90	11.14	13.54	8.80
	23.77	20.00	6.42	7.78	5.34	10.16	12.28	7.98
	25.04	20.00	5.91	7.24	4.68	8.92	10.87	6.81

B–3.3 Total Axial Heat Generation Fit

The total axial heat generation data was fit to an exponential curve of the form:

$$q_{material} = q_{peak} \times exp\left[-\left(\frac{z}{s}\right)^2\right]$$

Where *s* is a correlating parameter (cm) for each material, it was assumed that this parameter is symmetric about the axial midplane.

The following curves represent heat generation rates of the center channel rabbits

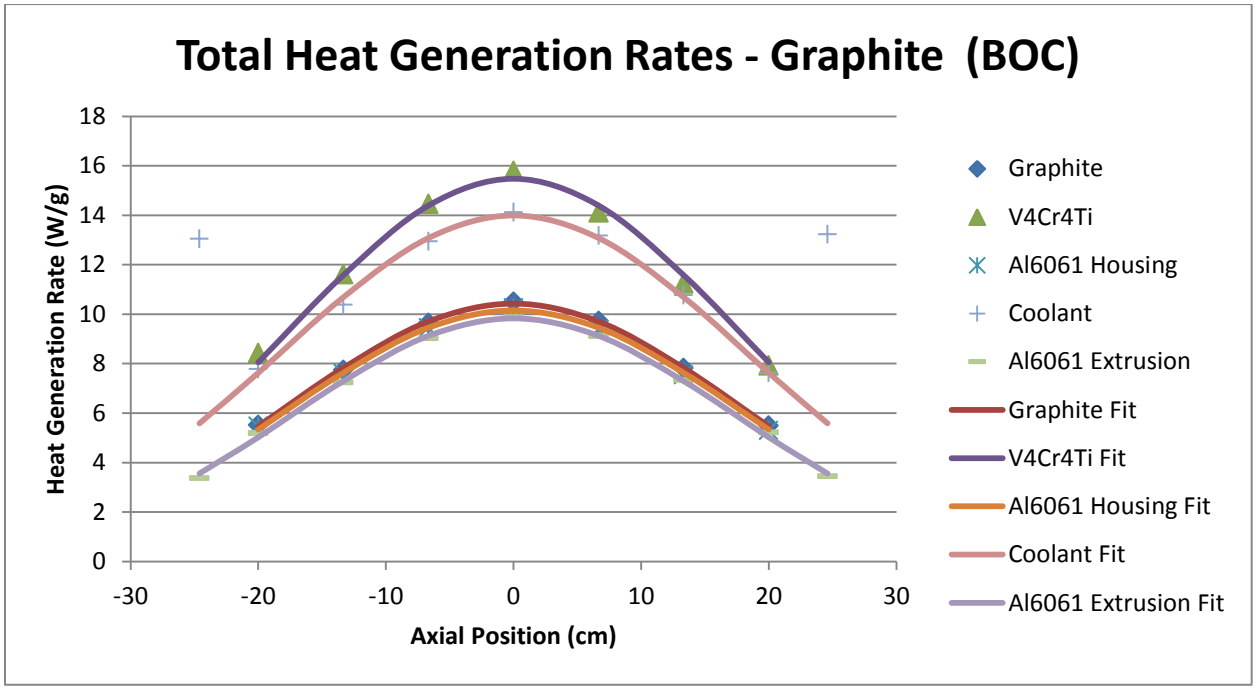

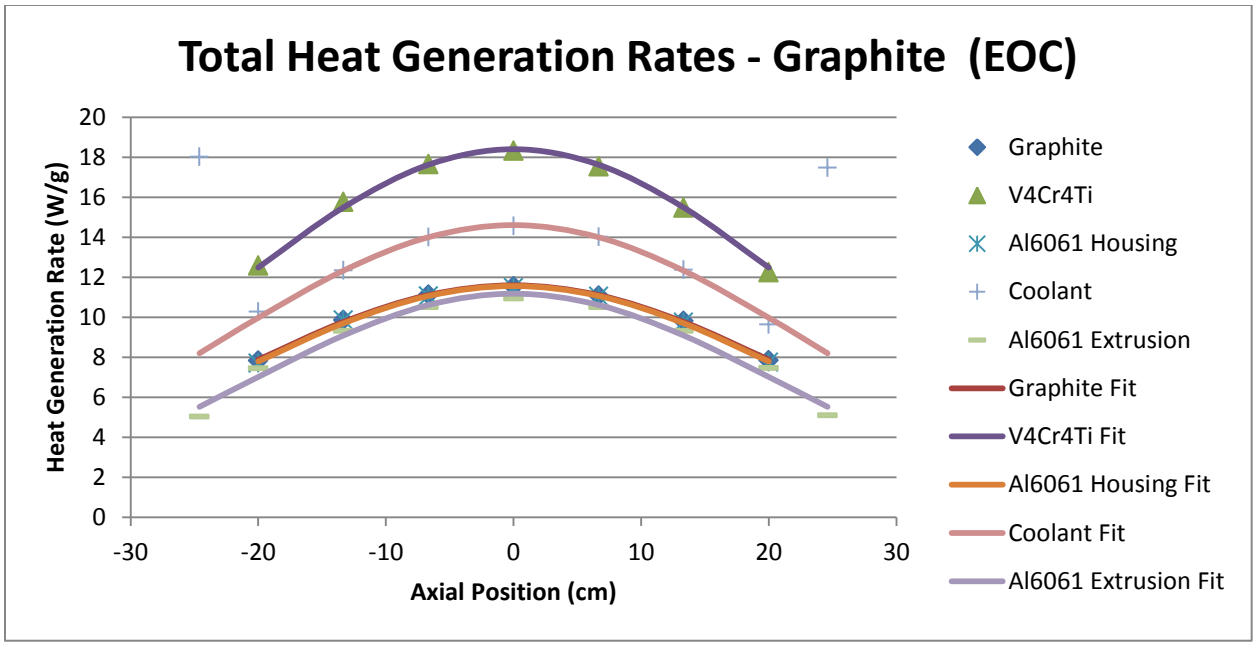

Material	Fit Parameters (Graphite)			
	BOC		EOC	
	Peak (W/g)	s(cm)	Peak (W/g)	s(cm)
Graphite	10.43	24.89	11.60	32.18
V4Cr4Ti	15.48	24.75	18.40	32.12
Al6061 Housing	10.15	24.94	11.56	31.83
Water	13.99	25.67	14.61	32.39
Al6061 Extrusion	9.83	24.41	11.18	29.31

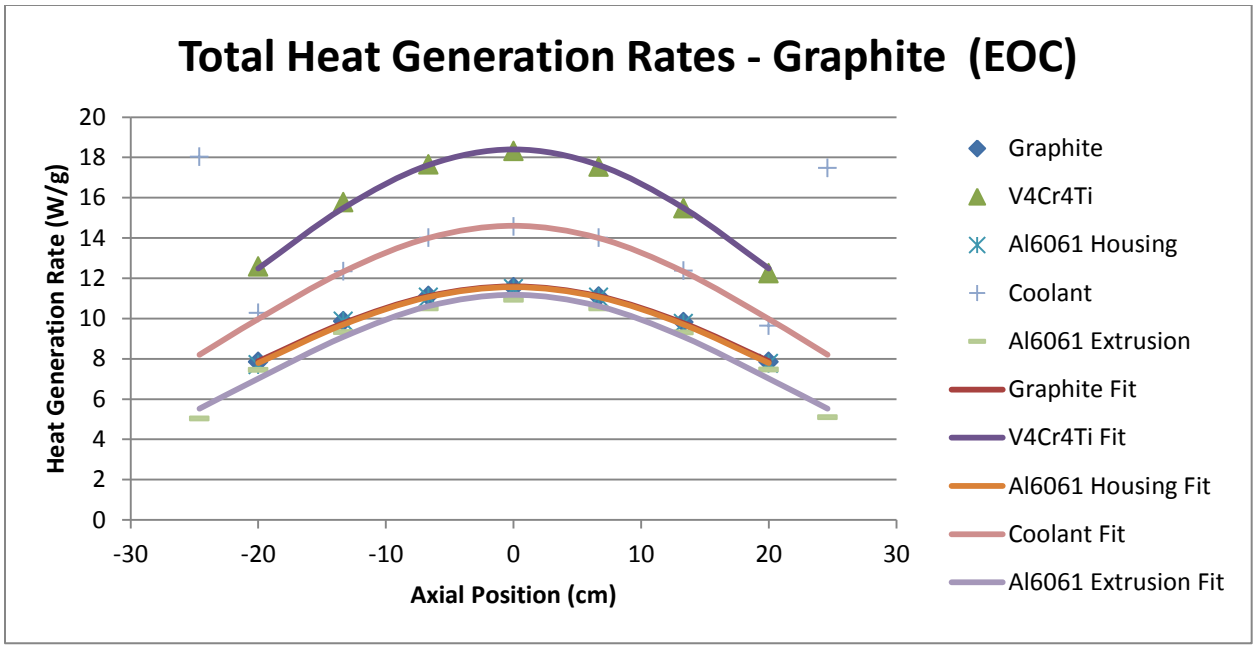

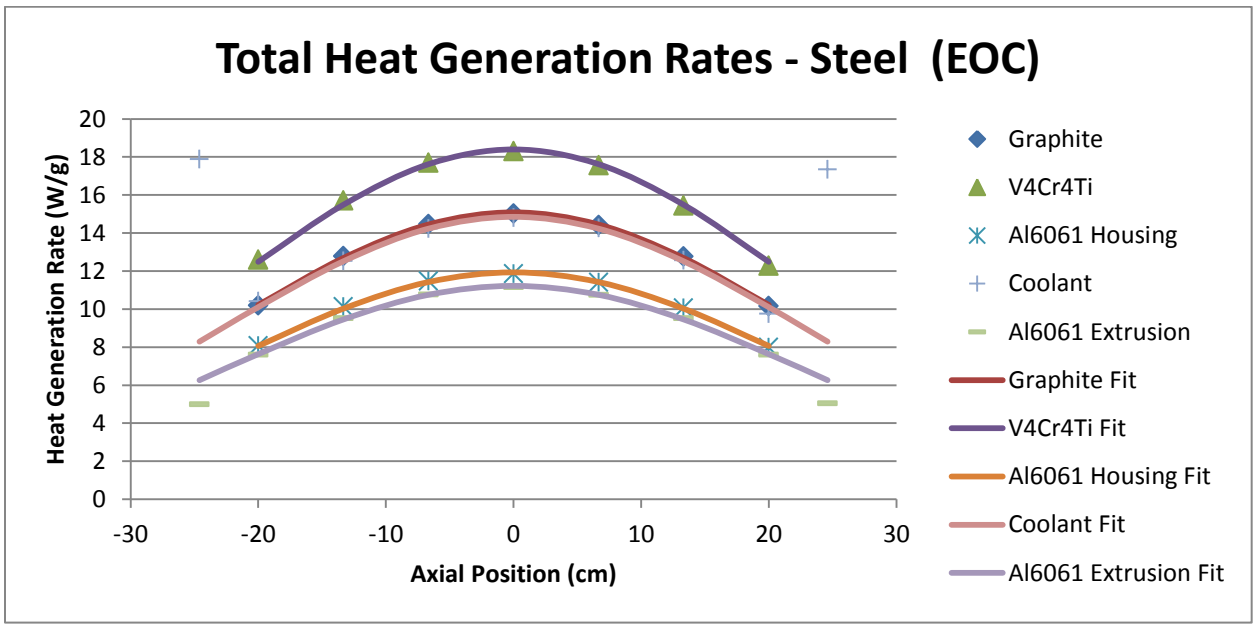

Material	Fit Parameters (Steel)			
	BOC		EOC	
	Peak (W/g)	s(cm)	Peak (W/g)	s(cm)
Steel	12.71	24.22	15.09	32.04
V4Cr4Ti	15.57	24.40	18.40	32.14
Al6061 Housing	10.42	24.69	11.93	31.95
Water	14.17	25.53	14.85	32.22
Al6061 Extrusion	10.02	24.16	11.22	32.22

APPENDIX C. NEUTRON FLUX

C–1 GRAPHITE SAMPLES, BEGINNING OF CYCLE

C–1.1 Center Channel Flux Tallies

Energy [MeV]	-20.0025 cm	-13.335 cm	-6.6675 cm	Midplane	+6.6675 cm	+13.335 cm	+20.0025 cm
3.00E-09	1.34E+12	1.79E+12	2.12E+12	2.50E+12	2.29E+12	1.72E+12	1.10E+12
7.50E-09	6.53E+12	9.17E+12	1.20E+13	1.28E+13	1.11E+13	8.05E+12	5.24E+12
1.00E-08	5.57E+12	7.87E+12	1.01E+13	1.09E+13	9.28E+12	7.03E+12	4.52E+12
2.53E-08	5.13E+13	7.30E+13	9.35E+13	1.02E+14	8.67E+13	6.46E+13	4.17E+13
3.00E-08	1.79E+13	2.52E+13	3.30E+13	3.61E+13	3.10E+13	2.27E+13	1.45E+13
4.00E-08	3.77E+13	5.42E+13	6.91E+13	7.56E+13	6.44E+13	4.75E+13	3.10E+13
5.00E-08	3.41E+13	4.86E+13	6.29E+13	6.89E+13	5.87E+13	4.36E+13	2.82E+13
7.00E-08	5.35E+13	7.58E+13	9.93E+13	1.08E+14	9.21E+13	6.89E+13	4.37E+13
1.00E-07	4.80E+13	7.03E+13	9.08E+13	9.97E+13	8.63E+13	6.34E+13	3.98E+13
1.50E-07	3.28E+13	4.97E+13	6.46E+13	7.04E+13	6.18E+13	4.63E+13	2.80E+13
2.00E-07	1.31E+13	1.99E+13	2.61E+13	2.84E+13	2.50E+13	1.85E+13	1.09E+13
2.25E-07	3.72E+12	5.91E+12	7.99E+12	8.84E+12	7.55E+12	5.67E+12	3.44E+12
2.50E-07	3.03E+12	4.83E+12	6.27E+12	6.98E+12	6.18E+12	4.80E+12	2.80E+12
2.75E-07	2.52E+12	4.14E+12	5.51E+12	6.17E+12	5.20E+12	4.13E+12	2.31E+12
3.35E-07	5.09E+12	8.10E+12	1.07E+13	1.19E+13	1.08E+13	8.08E+12	4.83E+12
3.50E-07	1.17E+12	1.71E+12	2.39E+12	2.54E+12	2.42E+12	1.67E+12	1.01E+12
3.75E-07	1.76E+12	2.83E+12	3.50E+12	3.96E+12	3.49E+12	2.58E+12	1.60E+12
4.00E-07	1.65E+12	2.62E+12	3.27E+12	3.66E+12	3.39E+12	2.55E+12	1.37E+12
6.25E-07	1.14E+13	1.74E+13	2.26E+13	2.54E+13	2.27E+13	1.71E+13	1.02E+13
1.00E-06	1.17E+13	1.77E+13	2.28E+13	2.62E+13	2.30E+13	1.76E+13	1.08E+13
1.77E-06	1.36E+13	2.21E+13	2.72E+13	3.06E+13	2.72E+13	2.09E+13	1.35E+13
3.00E-06	1.27E+13	1.99E+13	2.54E+13	2.80E+13	2.49E+13	1.95E+13	1.24E+13
4.75E-06	1.18E+13	1.71E+13	2.19E+13	2.43E+13	2.10E+13	1.64E+13	1.13E+13
6.00E-06	6.07E+12	9.26E+12	1.11E+13	1.25E+13	1.10E+13	8.85E+12	5.71E+12
8.10E-06	7.28E+12	1.16E+13	1.47E+13	1.61E+13	1.46E+13	1.16E+13	7.73E+12
1.00E-05	5.27E+12	8.36E+12	1.03E+13	1.12E+13	1.01E+13	8.39E+12	5.31E+12
3.00E-05	2.85E+13	4.26E+13	5.48E+13	6.01E+13	5.38E+13	4.30E+13	2.91E+13
1.00E-04	3.26E+13	4.91E+13	6.11E+13	6.65E+13	6.00E+13	4.89E+13	3.35E+13
5.50E-04	4.78E+13	6.94E+13	8.71E+13	9.44E+13	8.71E+13	7.11E+13	4.96E+13
3.00E-03	4.93E+13	7.26E+13	9.01E+13	9.78E+13	9.12E+13	7.58E+13	5.26E+13
1.70E-02	4.80E+13	7.11E+13	8.80E+13	9.39E+13	8.98E+13	7.31E+13	5.15E+13
2.50E-02	1.13E+13	1.68E+13	2.06E+13	2.27E+13	2.09E+13	1.75E+13	1.24E+13
1.00E-01	4.62E+13	6.84E+13	8.47E+13	9.29E+13	8.75E+13	7.23E+13	4.98E+13
4.00E-01	6.83E+13	1.02E+14	1.25E+14	1.36E+14	1.29E+14	1.06E+14	7.46E+13
9.00E-01	5.07E+13	7.43E+13	9.30E+13	1.00E+14	9.52E+13	7.91E+13	5.49E+13

1.40E+00	2.92E+13	4.31E+13	5.38E+13	5.84E+13	5.48E+13	4.52E+13	3.22E+13
1.85E+00	2.00E+13	2.89E+13	3.63E+13	3.90E+13	3.72E+13	2.97E+13	2.16E+13
2.35E+00	1.41E+13	2.03E+13	2.48E+13	2.72E+13	2.59E+13	2.10E+13	1.50E+13
2.48E+00	3.40E+12	4.89E+12	5.78E+12	6.72E+12	6.22E+12	4.89E+12	3.75E+12
3.00E+00	8.18E+12	1.17E+13	1.48E+13	1.58E+13	1.49E+13	1.25E+13	8.59E+12
4.80E+00	1.23E+13	1.81E+13	2.23E+13	2.42E+13	2.26E+13	1.86E+13	1.34E+13
6.43E+00	3.74E+12	5.17E+12	6.75E+12	7.06E+12	6.79E+12	5.56E+12	4.11E+12
8.19E+00	1.16E+12	1.80E+12	2.11E+12	2.38E+12	2.09E+12	1.87E+12	1.32E+12
2.00E+01	4.54E+11	6.41E+11	8.57E+11	8.28E+11	8.95E+11	6.48E+11	5.40E+11

C–1.2 Radial Flux Tallies

	Midplane			Bottom Row			Top Row		
Energy [MeV]	**Inner Column**	**Center Column**	**Outer Column**	**Inner Column**	**Center Column**	**Outer Column**	**Inner Column**	**Center Column**	**Outer Column**
3.00E-09	2.43E+12	2.50E+12	2.75E+12	1.07E+12	1.34E+12	1.53E+12	8.27E+11	1.10E+12	1.38E+12
7.50E-09	1.29E+13	1.28E+13	1.43E+13	5.70E+12	6.53E+12	7.78E+12	4.34E+12	5.24E+12	6.71E+12
1.00E-08	1.06E+13	1.09E+13	1.20E+13	4.70E+12	5.57E+12	6.66E+12	3.43E+12	4.52E+12	5.71E+12
2.53E-08	9.85E+13	1.02E+14	1.10E+14	4.29E+13	5.13E+13	5.99E+13	3.15E+13	4.17E+13	5.17E+13
3.00E-08	3.50E+13	3.61E+13	3.88E+13	1.51E+13	1.79E+13	2.12E+13	1.12E+13	1.45E+13	1.83E+13
4.00E-08	7.27E+13	7.56E+13	8.06E+13	3.17E+13	3.77E+13	4.37E+13	2.34E+13	3.10E+13	3.78E+13
5.00E-08	6.67E+13	6.89E+13	7.33E+13	2.89E+13	3.41E+13	3.98E+13	2.13E+13	2.82E+13	3.42E+13
7.00E-08	1.04E+14	1.08E+14	1.14E+14	4.48E+13	5.35E+13	6.07E+13	3.38E+13	4.37E+13	5.24E+13
1.00E-07	9.64E+13	9.97E+13	1.03E+14	4.11E+13	4.80E+13	5.40E+13	3.05E+13	3.98E+13	4.74E+13
1.50E-07	7.12E+13	7.04E+13	7.30E+13	2.91E+13	3.28E+13	3.67E+13	2.22E+13	2.80E+13	3.30E+13
2.00E-07	2.90E+13	2.84E+13	2.76E+13	1.15E+13	1.31E+13	1.35E+13	9.28E+12	1.09E+13	1.22E+13
2.25E-07	9.08E+12	8.84E+12	8.33E+12	3.61E+12	3.72E+12	3.83E+12	2.92E+12	3.44E+12	3.55E+12
2.50E-07	7.62E+12	6.98E+12	6.88E+12	2.92E+12	3.03E+12	3.16E+12	2.49E+12	2.80E+12	2.85E+12
2.75E-07	6.35E+12	6.17E+12	5.95E+12	2.35E+12	2.52E+12	2.55E+12	2.10E+12	2.31E+12	2.49E+12
3.35E-07	1.27E+13	1.19E+13	1.11E+13	4.95E+12	5.09E+12	5.11E+12	4.03E+12	4.83E+12	4.65E+12
3.50E-07	2.76E+12	2.54E+12	2.44E+12	1.02E+12	1.17E+12	1.05E+12	9.57E+11	1.01E+12	1.05E+12
3.75E-07	4.45E+12	3.96E+12	3.72E+12	1.59E+12	1.76E+12	1.71E+12	1.40E+12	1.60E+12	1.63E+12
4.00E-07	4.00E+12	3.66E+12	3.42E+12	1.49E+12	1.65E+12	1.65E+12	1.32E+12	1.37E+12	1.55E+12
6.25E-07	2.70E+13	2.54E+13	2.34E+13	1.08E+13	1.14E+13	1.09E+13	9.26E+12	1.02E+13	1.06E+13
1.00E-06	2.77E+13	2.62E+13	2.41E+13	1.13E+13	1.17E+13	1.12E+13	1.02E+13	1.08E+13	1.11E+13
1.77E-06	3.23E+13	3.06E+13	2.86E+13	1.35E+13	1.36E+13	1.35E+13	1.28E+13	1.35E+13	1.32E+13
3.00E-06	2.97E+13	2.80E+13	2.57E+13	1.30E+13	1.27E+13	1.29E+13	1.15E+13	1.24E+13	1.22E+13
4.75E-06	2.54E+13	2.43E+13	2.23E+13	1.14E+13	1.18E+13	1.10E+13	1.09E+13	1.13E+13	1.10E+13
6.00E-06	1.36E+13	1.25E+13	1.13E+13	5.84E+12	6.07E+12	5.86E+12	5.87E+12	5.71E+12	5.80E+12
8.10E-06	1.72E+13	1.61E+13	1.48E+13	7.62E+12	7.28E+12	7.22E+12	7.49E+12	7.73E+12	7.47E+12
1.00E-05	1.22E+13	1.12E+13	1.07E+13	5.47E+12	5.27E+12	5.12E+12	5.40E+12	5.31E+12	5.03E+12
3.00E-05	6.56E+13	6.01E+13	5.48E+13	2.90E+13	2.85E+13	2.72E+13	2.91E+13	2.91E+13	2.80E+13

1.00E-04	7.32E+13	6.65E+13	6.10E+13	3.40E+13	3.26E+13	3.05E+13	3.39E+13	3.35E+13	3.13E+13
5.50E-04	1.06E+14	9.44E+13	8.58E+13	5.17E+13	4.78E+13	4.41E+13	5.23E+13	4.96E+13	4.55E+13
3.00E-03	1.11E+14	9.78E+13	8.61E+13	5.55E+13	4.93E+13	4.44E+13	5.84E+13	5.26E+13	4.71E+13
1.70E-02	1.14E+14	9.39E+13	8.23E+13	5.69E+13	4.80E+13	4.16E+13	6.04E+13	5.15E+13	4.48E+13
2.50E-02	2.65E+13	2.27E+13	1.99E+13	1.34E+13	1.13E+13	9.82E+12	1.45E+13	1.24E+13	1.08E+13
1.00E-01	1.08E+14	9.29E+13	8.11E+13	5.35E+13	4.62E+13	4.10E+13	5.75E+13	4.98E+13	4.40E+13
4.00E-01	1.63E+14	1.36E+14	1.15E+14	8.12E+13	6.83E+13	5.88E+13	8.77E+13	7.46E+13	6.31E+13
9.00E-01	1.27E+14	1.00E+14	8.26E+13	6.33E+13	5.07E+13	4.23E+13	6.84E+13	5.49E+13	4.55E+13
1.40E+00	7.38E+13	5.84E+13	4.71E+13	3.73E+13	2.92E+13	2.40E+13	3.99E+13	3.22E+13	2.58E+13
1.85E+00	4.97E+13	3.90E+13	3.09E+13	2.50E+13	2.00E+13	1.65E+13	2.71E+13	2.16E+13	1.78E+13
2.35E+00	3.55E+13	2.72E+13	2.14E+13	1.80E+13	1.41E+13	1.14E+13	1.96E+13	1.50E+13	1.20E+13
2.48E+00	8.55E+12	6.72E+12	5.02E+12	4.43E+12	3.40E+12	2.53E+12	5.05E+12	3.75E+12	2.76E+12
3.00E+00	2.17E+13	1.58E+13	1.17E+13	1.08E+13	8.18E+12	6.41E+12	1.18E+13	8.59E+12	6.70E+12
4.80E+00	3.22E+13	2.42E+13	1.86E+13	1.62E+13	1.23E+13	9.83E+12	1.76E+13	1.34E+13	1.05E+13
6.43E+00	9.26E+12	7.06E+12	5.58E+12	4.86E+12	3.74E+12	2.75E+12	5.31E+12	4.11E+12	3.11E+12
8.19E+00	3.11E+12	2.38E+12	1.91E+12	1.50E+12	1.16E+12	9.73E+11	1.66E+12	1.32E+12	1.07E+12
2.00E+01	1.08E+12	8.28E+11	6.22E+11	6.09E+11	4.54E+11	3.89E+11	6.45E+11	5.40E+11	4.34E+11

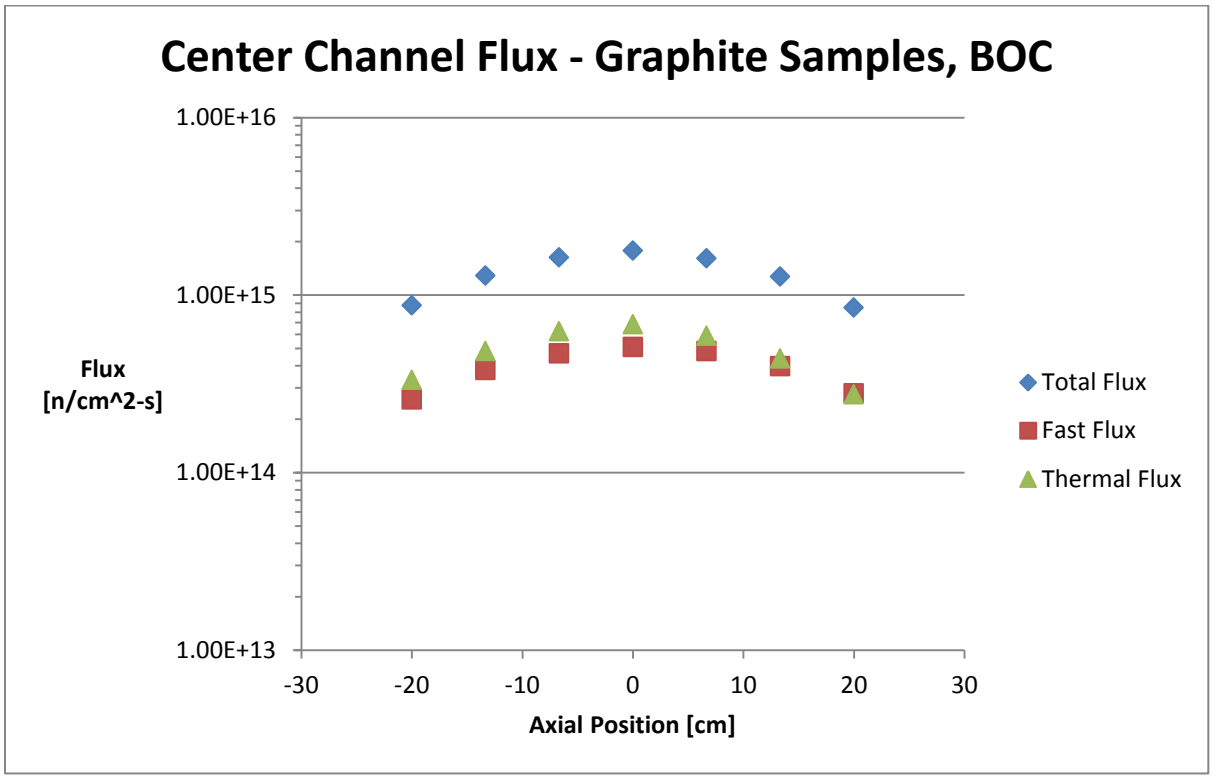

C–2 GRAPHITE SAMPLES, END OF CYCLE

C–2.1 Center Channel Flux Tallies

Energy [MeV]	-20.0025 cm	-13.335 cm	-6.6675 cm	Midplane	+6.6675 cm	+13.335 cm	+20.0025 cm
3.00E-09	2.35E+12	2.82E+12	3.35E+12	3.37E+12	3.30E+12	2.88E+12	2.25E+12
7.50E-09	1.21E+13	1.49E+13	1.69E+13	1.74E+13	1.70E+13	1.47E+13	1.17E+13
1.00E-08	1.02E+13	1.24E+13	1.43E+13	1.47E+13	1.42E+13	1.24E+13	1.00E+13
2.53E-08	9.63E+13	1.17E+14	1.33E+14	1.38E+14	1.33E+14	1.16E+14	9.32E+13
3.00E-08	3.33E+13	4.17E+13	4.71E+13	4.93E+13	4.70E+13	4.13E+13	3.26E+13
4.00E-08	7.06E+13	8.63E+13	9.81E+13	1.02E+14	9.81E+13	8.56E+13	6.84E+13
5.00E-08	6.38E+13	7.85E+13	8.89E+13	9.37E+13	8.98E+13	7.80E+13	6.26E+13
7.00E-08	9.95E+13	1.21E+14	1.39E+14	1.45E+14	1.39E+14	1.21E+14	9.62E+13
1.00E-07	8.92E+13	1.10E+14	1.26E+14	1.31E+14	1.25E+14	1.09E+14	8.65E+13
1.50E-07	6.07E+13	7.51E+13	8.69E+13	9.02E+13	8.70E+13	7.49E+13	5.91E+13
2.00E-07	2.16E+13	2.82E+13	3.23E+13	3.39E+13	3.22E+13	2.81E+13	2.15E+13
2.25E-07	6.21E+12	8.10E+12	9.50E+12	1.01E+13	9.36E+12	8.02E+12	5.96E+12
2.50E-07	5.14E+12	6.70E+12	7.49E+12	7.70E+12	7.43E+12	6.47E+12	4.80E+12
2.75E-07	4.11E+12	5.38E+12	6.34E+12	7.05E+12	6.20E+12	5.48E+12	4.12E+12
3.35E-07	8.03E+12	1.03E+13	1.22E+13	1.30E+13	1.25E+13	1.04E+13	8.34E+12
3.50E-07	1.64E+12	2.46E+12	2.73E+12	2.87E+12	2.74E+12	2.37E+12	1.74E+12
3.75E-07	2.78E+12	3.82E+12	4.38E+12	4.57E+12	4.26E+12	3.47E+12	2.74E+12
4.00E-07	2.50E+12	3.34E+12	3.99E+12	3.99E+12	3.89E+12	3.21E+12	2.50E+12
6.25E-07	1.67E+13	2.24E+13	2.65E+13	2.70E+13	2.62E+13	2.24E+13	1.68E+13
1.00E-06	1.69E+13	2.26E+13	2.65E+13	2.78E+13	2.63E+13	2.28E+13	1.69E+13
1.77E-06	1.98E+13	2.72E+13	3.12E+13	3.24E+13	3.15E+13	2.66E+13	1.98E+13
3.00E-06	1.83E+13	2.46E+13	2.83E+13	2.94E+13	2.86E+13	2.46E+13	1.81E+13
4.75E-06	1.56E+13	2.13E+13	2.45E+13	2.61E+13	2.46E+13	2.11E+13	1.56E+13
6.00E-06	8.04E+12	1.10E+13	1.25E+13	1.25E+13	1.24E+13	1.08E+13	8.15E+12
8.10E-06	1.01E+13	1.41E+13	1.60E+13	1.64E+13	1.64E+13	1.38E+13	1.04E+13
1.00E-05	7.26E+12	9.94E+12	1.17E+13	1.18E+13	1.13E+13	9.68E+12	7.36E+12
3.00E-05	3.75E+13	5.12E+13	5.82E+13	6.20E+13	5.87E+13	5.13E+13	3.78E+13
1.00E-04	4.15E+13	5.55E+13	6.42E+13	6.74E+13	6.47E+13	5.49E+13	4.20E+13
5.50E-04	5.90E+13	7.89E+13	9.13E+13	9.48E+13	9.07E+13	7.79E+13	5.81E+13
3.00E-03	5.83E+13	7.97E+13	9.17E+13	9.65E+13	9.18E+13	7.94E+13	5.86E+13
1.70E-02	5.64E+13	7.73E+13	8.83E+13	9.22E+13	8.83E+13	7.68E+13	5.71E+13
2.50E-02	1.34E+13	1.85E+13	2.07E+13	2.16E+13	2.08E+13	1.80E+13	1.33E+13
1.00E-01	5.51E+13	7.52E+13	8.59E+13	8.87E+13	8.50E+13	7.44E+13	5.53E+13
4.00E-01	8.09E+13	1.10E+14	1.25E+14	1.31E+14	1.26E+14	1.10E+14	8.15E+13
9.00E-01	6.08E+13	8.09E+13	9.37E+13	9.64E+13	9.30E+13	8.16E+13	6.04E+13
1.40E+00	3.58E+13	4.78E+13	5.46E+13	5.68E+13	5.43E+13	4.76E+13	3.61E+13

1.85E+00	2.41E+13	3.19E+13	3.68E+13	3.77E+13	3.60E+13	3.17E+13	2.40E+13
2.35E+00	1.71E+13	2.25E+13	2.54E+13	2.60E+13	2.57E+13	2.20E+13	1.72E+13
2.48E+00	4.00E+12	5.29E+12	6.33E+12	6.41E+12	5.87E+12	5.18E+12	3.90E+12
3.00E+00	9.71E+12	1.29E+13	1.47E+13	1.51E+13	1.45E+13	1.31E+13	1.01E+13
4.80E+00	1.48E+13	2.00E+13	2.22E+13	2.30E+13	2.28E+13	1.98E+13	1.50E+13
6.43E+00	4.41E+12	5.83E+12	6.79E+12	6.96E+12	6.61E+12	5.82E+12	4.58E+12
8.19E+00	1.38E+12	1.79E+12	2.06E+12	2.14E+12	2.09E+12	1.94E+12	1.49E+12
2.00E+01	4.96E+11	6.91E+11	8.60E+11	8.65E+11	7.10E+11	7.21E+11	5.67E+11

C–2.2 Radial Flux Tallies

	Midplane			Bottom Row			Top Row		
Energy [MeV]	**Inner Column**	**Center Column**	**Outer Column**	**Inner Column**	**Center Column**	**Outer Column**	**Inner Column**	**Center Column**	**Outer Column**
3.00E-09	3.49E+12	3.37E+12	3.78E+12	2.41E+12	2.35E+12	2.62E+12	2.29E+12	2.25E+12	2.50E+12
7.50E-09	1.85E+13	1.74E+13	1.91E+13	1.25E+13	1.21E+13	1.35E+13	1.21E+13	1.17E+13	1.29E+13
1.00E-08	1.54E+13	1.47E+13	1.57E+13	1.02E+13	1.02E+13	1.08E+13	9.79E+12	1.00E+13	1.08E+13
2.53E-08	1.41E+14	1.38E+14	1.46E+14	9.60E+13	9.63E+13	1.01E+14	9.29E+13	9.32E+13	9.94E+13
3.00E-08	5.02E+13	4.93E+13	5.12E+13	3.41E+13	3.33E+13	3.59E+13	3.24E+13	3.26E+13	3.47E+13
4.00E-08	1.04E+14	1.02E+14	1.07E+14	6.98E+13	7.06E+13	7.38E+13	6.83E+13	6.84E+13	7.21E+13
5.00E-08	9.44E+13	9.37E+13	9.76E+13	6.41E+13	6.38E+13	6.65E+13	6.16E+13	6.26E+13	6.59E+13
7.00E-08	1.47E+14	1.45E+14	1.49E+14	9.82E+13	9.95E+13	1.03E+14	9.56E+13	9.62E+13	1.01E+14
1.00E-07	1.32E+14	1.31E+14	1.34E+14	8.80E+13	8.92E+13	9.13E+13	8.68E+13	8.65E+13	9.01E+13
1.50E-07	9.29E+13	9.02E+13	9.03E+13	6.02E+13	6.07E+13	6.07E+13	5.99E+13	5.91E+13	5.97E+13
2.00E-07	3.47E+13	3.39E+13	3.28E+13	2.26E+13	2.16E+13	2.12E+13	2.21E+13	2.15E+13	2.08E+13
2.25E-07	1.05E+13	1.01E+13	9.60E+12	6.72E+12	6.21E+12	6.10E+12	6.79E+12	5.96E+12	5.71E+12
2.50E-07	8.75E+12	7.70E+12	7.50E+12	5.24E+12	5.14E+12	4.55E+12	5.26E+12	4.80E+12	4.66E+12
2.75E-07	7.27E+12	7.05E+12	6.12E+12	4.28E+12	4.11E+12	3.87E+12	4.31E+12	4.12E+12	3.84E+12
3.35E-07	1.45E+13	1.30E+13	1.20E+13	8.81E+12	8.03E+12	7.40E+12	8.64E+12	8.34E+12	7.50E+12
3.50E-07	3.12E+12	2.87E+12	2.70E+12	1.84E+12	1.64E+12	1.63E+12	1.87E+12	1.74E+12	1.54E+12
3.75E-07	4.87E+12	4.57E+12	4.18E+12	2.85E+12	2.78E+12	2.50E+12	2.91E+12	2.74E+12	2.52E+12
4.00E-07	4.26E+12	3.99E+12	3.67E+12	2.71E+12	2.50E+12	2.23E+12	2.74E+12	2.50E+12	2.30E+12
6.25E-07	3.01E+13	2.70E+13	2.50E+13	1.83E+13	1.67E+13	1.54E+13	1.83E+13	1.68E+13	1.54E+13
1.00E-06	3.02E+13	2.78E+13	2.54E+13	1.84E+13	1.69E+13	1.55E+13	1.82E+13	1.69E+13	1.56E+13
1.77E-06	3.59E+13	3.24E+13	2.94E+13	2.17E+13	1.98E+13	1.84E+13	2.18E+13	1.98E+13	1.78E+13
3.00E-06	3.17E+13	2.94E+13	2.68E+13	1.97E+13	1.83E+13	1.67E+13	2.00E+13	1.81E+13	1.67E+13
4.75E-06	2.77E+13	2.61E+13	2.32E+13	1.70E+13	1.56E+13	1.44E+13	1.73E+13	1.56E+13	1.46E+13
6.00E-06	1.38E+13	1.25E+13	1.22E+13	8.88E+12	8.04E+12	7.64E+12	8.74E+12	8.15E+12	7.49E+12
8.10E-06	1.83E+13	1.64E+13	1.57E+13	1.10E+13	1.01E+13	9.39E+12	1.11E+13	1.04E+13	9.27E+12
1.00E-05	1.31E+13	1.18E+13	1.10E+13	7.95E+12	7.26E+12	6.70E+12	7.87E+12	7.36E+12	6.70E+12
3.00E-05	6.72E+13	6.20E+13	5.61E+13	4.13E+13	3.75E+13	3.45E+13	4.16E+13	3.78E+13	3.46E+13

1.00E-04	7.44E+13	6.74E+13	6.07E+13	4.61E+13	4.15E+13	3.73E+13	4.57E+13	4.20E+13	3.80E+13
5.50E-04	1.05E+14	9.48E+13	8.43E+13	6.55E+13	5.90E+13	5.18E+13	6.59E+13	5.81E+13	5.21E+13
3.00E-03	1.08E+14	9.65E+13	8.46E+13	6.59E+13	5.83E+13	5.11E+13	6.68E+13	5.86E+13	5.16E+13
1.70E-02	1.09E+14	9.22E+13	7.91E+13	6.74E+13	5.64E+13	4.87E+13	6.73E+13	5.71E+13	4.90E+13
2.50E-02	2.54E+13	2.16E+13	1.93E+13	1.59E+13	1.34E+13	1.17E+13	1.58E+13	1.33E+13	1.17E+13
1.00E-01	1.03E+14	8.87E+13	7.80E+13	6.36E+13	5.51E+13	4.74E+13	6.40E+13	5.53E+13	4.84E+13
4.00E-01	1.55E+14	1.31E+14	1.12E+14	9.67E+13	8.09E+13	6.91E+13	9.79E+13	8.15E+13	6.95E+13
9.00E-01	1.21E+14	9.64E+13	7.99E+13	7.52E+13	6.08E+13	4.95E+13	7.58E+13	6.04E+13	4.97E+13
1.40E+00	7.17E+13	5.68E+13	4.56E+13	4.52E+13	3.58E+13	2.87E+13	4.54E+13	3.61E+13	2.91E+13
1.85E+00	4.81E+13	3.77E+13	2.98E+13	3.03E+13	2.41E+13	1.90E+13	3.03E+13	2.40E+13	1.95E+13
2.35E+00	3.41E+13	2.60E+13	2.10E+13	2.21E+13	1.71E+13	1.34E+13	2.21E+13	1.72E+13	1.31E+13
2.48E+00	8.28E+12	6.41E+12	4.76E+12	5.28E+12	4.00E+12	3.09E+12	5.24E+12	3.90E+12	3.04E+12
3.00E+00	2.07E+13	1.51E+13	1.16E+13	1.32E+13	9.71E+12	7.22E+12	1.35E+13	1.01E+13	7.38E+12
4.80E+00	3.11E+13	2.30E+13	1.74E+13	1.97E+13	1.48E+13	1.13E+13	2.01E+13	1.50E+13	1.14E+13
6.43E+00	8.88E+12	6.96E+12	5.48E+12	5.69E+12	4.41E+12	3.30E+12	5.67E+12	4.58E+12	3.46E+12
8.19E+00	2.93E+12	2.14E+12	1.73E+12	1.86E+12	1.38E+12	1.12E+12	1.77E+12	1.49E+12	1.12E+12
2.00E+01	1.11E+12	8.65E+11	5.99E+11	7.13E+11	4.96E+11	4.36E+11	6.66E+11	5.67E+11	4.38E+11

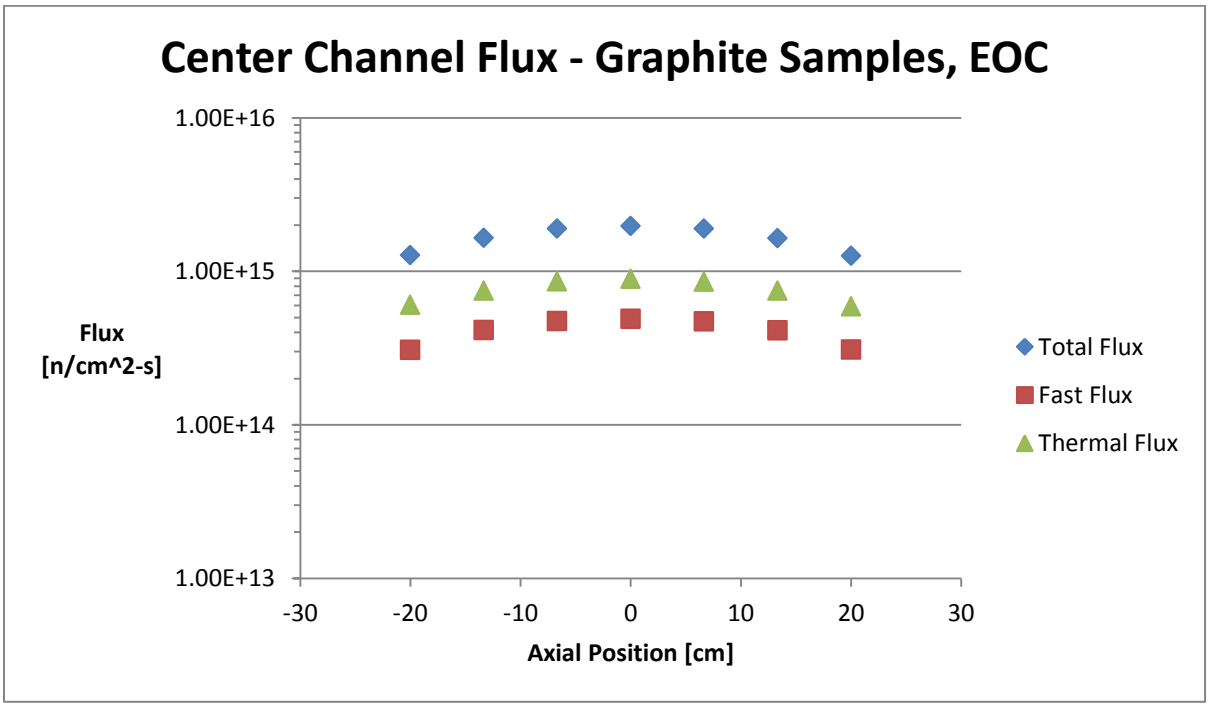

C–3 STEEL SAMPLES, BEGINNING OF CYCLE

C–3.1 Center Channel Flux Tallies

Energy [MeV]	-20.0025 cm	-13.335 cm	-6.6675 cm	Midplane	+6.6675 cm	+13.335 cm	+20.0025 cm
3.00E-09	7.03E+11	9.72E+11	1.20E+12	1.38E+12	1.20E+12	8.86E+11	5.89E+11
7.50E-09	4.19E+12	5.64E+12	7.48E+12	8.17E+12	7.07E+12	5.01E+12	3.39E+12
1.00E-08	3.67E+12	5.35E+12	6.57E+12	7.40E+12	6.07E+12	4.52E+12	3.12E+12
2.53E-08	3.65E+13	5.13E+13	6.68E+13	7.21E+13	6.20E+13	4.62E+13	2.97E+13
3.00E-08	1.36E+13	1.91E+13	2.46E+13	2.68E+13	2.32E+13	1.71E+13	1.11E+13
4.00E-08	2.87E+13	4.08E+13	5.30E+13	5.72E+13	4.95E+13	3.67E+13	2.34E+13
5.00E-08	2.70E+13	3.82E+13	4.92E+13	5.38E+13	4.65E+13	3.43E+13	2.20E+13
7.00E-08	4.27E+13	6.09E+13	7.91E+13	8.63E+13	7.47E+13	5.53E+13	3.54E+13
1.00E-07	3.91E+13	5.71E+13	7.46E+13	8.15E+13	7.06E+13	5.20E+13	3.23E+13
1.50E-07	2.85E+13	4.23E+13	5.56E+13	6.07E+13	5.29E+13	3.95E+13	2.36E+13
2.00E-07	1.11E+13	1.74E+13	2.30E+13	2.54E+13	2.26E+13	1.67E+13	9.85E+12
2.25E-07	3.53E+12	5.29E+12	7.18E+12	7.85E+12	7.19E+12	5.27E+12	3.22E+12
2.50E-07	2.83E+12	4.52E+12	6.06E+12	6.66E+12	5.85E+12	4.45E+12	2.59E+12
2.75E-07	2.42E+12	3.87E+12	5.29E+12	5.60E+12	4.94E+12	3.96E+12	2.17E+12
3.35E-07	4.64E+12	7.59E+12	1.03E+13	1.08E+13	9.90E+12	7.48E+12	4.44E+12
3.50E-07	1.02E+12	1.71E+12	2.19E+12	2.39E+12	2.10E+12	1.60E+12	9.45E+11
3.75E-07	1.60E+12	2.56E+12	3.44E+12	3.89E+12	3.30E+12	2.54E+12	1.49E+12
4.00E-07	1.56E+12	2.40E+12	3.21E+12	3.43E+12	3.11E+12	2.48E+12	1.46E+12
6.25E-07	1.04E+13	1.68E+13	2.17E+13	2.38E+13	2.14E+13	1.65E+13	9.59E+12
1.00E-06	1.07E+13	1.69E+13	2.19E+13	2.41E+13	2.18E+13	1.67E+13	1.04E+13
1.77E-06	1.35E+13	2.06E+13	2.63E+13	2.91E+13	2.63E+13	2.02E+13	1.30E+13
3.00E-06	1.23E+13	1.89E+13	2.43E+13	2.66E+13	2.36E+13	1.88E+13	1.23E+13
4.75E-06	1.08E+13	1.56E+13	1.95E+13	2.18E+13	1.93E+13	1.52E+13	9.87E+12
6.00E-06	5.70E+12	8.52E+12	1.11E+13	1.23E+13	1.10E+13	8.76E+12	5.67E+12
8.10E-06	7.33E+12	1.11E+13	1.45E+13	1.54E+13	1.40E+13	1.12E+13	7.14E+12
1.00E-05	5.27E+12	7.93E+12	9.73E+12	1.08E+13	9.88E+12	7.89E+12	5.20E+12
3.00E-05	2.67E+13	4.04E+13	5.13E+13	5.57E+13	5.09E+13	4.04E+13	2.64E+13
1.00E-04	3.23E+13	4.85E+13	5.92E+13	6.54E+13	5.93E+13	4.83E+13	3.27E+13
5.50E-04	4.77E+13	6.85E+13	8.53E+13	9.47E+13	8.51E+13	7.03E+13	4.92E+13
3.00E-03	4.89E+13	7.21E+13	8.95E+13	9.71E+13	9.02E+13	7.45E+13	5.18E+13
1.70E-02	4.74E+13	6.95E+13	8.75E+13	9.36E+13	8.87E+13	7.28E+13	5.06E+13
2.50E-02	1.13E+13	1.68E+13	2.11E+13	2.25E+13	2.15E+13	1.75E+13	1.23E+13
1.00E-01	4.59E+13	6.78E+13	8.36E+13	9.03E+13	8.59E+13	7.17E+13	4.95E+13
4.00E-01	6.89E+13	1.02E+14	1.26E+14	1.36E+14	1.29E+14	1.08E+14	7.42E+13
9.00E-01	5.20E+13	7.59E+13	9.48E+13	1.03E+14	9.65E+13	8.01E+13	5.58E+13
1.40E+00	3.03E+13	4.34E+13	5.43E+13	5.93E+13	5.57E+13	4.64E+13	3.19E+13

1.85E+00	2.01E+13	2.85E+13	3.58E+13	3.87E+13	3.66E+13	3.00E+13	2.11E+13
2.35E+00	1.34E+13	1.97E+13	2.41E+13	2.68E+13	2.51E+13	2.06E+13	1.51E+13
2.48E+00	3.19E+12	4.75E+12	5.76E+12	6.51E+12	5.95E+12	4.92E+12	3.57E+12
3.00E+00	7.84E+12	1.14E+13	1.44E+13	1.55E+13	1.47E+13	1.22E+13	8.64E+12
4.80E+00	1.19E+13	1.76E+13	2.16E+13	2.35E+13	2.17E+13	1.77E+13	1.29E+13
6.43E+00	3.69E+12	5.16E+12	6.24E+12	6.73E+12	6.23E+12	5.44E+12	3.77E+12
8.19E+00	1.06E+12	1.59E+12	2.01E+12	2.22E+12	2.15E+12	1.64E+12	1.17E+12
2.00E+01	4.33E+11	6.49E+11	7.42E+11	8.62E+11	8.90E+11	7.06E+11	4.48E+11

C–3.2 Radial Flux Tallies

	Midplane			Bottom Row			Top Row		
Energy [MeV]	**Inner Column**	**Center Column**	**Outer Column**	**Inner Column**	**Center Column**	**Outer Column**	**Inner Column**	**Center Column**	**Outer Column**
3.00E-09	1.40E+12	1.38E+12	1.62E+12	6.58E+11	7.03E+11	9.32E+11	4.25E+11	5.89E+11	8.46E+11
7.50E-09	8.37E+12	8.17E+12	9.56E+12	3.81E+12	4.19E+12	5.30E+12	2.59E+12	3.39E+12	4.74E+12
1.00E-08	7.46E+12	7.40E+12	8.39E+12	3.35E+12	3.67E+12	4.71E+12	2.20E+12	3.12E+12	3.95E+12
2.53E-08	7.38E+13	7.21E+13	8.29E+13	3.17E+13	3.65E+13	4.60E+13	2.22E+13	2.97E+13	3.98E+13
3.00E-08	2.70E+13	2.68E+13	3.04E+13	1.18E+13	1.36E+13	1.65E+13	8.22E+12	1.11E+13	1.45E+13
4.00E-08	5.76E+13	5.72E+13	6.46E+13	2.45E+13	2.87E+13	3.51E+13	1.78E+13	2.34E+13	3.09E+13
5.00E-08	5.35E+13	5.38E+13	5.90E+13	2.32E+13	2.70E+13	3.26E+13	1.65E+13	2.20E+13	2.82E+13
7.00E-08	8.56E+13	8.63E+13	9.42E+13	3.67E+13	4.27E+13	5.07E+13	2.69E+13	3.54E+13	4.48E+13
1.00E-07	8.15E+13	8.15E+13	8.67E+13	3.37E+13	3.91E+13	4.62E+13	2.50E+13	3.23E+13	4.10E+13
1.50E-07	6.13E+13	6.07E+13	6.28E+13	2.48E+13	2.85E+13	3.20E+13	1.89E+13	2.36E+13	2.88E+13
2.00E-07	2.65E+13	2.54E+13	2.50E+13	1.04E+13	1.11E+13	1.21E+13	7.96E+12	9.85E+12	1.11E+13
2.25E-07	8.64E+12	7.85E+12	7.58E+12	3.12E+12	3.53E+12	3.68E+12	2.67E+12	3.22E+12	3.49E+12
2.50E-07	7.17E+12	6.66E+12	5.90E+12	2.57E+12	2.83E+12	2.88E+12	2.26E+12	2.59E+12	2.75E+12
2.75E-07	6.18E+12	5.60E+12	5.08E+12	2.26E+12	2.42E+12	2.28E+12	1.91E+12	2.17E+12	2.34E+12
3.35E-07	1.22E+13	1.08E+13	1.01E+13	4.48E+12	4.64E+12	4.79E+12	3.83E+12	4.44E+12	4.63E+12
3.50E-07	2.67E+12	2.39E+12	2.25E+12	8.99E+11	1.02E+12	9.57E+11	8.26E+11	9.45E+11	1.01E+12
3.75E-07	3.96E+12	3.89E+12	3.51E+12	1.50E+12	1.60E+12	1.59E+12	1.33E+12	1.49E+12	1.52E+12
4.00E-07	3.95E+12	3.43E+12	3.21E+12	1.48E+12	1.56E+12	1.50E+12	1.10E+12	1.46E+12	1.53E+12
6.25E-07	2.63E+13	2.38E+13	2.20E+13	9.98E+12	1.04E+13	1.05E+13	8.62E+12	9.59E+12	1.00E+13
1.00E-06	2.68E+13	2.41E+13	2.24E+13	1.06E+13	1.07E+13	1.08E+13	9.70E+12	1.04E+13	1.04E+13
1.77E-06	3.22E+13	2.91E+13	2.71E+13	1.29E+13	1.35E+13	1.29E+13	1.21E+13	1.30E+13	1.26E+13
3.00E-06	2.93E+13	2.66E+13	2.42E+13	1.23E+13	1.23E+13	1.21E+13	1.13E+13	1.23E+13	1.19E+13
4.75E-06	2.45E+13	2.18E+13	2.04E+13	1.08E+13	1.08E+13	1.01E+13	9.71E+12	9.87E+12	9.83E+12
6.00E-06	1.32E+13	1.23E+13	1.07E+13	5.82E+12	5.70E+12	5.34E+12	5.40E+12	5.67E+12	5.59E+12
8.10E-06	1.70E+13	1.54E+13	1.41E+13	7.50E+12	7.33E+12	6.99E+12	7.15E+12	7.14E+12	7.17E+12
1.00E-05	1.24E+13	1.08E+13	1.01E+13	5.53E+12	5.27E+12	5.06E+12	5.10E+12	5.20E+12	4.88E+12
3.00E-05	6.24E+13	5.57E+13	5.00E+13	2.84E+13	2.67E+13	2.54E+13	2.71E+13	2.64E+13	2.59E+13

1.00E-04	7.30E+13	6.54E+13	5.94E+13	3.45E+13	3.23E+13	2.99E+13	3.38E+13	3.27E+13	3.12E+13
5.50E-04	1.05E+14	9.47E+13	8.31E+13	5.13E+13	4.77E+13	4.31E+13	5.23E+13	4.92E+13	4.51E+13
3.00E-03	1.10E+14	9.71E+13	8.43E+13	5.53E+13	4.89E+13	4.33E+13	5.79E+13	5.18E+13	4.58E+13
1.70E-02	1.12E+14	9.36E+13	8.05E+13	5.63E+13	4.74E+13	4.06E+13	6.10E+13	5.06E+13	4.45E+13
2.50E-02	2.68E+13	2.25E+13	2.00E+13	1.37E+13	1.13E+13	9.74E+12	1.46E+13	1.23E+13	1.12E+13
1.00E-01	1.06E+14	9.03E+13	7.92E+13	5.24E+13	4.59E+13	4.07E+13	5.83E+13	4.95E+13	4.28E+13
4.00E-01	1.63E+14	1.36E+14	1.17E+14	8.20E+13	6.89E+13	5.91E+13	8.78E+13	7.42E+13	6.42E+13
9.00E-01	1.28E+14	1.03E+14	8.38E+13	6.33E+13	5.20E+13	4.33E+13	6.94E+13	5.58E+13	4.60E+13
1.40E+00	7.57E+13	5.93E+13	4.76E+13	3.74E+13	3.03E+13	2.46E+13	4.04E+13	3.19E+13	2.60E+13
1.85E+00	4.85E+13	3.87E+13	3.14E+13	2.50E+13	2.01E+13	1.63E+13	2.65E+13	2.11E+13	1.76E+13
2.35E+00	3.49E+13	2.68E+13	2.09E+13	1.72E+13	1.34E+13	1.08E+13	1.93E+13	1.51E+13	1.20E+13
2.48E+00	8.31E+12	6.51E+12	4.86E+12	4.47E+12	3.19E+12	2.51E+12	4.81E+12	3.57E+12	2.70E+12
3.00E+00	2.10E+13	1.55E+13	1.16E+13	1.05E+13	7.84E+12	6.03E+12	1.15E+13	8.64E+12	6.05E+12
4.80E+00	3.15E+13	2.35E+13	1.78E+13	1.56E+13	1.19E+13	9.08E+12	1.73E+13	1.29E+13	9.83E+12
6.43E+00	9.14E+12	6.73E+12	5.24E+12	4.60E+12	3.69E+12	2.77E+12	4.70E+12	3.77E+12	3.01E+12
8.19E+00	2.73E+12	2.22E+12	1.72E+12	1.52E+12	1.06E+12	8.53E+11	1.56E+12	1.17E+12	1.04E+12
2.00E+01	1.12E+12	8.62E+11	6.78E+11	5.37E+11	4.33E+11	3.29E+11	6.87E+11	4.48E+11	3.79E+11

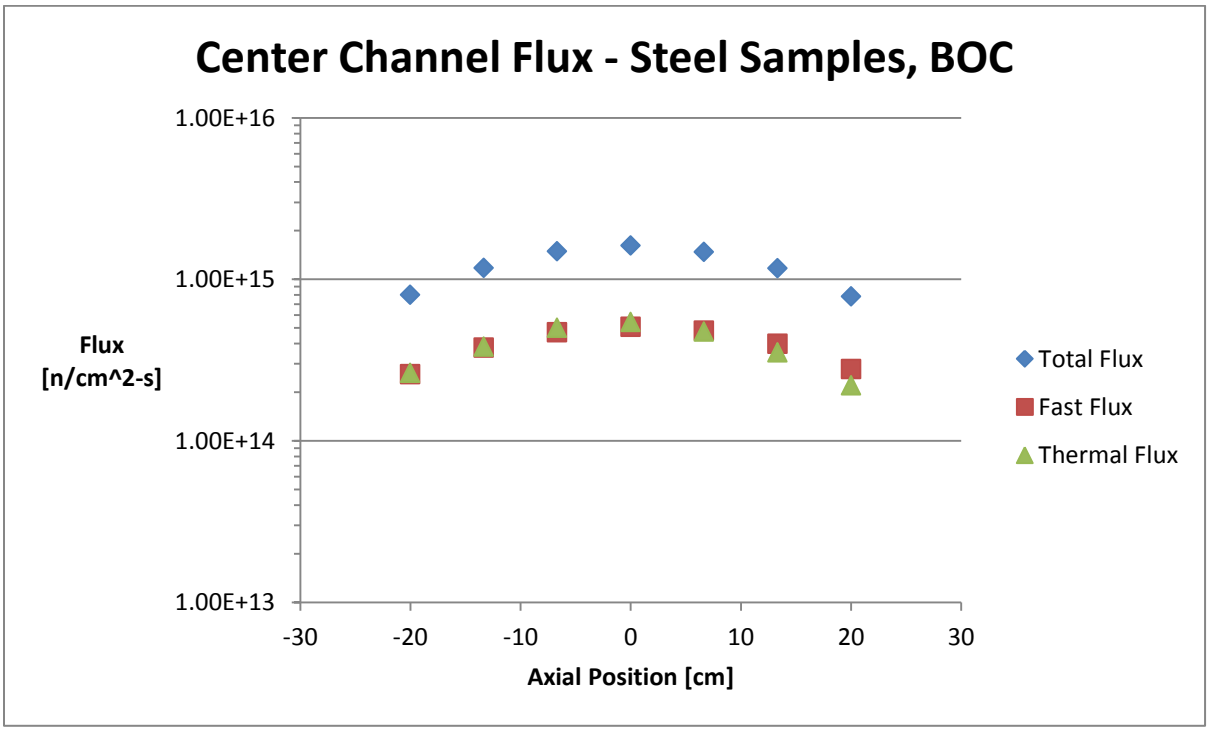

C–4 STEEL SAMPLES, END OF CYCLE

C–4.1 Center Channel Flux Tallies

Energy [MeV]	-20.0025 cm	-13.335 cm	-6.6675 cm	Midplane	+6.6675 cm	+13.335 cm	+20.0025 cm
3.00E-09	7.03E+11	9.72E+11	1.20E+12	1.38E+12	1.20E+12	8.86E+11	5.89E+11
7.50E-09	4.19E+12	5.64E+12	7.48E+12	8.17E+12	7.07E+12	5.01E+12	3.39E+12
1.00E-08	3.67E+12	5.35E+12	6.57E+12	7.40E+12	6.07E+12	4.52E+12	3.12E+12
2.53E-08	3.65E+13	5.13E+13	6.68E+13	7.21E+13	6.20E+13	4.62E+13	2.97E+13
3.00E-08	1.36E+13	1.91E+13	2.46E+13	2.68E+13	2.32E+13	1.71E+13	1.11E+13
4.00E-08	2.87E+13	4.08E+13	5.30E+13	5.72E+13	4.95E+13	3.67E+13	2.34E+13
5.00E-08	2.70E+13	3.82E+13	4.92E+13	5.38E+13	4.65E+13	3.43E+13	2.20E+13
7.00E-08	4.27E+13	6.09E+13	7.91E+13	8.63E+13	7.47E+13	5.53E+13	3.54E+13
1.00E-07	3.91E+13	5.71E+13	7.46E+13	8.15E+13	7.06E+13	5.20E+13	3.23E+13
1.50E-07	2.85E+13	4.23E+13	5.56E+13	6.07E+13	5.29E+13	3.95E+13	2.36E+13
2.00E-07	1.11E+13	1.74E+13	2.30E+13	2.54E+13	2.26E+13	1.67E+13	9.85E+12
2.25E-07	3.53E+12	5.29E+12	7.18E+12	7.85E+12	7.19E+12	5.27E+12	3.22E+12
2.50E-07	2.83E+12	4.52E+12	6.06E+12	6.66E+12	5.85E+12	4.45E+12	2.59E+12
2.75E-07	2.42E+12	3.87E+12	5.29E+12	5.60E+12	4.94E+12	3.96E+12	2.17E+12
3.35E-07	4.64E+12	7.59E+12	1.03E+13	1.08E+13	9.90E+12	7.48E+12	4.44E+12
3.50E-07	1.02E+12	1.71E+12	2.19E+12	2.39E+12	2.10E+12	1.60E+12	9.45E+11
3.75E-07	1.60E+12	2.56E+12	3.44E+12	3.89E+12	3.30E+12	2.54E+12	1.49E+12
4.00E-07	1.56E+12	2.40E+12	3.21E+12	3.43E+12	3.11E+12	2.48E+12	1.46E+12
6.25E-07	1.04E+13	1.68E+13	2.17E+13	2.38E+13	2.14E+13	1.65E+13	9.59E+12
1.00E-06	1.07E+13	1.69E+13	2.19E+13	2.41E+13	2.18E+13	1.67E+13	1.04E+13
1.77E-06	1.35E+13	2.06E+13	2.63E+13	2.91E+13	2.63E+13	2.02E+13	1.30E+13
3.00E-06	1.23E+13	1.89E+13	2.43E+13	2.66E+13	2.36E+13	1.88E+13	1.23E+13
4.75E-06	1.08E+13	1.56E+13	1.95E+13	2.18E+13	1.93E+13	1.52E+13	9.87E+12
6.00E-06	5.70E+12	8.52E+12	1.11E+13	1.23E+13	1.10E+13	8.76E+12	5.67E+12
8.10E-06	7.33E+12	1.11E+13	1.45E+13	1.54E+13	1.40E+13	1.12E+13	7.14E+12
1.00E-05	5.27E+12	7.93E+12	9.73E+12	1.08E+13	9.88E+12	7.89E+12	5.20E+12
3.00E-05	2.67E+13	4.04E+13	5.13E+13	5.57E+13	5.09E+13	4.04E+13	2.64E+13
1.00E-04	3.23E+13	4.85E+13	5.92E+13	6.54E+13	5.93E+13	4.83E+13	3.27E+13
5.50E-04	4.77E+13	6.85E+13	8.53E+13	9.47E+13	8.51E+13	7.03E+13	4.92E+13
3.00E-03	4.89E+13	7.21E+13	8.95E+13	9.71E+13	9.02E+13	7.45E+13	5.18E+13
1.70E-02	4.74E+13	6.95E+13	8.75E+13	9.36E+13	8.87E+13	7.28E+13	5.06E+13
2.50E-02	1.13E+13	1.68E+13	2.11E+13	2.25E+13	2.15E+13	1.75E+13	1.23E+13
1.00E-01	4.59E+13	6.78E+13	8.36E+13	9.03E+13	8.59E+13	7.17E+13	4.95E+13
4.00E-01	6.89E+13	1.02E+14	1.26E+14	1.36E+14	1.29E+14	1.08E+14	7.42E+13
9.00E-01	5.20E+13	7.59E+13	9.48E+13	1.03E+14	9.65E+13	8.01E+13	5.58E+13
1.40E+00	3.03E+13	4.34E+13	5.43E+13	5.93E+13	5.57E+13	4.64E+13	3.19E+13

1.85E+00	2.01E+13	2.85E+13	3.58E+13	3.87E+13	3.66E+13	3.00E+13	2.11E+13
2.35E+00	1.34E+13	1.97E+13	2.41E+13	2.68E+13	2.51E+13	2.06E+13	1.51E+13
2.48E+00	3.19E+12	4.75E+12	5.76E+12	6.51E+12	5.95E+12	4.92E+12	3.57E+12
3.00E+00	7.84E+12	1.14E+13	1.44E+13	1.55E+13	1.47E+13	1.22E+13	8.64E+12
4.80E+00	1.19E+13	1.76E+13	2.16E+13	2.35E+13	2.17E+13	1.77E+13	1.29E+13
6.43E+00	3.69E+12	5.16E+12	6.24E+12	6.73E+12	6.23E+12	5.44E+12	3.77E+12
8.19E+00	1.06E+12	1.59E+12	2.01E+12	2.22E+12	2.15E+12	1.64E+12	1.17E+12
2.00E+01	4.33E+11	6.49E+11	7.42E+11	8.62E+11	8.90E+11	7.06E+11	4.48E+11

C–4.2 Radial Flux Tallies

	Midplane			Bottom Row			Top Row		
Energy [MeV]	**Inner Column**	**Center Column**	**Outer Column**	**Inner Column**	**Center Column**	**Outer Column**	**Inner Column**	**Center Column**	**Outer Column**
3.00E-09	2.02E+12	1.82E+12	2.15E+12	1.39E+12	1.24E+12	1.48E+12	1.34E+12	1.25E+12	1.42E+12
7.50E-09	1.21E+13	1.09E+13	1.24E+13	8.45E+12	7.62E+12	8.77E+12	8.12E+12	7.37E+12	8.82E+12
1.00E-08	1.06E+13	9.62E+12	1.11E+13	7.46E+12	6.70E+12	7.79E+12	7.17E+12	6.63E+12	7.46E+12
2.53E-08	1.06E+14	9.79E+13	1.08E+14	7.19E+13	6.82E+13	7.66E+13	6.99E+13	6.67E+13	7.44E+13
3.00E-08	3.90E+13	3.63E+13	3.98E+13	2.61E+13	2.54E+13	2.76E+13	2.55E+13	2.45E+13	2.73E+13
4.00E-08	8.19E+13	7.80E+13	8.36E+13	5.59E+13	5.44E+13	5.90E+13	5.44E+13	5.28E+13	5.73E+13
5.00E-08	7.53E+13	7.18E+13	7.74E+13	5.11E+13	5.04E+13	5.40E+13	5.02E+13	4.89E+13	5.30E+13
7.00E-08	1.20E+14	1.15E+14	1.21E+14	8.16E+13	7.95E+13	8.52E+13	7.94E+13	7.74E+13	8.33E+13
1.00E-07	1.12E+14	1.07E+14	1.11E+14	7.50E+13	7.26E+13	7.71E+13	7.29E+13	7.16E+13	7.47E+13
1.50E-07	8.06E+13	7.68E+13	7.76E+13	5.32E+13	5.16E+13	5.27E+13	5.15E+13	5.02E+13	5.17E+13
2.00E-07	3.17E+13	2.99E+13	2.91E+13	2.07E+13	1.90E+13	1.87E+13	2.01E+13	1.88E+13	1.85E+13
2.25E-07	9.74E+12	9.17E+12	8.50E+12	6.00E+12	5.42E+12	5.27E+12	6.22E+12	5.52E+12	5.67E+12
2.50E-07	7.76E+12	7.44E+12	6.80E+12	5.02E+12	4.54E+12	4.17E+12	4.79E+12	4.61E+12	4.40E+12
2.75E-07	6.71E+12	5.95E+12	6.00E+12	4.28E+12	3.65E+12	3.52E+12	4.22E+12	3.89E+12	3.50E+12
3.35E-07	1.34E+13	1.18E+13	1.08E+13	8.30E+12	7.44E+12	6.84E+12	8.00E+12	7.78E+12	7.09E+12
3.50E-07	2.95E+12	2.64E+12	2.46E+12	1.78E+12	1.59E+12	1.49E+12	1.68E+12	1.74E+12	1.56E+12
3.75E-07	4.47E+12	4.08E+12	3.78E+12	2.77E+12	2.51E+12	2.29E+12	2.69E+12	2.59E+12	2.38E+12
4.00E-07	4.31E+12	3.78E+12	3.59E+12	2.50E+12	2.35E+12	2.05E+12	2.52E+12	2.17E+12	2.19E+12
6.25E-07	2.88E+13	2.58E+13	2.35E+13	1.78E+13	1.61E+13	1.43E+13	1.76E+13	1.61E+13	1.43E+13
1.00E-06	2.95E+13	2.67E+13	2.37E+13	1.79E+13	1.62E+13	1.47E+13	1.78E+13	1.67E+13	1.47E+13
1.77E-06	3.43E+13	3.14E+13	2.84E+13	2.13E+13	1.94E+13	1.75E+13	2.11E+13	1.89E+13	1.73E+13
3.00E-06	3.12E+13	2.81E+13	2.59E+13	1.93E+13	1.78E+13	1.59E+13	1.93E+13	1.68E+13	1.59E+13
4.75E-06	2.59E+13	2.34E+13	2.14E+13	1.60E+13	1.44E+13	1.31E+13	1.61E+13	1.43E+13	1.32E+13
6.00E-06	1.37E+13	1.23E+13	1.15E+13	8.67E+12	7.55E+12	7.17E+12	8.31E+12	8.12E+12	6.99E+12
8.10E-06	1.76E+13	1.60E+13	1.44E+13	1.11E+13	9.62E+12	8.99E+12	1.09E+13	9.89E+12	9.07E+12
1.00E-05	1.24E+13	1.13E+13	1.06E+13	7.72E+12	7.08E+12	6.51E+12	7.78E+12	6.90E+12	6.28E+12
3.00E-05	6.37E+13	5.66E+13	5.10E+13	3.92E+13	3.52E+13	3.13E+13	3.93E+13	3.53E+13	3.19E+13

1.00E-04	7.39E+13	6.58E+13	5.91E+13	4.50E+13	4.01E+13	3.66E+13	4.54E+13	4.11E+13	3.58E+13
5.50E-04	1.05E+14	9.30E+13	8.25E+13	6.54E+13	5.68E+13	5.02E+13	6.49E+13	5.71E+13	5.07E+13
3.00E-03	1.06E+14	9.31E+13	8.23E+13	6.60E+13	5.74E+13	4.92E+13	6.63E+13	5.73E+13	5.01E+13
1.70E-02	1.08E+14	9.05E+13	7.78E+13	6.77E+13	5.52E+13	4.77E+13	6.69E+13	5.57E+13	4.75E+13
2.50E-02	2.51E+13	2.15E+13	1.89E+13	1.61E+13	1.34E+13	1.19E+13	1.53E+13	1.35E+13	1.18E+13
1.00E-01	1.00E+14	8.64E+13	7.67E+13	6.26E+13	5.33E+13	4.73E+13	6.27E+13	5.35E+13	4.75E+13
4.00E-01	1.56E+14	1.30E+14	1.12E+14	9.67E+13	8.07E+13	6.95E+13	9.71E+13	8.16E+13	7.00E+13
9.00E-01	1.23E+14	9.78E+13	8.08E+13	7.73E+13	6.12E+13	5.03E+13	7.69E+13	6.20E+13	5.02E+13
1.40E+00	7.18E+13	5.71E+13	4.55E+13	4.56E+13	3.61E+13	2.90E+13	4.58E+13	3.61E+13	2.90E+13
1.85E+00	4.72E+13	3.74E+13	3.02E+13	3.03E+13	2.35E+13	1.88E+13	3.01E+13	2.39E+13	1.91E+13
2.35E+00	3.36E+13	2.62E+13	1.99E+13	2.15E+13	1.62E+13	1.28E+13	2.11E+13	1.63E+13	1.24E+13
2.48E+00	8.10E+12	6.15E+12	4.45E+12	5.29E+12	3.93E+12	2.90E+12	5.29E+12	3.92E+12	2.96E+12
3.00E+00	2.03E+13	1.49E+13	1.12E+13	1.28E+13	9.48E+12	6.64E+12	1.27E+13	9.75E+12	7.31E+12
4.80E+00	3.03E+13	2.23E+13	1.68E+13	1.94E+13	1.44E+13	1.07E+13	1.93E+13	1.45E+13	1.10E+13
6.43E+00	8.57E+12	6.61E+12	4.95E+12	5.27E+12	4.18E+12	3.18E+12	5.62E+12	4.22E+12	3.04E+12
8.19E+00	2.67E+12	1.96E+12	1.61E+12	1.76E+12	1.34E+12	1.01E+12	1.81E+12	1.30E+12	9.97E+11
2.00E+01	1.01E+12	8.02E+11	6.31E+11	7.24E+11	5.25E+11	4.01E+11	7.88E+11	5.04E+11	4.00E+11

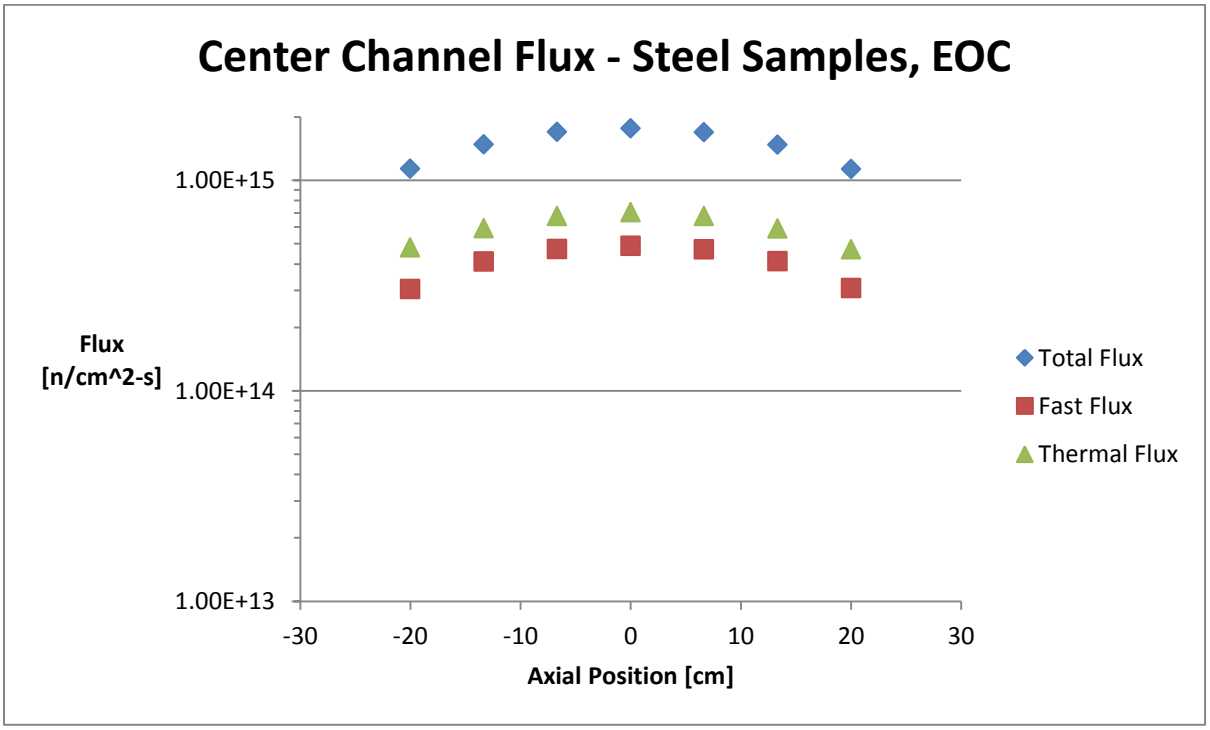

C–5 STEEL SAMPLES, BEGINNING OF CYCLE – TWO ASSEMBLIES (3B–7B)

C–5.1 7B Center Channel Flux Tallies

Energy [MeV]	-20.0025 cm	-13.335 cm	-6.6675 cm	Midplane	+6.6675 cm	+13.335 cm	+20.0025 cm
3.00E-09	6.91E+11	9.94E+11	1.27E+12	1.43E+12	1.14E+12	8.30E+11	5.42E+11
7.50E-09	4.24E+12	5.88E+12	7.45E+12	8.13E+12	7.24E+12	5.15E+12	3.45E+12
1.00E-08	3.61E+12	5.17E+12	6.62E+12	7.25E+12	6.16E+12	4.58E+12	2.98E+12
2.53E-08	3.69E+13	5.20E+13	6.77E+13	7.27E+13	6.24E+13	4.67E+13	3.02E+13
3.00E-08	1.36E+13	1.89E+13	2.47E+13	2.69E+13	2.34E+13	1.72E+13	1.13E+13
4.00E-08	2.91E+13	4.15E+13	5.32E+13	5.78E+13	5.01E+13	3.69E+13	2.41E+13
5.00E-08	2.70E+13	3.80E+13	4.95E+13	5.42E+13	4.62E+13	3.46E+13	2.21E+13
7.00E-08	4.30E+13	6.12E+13	8.02E+13	8.69E+13	7.51E+13	5.49E+13	3.54E+13
1.00E-07	3.94E+13	5.72E+13	7.49E+13	8.16E+13	7.14E+13	5.22E+13	3.31E+13
1.50E-07	2.90E+13	4.30E+13	5.59E+13	6.09E+13	5.34E+13	3.96E+13	2.44E+13
2.00E-07	1.11E+13	1.78E+13	2.30E+13	2.52E+13	2.23E+13	1.65E+13	9.82E+12
2.25E-07	3.45E+12	5.39E+12	7.23E+12	7.90E+12	6.98E+12	5.34E+12	3.10E+12
2.50E-07	2.92E+12	4.46E+12	6.03E+12	6.86E+12	5.98E+12	4.45E+12	2.55E+12
2.75E-07	2.47E+12	3.83E+12	5.12E+12	5.64E+12	5.06E+12	3.76E+12	2.16E+12
3.35E-07	4.91E+12	7.66E+12	1.01E+13	1.10E+13	9.61E+12	7.46E+12	4.41E+12
3.50E-07	1.04E+12	1.67E+12	2.28E+12	2.42E+12	2.12E+12	1.70E+12	9.18E+11
3.75E-07	1.68E+12	2.69E+12	3.19E+12	4.08E+12	3.63E+12	2.66E+12	1.56E+12
4.00E-07	1.64E+12	2.44E+12	3.26E+12	3.51E+12	3.24E+12	2.30E+12	1.42E+12
6.25E-07	1.02E+13	1.66E+13	2.18E+13	2.42E+13	2.15E+13	1.63E+13	1.02E+13
1.00E-06	1.10E+13	1.70E+13	2.25E+13	2.42E+13	2.21E+13	1.71E+13	1.06E+13
1.77E-06	1.37E+13	2.09E+13	2.65E+13	2.91E+13	2.64E+13	2.06E+13	1.33E+13
3.00E-06	1.27E+13	1.93E+13	2.45E+13	2.73E+13	2.42E+13	1.83E+13	1.20E+13
4.75E-06	1.04E+13	1.57E+13	2.02E+13	2.23E+13	1.97E+13	1.55E+13	1.05E+13
6.00E-06	5.88E+12	8.82E+12	1.10E+13	1.21E+13	1.09E+13	8.63E+12	5.80E+12
8.10E-06	7.46E+12	1.14E+13	1.43E+13	1.53E+13	1.42E+13	1.12E+13	7.42E+12
1.00E-05	5.42E+12	8.14E+12	1.02E+13	1.12E+13	1.00E+13	8.02E+12	5.40E+12
3.00E-05	2.70E+13	4.11E+13	5.08E+13	5.60E+13	5.08E+13	4.11E+13	2.75E+13
1.00E-04	3.26E+13	4.83E+13	6.02E+13	6.67E+13	5.89E+13	4.79E+13	3.34E+13
5.50E-04	4.77E+13	6.92E+13	8.59E+13	9.33E+13	8.67E+13	7.07E+13	4.94E+13
3.00E-03	4.94E+13	7.22E+13	9.01E+13	9.62E+13	9.03E+13	7.54E+13	5.18E+13
1.70E-02	4.74E+13	7.13E+13	8.77E+13	9.41E+13	8.98E+13	7.27E+13	5.11E+13
2.50E-02	1.14E+13	1.72E+13	2.15E+13	2.29E+13	2.13E+13	1.80E+13	1.24E+13
1.00E-01	4.62E+13	6.86E+13	8.35E+13	9.06E+13	8.61E+13	7.13E+13	4.86E+13
4.00E-01	6.90E+13	1.04E+14	1.28E+14	1.37E+14	1.31E+14	1.08E+14	7.55E+13
9.00E-01	5.29E+13	7.68E+13	9.69E+13	1.03E+14	9.76E+13	8.11E+13	5.63E+13
1.40E+00	3.04E+13	4.36E+13	5.44E+13	6.00E+13	5.60E+13	4.64E+13	3.29E+13

1.85E+00	1.98E+13	2.88E+13	3.60E+13	3.85E+13	3.62E+13	3.02E+13	2.16E+13
2.35E+00	1.38E+13	1.99E+13	2.50E+13	2.71E+13	2.54E+13	2.09E+13	1.52E+13
2.48E+00	3.29E+12	4.91E+12	5.91E+12	6.29E+12	5.96E+12	4.95E+12	3.60E+12
3.00E+00	7.89E+12	1.16E+13	1.45E+13	1.55E+13	1.47E+13	1.22E+13	8.48E+12
4.80E+00	1.20E+13	1.73E+13	2.14E+13	2.36E+13	2.24E+13	1.82E+13	1.32E+13
6.43E+00	3.50E+12	4.97E+12	6.03E+12	6.89E+12	6.39E+12	5.30E+12	3.94E+12
8.19E+00	1.21E+12	1.66E+12	1.98E+12	2.15E+12	2.09E+12	1.66E+12	1.24E+12
2.00E+01	4.83E+11	6.48E+11	7.64E+11	9.14E+11	7.58E+11	6.38E+11	4.51E+11

C–5.2 7B Radial Flux Tallies

	Midplane			Bottom Row			Top Row		
Energy [MeV]	**Inner Column**	**Center Column**	**Outer Column**	**Inner Column**	**Center Column**	**Outer Column**	**Inner Column**	**Center Column**	**Outer Column**
3.00E-09	1.47E+12	1.43E+12	1.64E+12	6.44E+11	6.91E+11	9.17E+11	4.43E+11	5.42E+11	8.35E+11
7.50E-09	8.62E+12	8.13E+12	9.59E+12	3.66E+12	4.24E+12	5.21E+12	2.66E+12	3.45E+12	4.58E+12
1.00E-08	7.56E+12	7.25E+12	8.64E+12	3.19E+12	3.61E+12	4.52E+12	2.32E+12	2.98E+12	4.08E+12
2.53E-08	7.45E+13	7.27E+13	8.38E+13	3.18E+13	3.69E+13	4.63E+13	2.29E+13	3.02E+13	4.03E+13
3.00E-08	2.70E+13	2.69E+13	3.07E+13	1.18E+13	1.36E+13	1.65E+13	8.46E+12	1.13E+13	1.48E+13
4.00E-08	5.74E+13	5.78E+13	6.49E+13	2.50E+13	2.91E+13	3.56E+13	1.85E+13	2.41E+13	3.12E+13
5.00E-08	5.46E+13	5.42E+13	6.00E+13	2.30E+13	2.70E+13	3.23E+13	1.67E+13	2.21E+13	2.85E+13
7.00E-08	8.68E+13	8.69E+13	9.47E+13	3.65E+13	4.30E+13	5.13E+13	2.69E+13	3.54E+13	4.49E+13
1.00E-07	8.18E+13	8.16E+13	8.71E+13	3.40E+13	3.94E+13	4.65E+13	2.55E+13	3.31E+13	4.08E+13
1.50E-07	6.21E+13	6.09E+13	6.35E+13	2.50E+13	2.90E+13	3.29E+13	1.94E+13	2.44E+13	2.92E+13
2.00E-07	2.69E+13	2.52E+13	2.50E+13	1.01E+13	1.11E+13	1.24E+13	8.17E+12	9.82E+12	1.12E+13
2.25E-07	8.37E+12	7.90E+12	7.65E+12	3.26E+12	3.45E+12	3.48E+12	2.90E+12	3.10E+12	3.55E+12
2.50E-07	7.03E+12	6.86E+12	6.12E+12	2.70E+12	2.92E+12	2.89E+12	2.29E+12	2.55E+12	2.68E+12
2.75E-07	6.15E+12	5.64E+12	5.36E+12	2.27E+12	2.47E+12	2.38E+12	1.88E+12	2.16E+12	2.26E+12
3.35E-07	1.22E+13	1.10E+13	1.04E+13	4.66E+12	4.91E+12	4.89E+12	3.90E+12	4.41E+12	4.56E+12
3.50E-07	2.69E+12	2.42E+12	2.23E+12	9.60E+11	1.04E+12	1.10E+12	8.95E+11	9.18E+11	1.02E+12
3.75E-07	4.37E+12	4.08E+12	3.44E+12	1.50E+12	1.68E+12	1.57E+12	1.37E+12	1.56E+12	1.61E+12
4.00E-07	3.86E+12	3.51E+12	3.19E+12	1.40E+12	1.64E+12	1.45E+12	1.32E+12	1.42E+12	1.45E+12
6.25E-07	2.59E+13	2.42E+13	2.22E+13	1.00E+13	1.02E+13	1.05E+13	8.83E+12	1.02E+13	1.00E+13
1.00E-06	2.68E+13	2.42E+13	2.28E+13	1.09E+13	1.10E+13	1.06E+13	9.38E+12	1.06E+13	1.09E+13
1.77E-06	3.24E+13	2.91E+13	2.67E+13	1.33E+13	1.37E+13	1.32E+13	1.22E+13	1.33E+13	1.30E+13
3.00E-06	2.93E+13	2.73E+13	2.47E+13	1.24E+13	1.27E+13	1.16E+13	1.14E+13	1.20E+13	1.19E+13
4.75E-06	2.42E+13	2.23E+13	2.06E+13	1.05E+13	1.04E+13	1.00E+13	1.00E+13	1.05E+13	1.04E+13
6.00E-06	1.32E+13	1.21E+13	1.12E+13	5.98E+12	5.88E+12	5.40E+12	5.66E+12	5.80E+12	5.41E+12
8.10E-06	1.69E+13	1.53E+13	1.44E+13	7.41E+12	7.46E+12	7.16E+12	7.24E+12	7.42E+12	6.77E+12
1.00E-05	1.20E+13	1.12E+13	9.94E+12	5.35E+12	5.42E+12	4.91E+12	5.36E+12	5.40E+12	4.89E+12
3.00E-05	6.29E+13	5.60E+13	5.10E+13	2.83E+13	2.70E+13	2.54E+13	2.80E+13	2.75E+13	2.63E+13
1.00E-04	7.33E+13	6.67E+13	5.97E+13	3.45E+13	3.26E+13	2.97E+13	3.41E+13	3.34E+13	3.16E+13

5.50E-04	1.06E+14	9.33E+13	8.49E+13	5.17E+13	4.77E+13	4.30E+13	5.31E+13	4.94E+13	4.50E+13
3.00E-03	1.11E+14	9.62E+13	8.41E+13	5.62E+13	4.94E+13	4.39E+13	5.77E+13	5.18E+13	4.61E+13
1.70E-02	1.13E+14	9.41E+13	8.10E+13	5.74E+13	4.74E+13	4.13E+13	6.10E+13	5.11E+13	4.52E+13
2.50E-02	2.68E+13	2.29E+13	1.99E+13	1.33E+13	1.14E+13	1.05E+13	1.44E+13	1.24E+13	1.10E+13
1.00E-01	1.06E+14	9.06E+13	8.00E+13	5.31E+13	4.62E+13	4.03E+13	5.73E+13	4.86E+13	4.33E+13
4.00E-01	1.65E+14	1.37E+14	1.18E+14	8.23E+13	6.90E+13	6.05E+13	8.87E+13	7.55E+13	6.55E+13
9.00E-01	1.30E+14	1.03E+14	8.51E+13	6.42E+13	5.29E+13	4.35E+13	6.96E+13	5.63E+13	4.61E+13
1.40E+00	7.58E+13	6.00E+13	4.82E+13	3.74E+13	3.04E+13	2.43E+13	4.09E+13	3.29E+13	2.57E+13
1.85E+00	4.94E+13	3.85E+13	3.15E+13	2.51E+13	1.98E+13	1.65E+13	2.68E+13	2.16E+13	1.77E+13
2.35E+00	3.55E+13	2.71E+13	2.10E+13	1.82E+13	1.38E+13	1.08E+13	1.91E+13	1.52E+13	1.18E+13
2.48E+00	8.76E+12	6.29E+12	4.90E+12	4.39E+12	3.29E+12	2.46E+12	4.82E+12	3.60E+12	2.72E+12
3.00E+00	2.14E+13	1.55E+13	1.16E+13	1.07E+13	7.89E+12	5.95E+12	1.16E+13	8.48E+12	6.27E+12
4.80E+00	3.21E+13	2.36E+13	1.73E+13	1.60E+13	1.20E+13	9.31E+12	1.72E+13	1.32E+13	9.82E+12
6.43E+00	8.98E+12	6.89E+12	4.93E+12	4.55E+12	3.50E+12	2.74E+12	5.04E+12	3.94E+12	2.88E+12
8.19E+00	2.91E+12	2.15E+12	1.65E+12	1.67E+12	1.21E+12	8.69E+11	1.68E+12	1.24E+12	9.69E+11
2.00E+01	1.15E+12	9.14E+11	6.01E+11	4.60E+11	4.83E+11	3.72E+11	6.10E+11	4.51E+11	3.53E+11

C–5.3 3B Center Channel Flux Tallies

Energy [MeV]	-20.0025 cm	-13.335 cm	-6.6675 cm	Midplane	+6.6675 cm	+13.335 cm	+20.0025 cm
3.00E-09	7.28E+11	9.65E+11	1.26E+12	1.39E+12	1.18E+12	8.92E+11	5.09E+11
7.50E-09	4.15E+12	5.87E+12	7.52E+12	8.19E+12	7.00E+12	5.16E+12	3.55E+12
1.00E-08	3.67E+12	5.24E+12	6.87E+12	7.12E+12	6.10E+12	4.64E+12	3.08E+12
2.53E-08	3.74E+13	5.27E+13	6.69E+13	7.26E+13	6.22E+13	4.66E+13	3.08E+13
3.00E-08	1.37E+13	1.95E+13	2.48E+13	2.71E+13	2.30E+13	1.70E+13	1.14E+13
4.00E-08	2.95E+13	4.20E+13	5.36E+13	5.77E+13	4.96E+13	3.71E+13	2.44E+13
5.00E-08	2.71E+13	3.86E+13	4.99E+13	5.40E+13	4.68E+13	3.42E+13	2.23E+13
7.00E-08	4.34E+13	6.26E+13	8.05E+13	8.70E+13	7.52E+13	5.60E+13	3.58E+13
1.00E-07	4.05E+13	5.86E+13	7.57E+13	8.14E+13	7.09E+13	5.28E+13	3.34E+13
1.50E-07	2.90E+13	4.31E+13	5.60E+13	6.10E+13	5.32E+13	4.02E+13	2.44E+13
2.00E-07	1.11E+13	1.77E+13	2.30E+13	2.57E+13	2.22E+13	1.68E+13	1.02E+13
2.25E-07	3.54E+12	5.55E+12	7.19E+12	7.94E+12	6.82E+12	5.45E+12	3.16E+12
2.50E-07	2.58E+12	4.60E+12	5.85E+12	6.59E+12	5.81E+12	4.39E+12	2.65E+12
2.75E-07	2.35E+12	3.90E+12	5.21E+12	5.59E+12	5.04E+12	3.70E+12	2.17E+12
3.35E-07	4.99E+12	7.77E+12	9.70E+12	1.12E+13	1.00E+13	7.54E+12	4.49E+12
3.50E-07	1.11E+12	1.73E+12	2.17E+12	2.41E+12	2.20E+12	1.64E+12	9.72E+11
3.75E-07	1.63E+12	2.55E+12	3.45E+12	3.64E+12	3.33E+12	2.51E+12	1.60E+12
4.00E-07	1.49E+12	2.39E+12	3.22E+12	3.51E+12	3.08E+12	2.32E+12	1.44E+12
6.25E-07	1.04E+13	1.67E+13	2.15E+13	2.41E+13	2.18E+13	1.65E+13	9.61E+12
1.00E-06	1.16E+13	1.71E+13	2.24E+13	2.46E+13	2.18E+13	1.73E+13	1.05E+13

1.77E-06	1.34E+13	2.05E+13	2.68E+13	2.94E+13	2.67E+13	2.03E+13	1.30E+13
3.00E-06	1.24E+13	1.96E+13	2.46E+13	2.72E+13	2.39E+13	1.89E+13	1.23E+13
4.75E-06	1.07E+13	1.61E+13	1.98E+13	2.21E+13	1.93E+13	1.49E+13	1.02E+13
6.00E-06	5.85E+12	8.45E+12	1.12E+13	1.21E+13	1.12E+13	8.59E+12	5.87E+12
8.10E-06	7.36E+12	1.12E+13	1.42E+13	1.61E+13	1.41E+13	1.13E+13	7.27E+12
1.00E-05	5.41E+12	7.99E+12	1.02E+13	1.11E+13	9.98E+12	8.16E+12	5.29E+12
3.00E-05	2.77E+13	4.02E+13	5.13E+13	5.63E+13	5.15E+13	4.15E+13	2.74E+13
1.00E-04	3.27E+13	4.83E+13	6.04E+13	6.50E+13	6.04E+13	4.84E+13	3.31E+13
5.50E-04	4.77E+13	7.03E+13	8.66E+13	9.43E+13	8.74E+13	7.12E+13	4.95E+13
3.00E-03	4.96E+13	7.25E+13	8.94E+13	9.77E+13	9.03E+13	7.54E+13	5.22E+13
1.70E-02	4.79E+13	7.03E+13	8.74E+13	9.49E+13	8.94E+13	7.39E+13	5.07E+13
2.50E-02	1.13E+13	1.70E+13	2.09E+13	2.28E+13	2.21E+13	1.80E+13	1.29E+13
1.00E-01	4.61E+13	6.70E+13	8.47E+13	8.99E+13	8.64E+13	7.18E+13	4.91E+13
4.00E-01	7.05E+13	1.03E+14	1.28E+14	1.38E+14	1.31E+14	1.08E+14	7.49E+13
9.00E-01	5.29E+13	7.67E+13	9.53E+13	1.04E+14	9.76E+13	8.11E+13	5.76E+13
1.40E+00	3.11E+13	4.46E+13	5.39E+13	6.00E+13	5.61E+13	4.66E+13	3.25E+13
1.85E+00	1.99E+13	2.89E+13	3.57E+13	3.89E+13	3.65E+13	3.02E+13	2.15E+13
2.35E+00	1.39E+13	1.98E+13	2.48E+13	2.68E+13	2.54E+13	2.08E+13	1.49E+13
2.48E+00	3.42E+12	4.80E+12	5.91E+12	6.54E+12	6.21E+12	4.94E+12	3.70E+12
3.00E+00	7.87E+12	1.14E+13	1.42E+13	1.60E+13	1.49E+13	1.22E+13	8.59E+12
4.80E+00	1.18E+13	1.75E+13	2.17E+13	2.37E+13	2.26E+13	1.83E+13	1.30E+13
6.43E+00	3.48E+12	5.22E+12	6.01E+12	6.91E+12	6.48E+12	5.41E+12	3.81E+12
8.19E+00	1.23E+12	1.73E+12	2.10E+12	2.28E+12	2.02E+12	1.67E+12	1.14E+12
2.00E+01	3.72E+11	6.08E+11	7.87E+11	8.62E+11	7.78E+11	7.42E+11	5.21E+11

C–5.4 3B Radial Flux Tallies

	Midplane			Bottom Row			Top Row		
Energy [MeV]	**Inner Column**	**Center Column**	**Outer Column**	**Inner Column**	**Center Column**	**Outer Column**	**Inner Column**	**Center Column**	**Outer Column**
3.00E-09	1.38E+12	1.39E+12	1.65E+12	6.26E+11	7.28E+11	9.29E+11	4.36E+11	5.09E+11	7.93E+11
7.50E-09	8.41E+12	8.19E+12	9.73E+12	3.72E+12	4.15E+12	5.45E+12	2.74E+12	3.55E+12	4.86E+12
1.00E-08	7.35E+12	7.12E+12	8.65E+12	3.23E+12	3.67E+12	4.80E+12	2.34E+12	3.08E+12	4.32E+12
2.53E-08	7.37E+13	7.26E+13	8.35E+13	3.22E+13	3.74E+13	4.73E+13	2.27E+13	3.08E+13	4.13E+13
3.00E-08	2.69E+13	2.71E+13	3.07E+13	1.16E+13	1.37E+13	1.70E+13	8.36E+12	1.14E+13	1.50E+13
4.00E-08	5.79E+13	5.77E+13	6.47E+13	2.52E+13	2.95E+13	3.60E+13	1.80E+13	2.44E+13	3.15E+13
5.00E-08	5.40E+13	5.40E+13	5.95E+13	2.31E+13	2.71E+13	3.31E+13	1.70E+13	2.23E+13	2.93E+13
7.00E-08	8.67E+13	8.70E+13	9.51E+13	3.72E+13	4.34E+13	5.23E+13	2.74E+13	3.58E+13	4.60E+13
1.00E-07	8.12E+13	8.14E+13	8.77E+13	3.51E+13	4.05E+13	4.70E+13	2.57E+13	3.34E+13	4.19E+13
1.50E-07	6.19E+13	6.10E+13	6.39E+13	2.53E+13	2.90E+13	3.28E+13	1.91E+13	2.44E+13	2.96E+13
2.00E-07	2.67E+13	2.57E+13	2.52E+13	1.04E+13	1.11E+13	1.23E+13	7.92E+12	1.02E+13	1.13E+13

2.25E-07	8.68E+12	7.94E+12	7.74E+12	3.35E+12	3.54E+12	3.61E+12	2.46E+12	3.16E+12	3.32E+12
2.50E-07	7.03E+12	6.59E+12	6.48E+12	2.63E+12	2.58E+12	2.98E+12	2.16E+12	2.65E+12	2.62E+12
2.75E-07	5.89E+12	5.59E+12	5.13E+12	2.26E+12	2.35E+12	2.54E+12	1.82E+12	2.17E+12	2.37E+12
3.35E-07	1.24E+13	1.12E+13	1.05E+13	4.34E+12	4.99E+12	5.08E+12	3.79E+12	4.49E+12	4.65E+12
3.50E-07	2.62E+12	2.41E+12	2.28E+12	9.93E+11	1.11E+12	1.06E+12	8.25E+11	9.72E+11	9.72E+11
3.75E-07	4.34E+12	3.64E+12	3.40E+12	1.60E+12	1.63E+12	1.63E+12	1.31E+12	1.60E+12	1.61E+12
4.00E-07	4.02E+12	3.51E+12	3.29E+12	1.46E+12	1.49E+12	1.51E+12	1.13E+12	1.44E+12	1.44E+12
6.25E-07	2.62E+13	2.41E+13	2.20E+13	1.03E+13	1.04E+13	1.07E+13	8.67E+12	9.61E+12	1.02E+13
1.00E-06	2.72E+13	2.46E+13	2.26E+13	1.10E+13	1.16E+13	1.10E+13	9.55E+12	1.05E+13	1.04E+13
1.77E-06	3.26E+13	2.94E+13	2.64E+13	1.35E+13	1.34E+13	1.32E+13	1.24E+13	1.30E+13	1.26E+13
3.00E-06	2.89E+13	2.72E+13	2.47E+13	1.26E+13	1.24E+13	1.20E+13	1.14E+13	1.23E+13	1.21E+13
4.75E-06	2.44E+13	2.21E+13	2.03E+13	1.06E+13	1.07E+13	1.03E+13	9.70E+12	1.02E+13	9.98E+12
6.00E-06	1.34E+13	1.21E+13	1.13E+13	5.72E+12	5.85E+12	5.48E+12	5.80E+12	5.87E+12	5.33E+12
8.10E-06	1.73E+13	1.61E+13	1.42E+13	7.62E+12	7.36E+12	6.99E+12	7.46E+12	7.27E+12	6.93E+12
1.00E-05	1.21E+13	1.11E+13	1.03E+13	5.50E+12	5.41E+12	5.10E+12	5.31E+12	5.29E+12	5.15E+12
3.00E-05	6.25E+13	5.63E+13	5.12E+13	2.82E+13	2.77E+13	2.53E+13	2.73E+13	2.74E+13	2.61E+13
1.00E-04	7.32E+13	6.50E+13	5.92E+13	3.44E+13	3.27E+13	3.03E+13	3.37E+13	3.31E+13	3.10E+13
5.50E-04	1.06E+14	9.43E+13	8.43E+13	5.21E+13	4.77E+13	4.37E+13	5.24E+13	4.95E+13	4.55E+13
3.00E-03	1.11E+14	9.77E+13	8.63E+13	5.55E+13	4.96E+13	4.33E+13	5.75E+13	5.22E+13	4.64E+13
1.70E-02	1.13E+14	9.49E+13	8.22E+13	5.68E+13	4.79E+13	4.09E+13	6.13E+13	5.07E+13	4.46E+13
2.50E-02	2.76E+13	2.28E+13	1.99E+13	1.34E+13	1.13E+13	1.01E+13	1.42E+13	1.29E+13	1.09E+13
1.00E-01	1.07E+14	8.99E+13	7.98E+13	5.38E+13	4.61E+13	4.04E+13	5.78E+13	4.91E+13	4.37E+13
4.00E-01	1.64E+14	1.38E+14	1.17E+14	8.24E+13	7.05E+13	6.04E+13	9.00E+13	7.49E+13	6.41E+13
9.00E-01	1.30E+14	1.04E+14	8.41E+13	6.41E+13	5.29E+13	4.29E+13	7.06E+13	5.76E+13	4.66E+13
1.40E+00	7.58E+13	6.00E+13	4.81E+13	3.77E+13	3.11E+13	2.46E+13	4.13E+13	3.25E+13	2.67E+13
1.85E+00	4.86E+13	3.89E+13	3.11E+13	2.47E+13	1.99E+13	1.63E+13	2.71E+13	2.15E+13	1.75E+13
2.35E+00	3.56E+13	2.68E+13	2.13E+13	1.79E+13	1.39E+13	1.07E+13	1.95E+13	1.49E+13	1.16E+13
2.48E+00	8.88E+12	6.54E+12	5.09E+12	4.50E+12	3.42E+12	2.56E+12	4.66E+12	3.70E+12	2.66E+12
3.00E+00	2.16E+13	1.60E+13	1.22E+13	1.09E+13	7.87E+12	5.81E+12	1.19E+13	8.59E+12	6.27E+12
4.80E+00	3.23E+13	2.37E+13	1.74E+13	1.59E+13	1.18E+13	9.30E+12	1.73E+13	1.30E+13	9.73E+12
6.43E+00	9.12E+12	6.91E+12	5.22E+12	4.66E+12	3.48E+12	2.63E+12	5.14E+12	3.81E+12	3.03E+12
8.19E+00	2.93E+12	2.28E+12	1.63E+12	1.48E+12	1.23E+12	8.92E+11	1.55E+12	1.14E+12	8.82E+11
2.00E+01	1.07E+12	8.62E+11	7.48E+11	6.04E+11	3.72E+11	3.04E+11	6.49E+11	5.21E+11	4.08E+11

C–6 STEEL SAMPLES, BEGINNING OF CYCLE – TWO ASSEMBLIES (7A–7B)

C–6.1 7B Center Channel Flux Tallies

Energy [MeV]	-20.0025 cm	-13.335 cm	-6.6675 cm	Midplane	+6.6675 cm	+13.335 cm	+20.0025 cm
3.00E-09	6.91E+11	9.94E+11	1.27E+12	1.43E+12	1.14E+12	8.30E+11	5.42E+11
7.50E-09	4.24E+12	5.88E+12	7.45E+12	8.13E+12	7.24E+12	5.15E+12	3.45E+12
1.00E-08	3.61E+12	5.17E+12	6.62E+12	7.25E+12	6.16E+12	4.58E+12	2.98E+12
2.53E-08	3.69E+13	5.20E+13	6.77E+13	7.27E+13	6.24E+13	4.67E+13	3.02E+13
3.00E-08	1.36E+13	1.89E+13	2.47E+13	2.69E+13	2.34E+13	1.72E+13	1.13E+13
4.00E-08	2.91E+13	4.15E+13	5.32E+13	5.78E+13	5.01E+13	3.69E+13	2.41E+13
5.00E-08	2.70E+13	3.80E+13	4.95E+13	5.42E+13	4.62E+13	3.46E+13	2.21E+13
7.00E-08	4.30E+13	6.12E+13	8.02E+13	8.69E+13	7.51E+13	5.49E+13	3.54E+13
1.00E-07	3.94E+13	5.72E+13	7.49E+13	8.16E+13	7.14E+13	5.22E+13	3.31E+13
1.50E-07	2.90E+13	4.30E+13	5.59E+13	6.09E+13	5.34E+13	3.96E+13	2.44E+13
2.00E-07	1.11E+13	1.78E+13	2.30E+13	2.52E+13	2.23E+13	1.65E+13	9.82E+12
2.25E-07	3.45E+12	5.39E+12	7.23E+12	7.90E+12	6.98E+12	5.34E+12	3.10E+12
2.50E-07	2.92E+12	4.46E+12	6.03E+12	6.86E+12	5.98E+12	4.45E+12	2.55E+12
2.75E-07	2.47E+12	3.83E+12	5.12E+12	5.64E+12	5.06E+12	3.76E+12	2.16E+12
3.35E-07	4.91E+12	7.66E+12	1.01E+13	1.10E+13	9.61E+12	7.46E+12	4.41E+12
3.50E-07	1.04E+12	1.67E+12	2.28E+12	2.42E+12	2.12E+12	1.70E+12	9.18E+11
3.75E-07	1.68E+12	2.69E+12	3.19E+12	4.08E+12	3.63E+12	2.66E+12	1.56E+12
4.00E-07	1.64E+12	2.44E+12	3.26E+12	3.51E+12	3.24E+12	2.30E+12	1.42E+12
6.25E-07	1.02E+13	1.66E+13	2.18E+13	2.42E+13	2.15E+13	1.63E+13	1.02E+13
1.00E-06	1.10E+13	1.70E+13	2.25E+13	2.42E+13	2.21E+13	1.71E+13	1.06E+13
1.77E-06	1.37E+13	2.09E+13	2.65E+13	2.91E+13	2.64E+13	2.06E+13	1.33E+13
3.00E-06	1.27E+13	1.93E+13	2.45E+13	2.73E+13	2.42E+13	1.83E+13	1.20E+13
4.75E-06	1.04E+13	1.57E+13	2.02E+13	2.23E+13	1.97E+13	1.55E+13	1.05E+13
6.00E-06	5.88E+12	8.82E+12	1.10E+13	1.21E+13	1.09E+13	8.63E+12	5.80E+12
8.10E-06	7.46E+12	1.14E+13	1.43E+13	1.53E+13	1.42E+13	1.12E+13	7.42E+12
1.00E-05	5.42E+12	8.14E+12	1.02E+13	1.12E+13	1.00E+13	8.02E+12	5.40E+12
3.00E-05	2.70E+13	4.11E+13	5.08E+13	5.60E+13	5.08E+13	4.11E+13	2.75E+13
1.00E-04	3.26E+13	4.83E+13	6.02E+13	6.67E+13	5.89E+13	4.79E+13	3.34E+13
5.50E-04	4.77E+13	6.92E+13	8.59E+13	9.33E+13	8.67E+13	7.07E+13	4.94E+13
3.00E-03	4.94E+13	7.22E+13	9.01E+13	9.62E+13	9.03E+13	7.54E+13	5.18E+13
1.70E-02	4.74E+13	7.13E+13	8.77E+13	9.41E+13	8.98E+13	7.27E+13	5.11E+13
2.50E-02	1.14E+13	1.72E+13	2.15E+13	2.29E+13	2.13E+13	1.80E+13	1.24E+13
1.00E-01	4.62E+13	6.86E+13	8.35E+13	9.06E+13	8.61E+13	7.13E+13	4.86E+13
4.00E-01	6.90E+13	1.04E+14	1.28E+14	1.37E+14	1.31E+14	1.08E+14	7.55E+13
9.00E-01	5.29E+13	7.68E+13	9.69E+13	1.03E+14	9.76E+13	8.11E+13	5.63E+13
1.40E+00	3.04E+13	4.36E+13	5.44E+13	6.00E+13	5.60E+13	4.64E+13	3.29E+13

1.85E+00	1.98E+13	2.88E+13	3.60E+13	3.85E+13	3.62E+13	3.02E+13	2.16E+13
2.35E+00	1.38E+13	1.99E+13	2.50E+13	2.71E+13	2.54E+13	2.09E+13	1.52E+13
2.48E+00	3.29E+12	4.91E+12	5.91E+12	6.29E+12	5.96E+12	4.95E+12	3.60E+12
3.00E+00	7.89E+12	1.16E+13	1.45E+13	1.55E+13	1.47E+13	1.22E+13	8.48E+12
4.80E+00	1.20E+13	1.73E+13	2.14E+13	2.36E+13	2.24E+13	1.82E+13	1.32E+13
6.43E+00	3.50E+12	4.97E+12	6.03E+12	6.89E+12	6.39E+12	5.30E+12	3.94E+12
8.19E+00	1.21E+12	1.66E+12	1.98E+12	2.15E+12	2.09E+12	1.66E+12	1.24E+12
2.00E+01	4.83E+11	6.48E+11	7.64E+11	9.14E+11	7.58E+11	6.38E+11	4.51E+11

C–6.2 7B Radial Flux Tallies

	Midplane			Bottom Row			Top Row		
Energy [MeV]	**Inner Column**	**Center Column**	**Outer Column**	**Inner Column**	**Center Column**	**Outer Column**	**Inner Column**	**Center Column**	**Outer Column**
3.00E-09	1.47E+12	1.43E+12	1.64E+12	6.44E+11	6.91E+11	9.17E+11	4.43E+11	5.42E+11	8.35E+11
7.50E-09	8.62E+12	8.13E+12	9.59E+12	3.66E+12	4.24E+12	5.21E+12	2.66E+12	3.45E+12	4.58E+12
1.00E-08	7.56E+12	7.25E+12	8.64E+12	3.19E+12	3.61E+12	4.52E+12	2.32E+12	2.98E+12	4.08E+12
2.53E-08	7.45E+13	7.27E+13	8.38E+13	3.18E+13	3.69E+13	4.63E+13	2.29E+13	3.02E+13	4.03E+13
3.00E-08	2.70E+13	2.69E+13	3.07E+13	1.18E+13	1.36E+13	1.65E+13	8.46E+12	1.13E+13	1.48E+13
4.00E-08	5.74E+13	5.78E+13	6.49E+13	2.50E+13	2.91E+13	3.56E+13	1.85E+13	2.41E+13	3.12E+13
5.00E-08	5.46E+13	5.42E+13	6.00E+13	2.30E+13	2.70E+13	3.23E+13	1.67E+13	2.21E+13	2.85E+13
7.00E-08	8.68E+13	8.69E+13	9.47E+13	3.65E+13	4.30E+13	5.13E+13	2.69E+13	3.54E+13	4.49E+13
1.00E-07	8.18E+13	8.16E+13	8.71E+13	3.40E+13	3.94E+13	4.65E+13	2.55E+13	3.31E+13	4.08E+13
1.50E-07	6.21E+13	6.09E+13	6.35E+13	2.50E+13	2.90E+13	3.29E+13	1.94E+13	2.44E+13	2.92E+13
2.00E-07	2.69E+13	2.52E+13	2.50E+13	1.01E+13	1.11E+13	1.24E+13	8.17E+12	9.82E+12	1.12E+13
2.25E-07	8.37E+12	7.90E+12	7.65E+12	3.26E+12	3.45E+12	3.48E+12	2.90E+12	3.10E+12	3.55E+12
2.50E-07	7.03E+12	6.86E+12	6.12E+12	2.70E+12	2.92E+12	2.89E+12	2.29E+12	2.55E+12	2.68E+12
2.75E-07	6.15E+12	5.64E+12	5.36E+12	2.27E+12	2.47E+12	2.38E+12	1.88E+12	2.16E+12	2.26E+12
3.35E-07	1.22E+13	1.10E+13	1.04E+13	4.66E+12	4.91E+12	4.89E+12	3.90E+12	4.41E+12	4.56E+12
3.50E-07	2.69E+12	2.42E+12	2.23E+12	9.60E+11	1.04E+12	1.10E+12	8.95E+11	9.18E+11	1.02E+12
3.75E-07	4.37E+12	4.08E+12	3.44E+12	1.50E+12	1.68E+12	1.57E+12	1.37E+12	1.56E+12	1.61E+12
4.00E-07	3.86E+12	3.51E+12	3.19E+12	1.40E+12	1.64E+12	1.45E+12	1.32E+12	1.42E+12	1.45E+12
6.25E-07	2.59E+13	2.42E+13	2.22E+13	1.00E+13	1.02E+13	1.05E+13	8.83E+12	1.02E+13	1.00E+13
1.00E-06	2.68E+13	2.42E+13	2.28E+13	1.09E+13	1.10E+13	1.06E+13	9.38E+12	1.06E+13	1.09E+13
1.77E-06	3.24E+13	2.91E+13	2.67E+13	1.33E+13	1.37E+13	1.32E+13	1.22E+13	1.33E+13	1.30E+13
3.00E-06	2.93E+13	2.73E+13	2.47E+13	1.24E+13	1.27E+13	1.16E+13	1.14E+13	1.20E+13	1.19E+13
4.75E-06	2.42E+13	2.23E+13	2.06E+13	1.05E+13	1.04E+13	1.00E+13	1.00E+13	1.05E+13	1.04E+13
6.00E-06	1.32E+13	1.21E+13	1.12E+13	5.98E+12	5.88E+12	5.40E+12	5.66E+12	5.80E+12	5.41E+12
8.10E-06	1.69E+13	1.53E+13	1.44E+13	7.41E+12	7.46E+12	7.16E+12	7.24E+12	7.42E+12	6.77E+12
1.00E-05	1.20E+13	1.12E+13	9.94E+12	5.35E+12	5.42E+12	4.91E+12	5.36E+12	5.40E+12	4.89E+12
3.00E-05	6.29E+13	5.60E+13	5.10E+13	2.83E+13	2.70E+13	2.54E+13	2.80E+13	2.75E+13	2.63E+13

1.00E-04	7.33E+13	6.67E+13	5.97E+13	3.45E+13	3.26E+13	2.97E+13	3.41E+13	3.34E+13	3.16E+13
5.50E-04	1.06E+14	9.33E+13	8.49E+13	5.17E+13	4.77E+13	4.30E+13	5.31E+13	4.94E+13	4.50E+13
3.00E-03	1.11E+14	9.62E+13	8.41E+13	5.62E+13	4.94E+13	4.39E+13	5.77E+13	5.18E+13	4.61E+13
1.70E-02	1.13E+14	9.41E+13	8.10E+13	5.74E+13	4.74E+13	4.13E+13	6.10E+13	5.11E+13	4.52E+13
2.50E-02	2.68E+13	2.29E+13	1.99E+13	1.33E+13	1.14E+13	1.05E+13	1.44E+13	1.24E+13	1.10E+13
1.00E-01	1.06E+14	9.06E+13	8.00E+13	5.31E+13	4.62E+13	4.03E+13	5.73E+13	4.86E+13	4.33E+13
4.00E-01	1.65E+14	1.37E+14	1.18E+14	8.23E+13	6.90E+13	6.05E+13	8.87E+13	7.55E+13	6.55E+13
9.00E-01	1.30E+14	1.03E+14	8.51E+13	6.42E+13	5.29E+13	4.35E+13	6.96E+13	5.63E+13	4.61E+13
1.40E+00	7.58E+13	6.00E+13	4.82E+13	3.74E+13	3.04E+13	2.43E+13	4.09E+13	3.29E+13	2.57E+13
1.85E+00	4.94E+13	3.85E+13	3.15E+13	2.51E+13	1.98E+13	1.65E+13	2.68E+13	2.16E+13	1.77E+13
2.35E+00	3.55E+13	2.71E+13	2.10E+13	1.82E+13	1.38E+13	1.08E+13	1.91E+13	1.52E+13	1.18E+13
2.48E+00	8.76E+12	6.29E+12	4.90E+12	4.39E+12	3.29E+12	2.46E+12	4.82E+12	3.60E+12	2.72E+12
3.00E+00	2.14E+13	1.55E+13	1.16E+13	1.07E+13	7.89E+12	5.95E+12	1.16E+13	8.48E+12	6.27E+12
4.80E+00	3.21E+13	2.36E+13	1.73E+13	1.60E+13	1.20E+13	9.31E+12	1.72E+13	1.32E+13	9.82E+12
6.43E+00	8.98E+12	6.89E+12	4.93E+12	4.55E+12	3.50E+12	2.74E+12	5.04E+12	3.94E+12	2.88E+12
8.19E+00	2.91E+12	2.15E+12	1.65E+12	1.67E+12	1.21E+12	8.69E+11	1.68E+12	1.24E+12	9.69E+11
2.00E+01	1.15E+12	9.14E+11	6.01E+11	4.60E+11	4.83E+11	3.72E+11	6.10E+11	4.51E+11	3.53E+11

C–6.3 7A Center Channel Flux Tallies

Energy [MeV]	-20.0025 cm	-13.335 cm	-6.6675 cm	Midplane	+6.6675 cm	+13.335 cm	+20.0025 cm
3.00E-09	6.63E+11	9.29E+11	1.16E+12	1.14E+12	9.92E+11	7.10E+11	5.62E+11
7.50E-09	3.97E+12	5.19E+12	6.46E+12	7.02E+12	6.12E+12	4.74E+12	3.16E+12
1.00E-08	3.39E+12	4.61E+12	5.80E+12	6.31E+12	5.42E+12	4.11E+12	2.87E+12
2.53E-08	3.40E+13	4.61E+13	5.88E+13	6.30E+13	5.55E+13	4.20E+13	2.80E+13
3.00E-08	1.27E+13	1.71E+13	2.16E+13	2.34E+13	2.07E+13	1.54E+13	1.00E+13
4.00E-08	2.71E+13	3.66E+13	4.69E+13	4.99E+13	4.44E+13	3.38E+13	2.24E+13
5.00E-08	2.46E+13	3.42E+13	4.39E+13	4.72E+13	4.12E+13	3.10E+13	2.06E+13
7.00E-08	3.97E+13	5.50E+13	7.05E+13	7.63E+13	6.71E+13	5.06E+13	3.29E+13
1.00E-07	3.68E+13	5.27E+13	6.68E+13	7.24E+13	6.41E+13	4.74E+13	3.09E+13
1.50E-07	2.67E+13	3.92E+13	5.01E+13	5.48E+13	4.86E+13	3.70E+13	2.29E+13
2.00E-07	1.06E+13	1.63E+13	2.12E+13	2.33E+13	2.04E+13	1.58E+13	9.54E+12
2.25E-07	3.35E+12	5.12E+12	6.65E+12	7.42E+12	6.72E+12	5.07E+12	3.01E+12
2.50E-07	2.63E+12	4.30E+12	5.47E+12	6.21E+12	5.51E+12	4.39E+12	2.49E+12
2.75E-07	2.39E+12	3.74E+12	4.87E+12	5.53E+12	4.75E+12	3.65E+12	2.25E+12
3.35E-07	4.65E+12	7.28E+12	9.83E+12	1.05E+13	9.34E+12	7.14E+12	4.36E+12
3.50E-07	1.08E+12	1.55E+12	2.19E+12	2.35E+12	2.22E+12	1.66E+12	9.00E+11
3.75E-07	1.57E+12	2.55E+12	3.19E+12	3.70E+12	3.23E+12	2.53E+12	1.44E+12
4.00E-07	1.54E+12	2.47E+12	3.02E+12	3.36E+12	3.20E+12	2.37E+12	1.26E+12
6.25E-07	1.01E+13	1.60E+13	2.09E+13	2.29E+13	2.11E+13	1.53E+13	9.40E+12

1.00E-06	1.04E+13	1.64E+13	2.09E+13	2.37E+13	2.12E+13	1.62E+13	9.79E+12
1.77E-06	1.30E+13	1.97E+13	2.49E+13	2.78E+13	2.53E+13	1.98E+13	1.21E+13
3.00E-06	1.19E+13	1.82E+13	2.30E+13	2.53E+13	2.31E+13	1.83E+13	1.17E+13
4.75E-06	1.02E+13	1.53E+13	1.89E+13	2.13E+13	1.95E+13	1.49E+13	1.00E+13
6.00E-06	5.42E+12	8.34E+12	1.03E+13	1.17E+13	1.07E+13	8.71E+12	5.36E+12
8.10E-06	7.08E+12	1.03E+13	1.35E+13	1.47E+13	1.34E+13	1.09E+13	6.92E+12
1.00E-05	5.02E+12	7.64E+12	9.65E+12	1.02E+13	9.34E+12	7.78E+12	5.07E+12
3.00E-05	2.58E+13	3.86E+13	4.87E+13	5.34E+13	4.85E+13	3.89E+13	2.58E+13
1.00E-04	3.08E+13	4.54E+13	5.70E+13	6.26E+13	5.76E+13	4.67E+13	3.15E+13
5.50E-04	4.53E+13	6.60E+13	8.22E+13	9.02E+13	8.23E+13	6.71E+13	4.70E+13
3.00E-03	4.73E+13	6.86E+13	8.48E+13	9.21E+13	8.53E+13	7.00E+13	5.00E+13
1.70E-02	4.44E+13	6.73E+13	8.35E+13	8.90E+13	8.43E+13	7.13E+13	4.93E+13
2.50E-02	1.07E+13	1.60E+13	1.99E+13	2.16E+13	2.03E+13	1.67E+13	1.16E+13
1.00E-01	4.36E+13	6.50E+13	7.99E+13	8.60E+13	8.21E+13	6.78E+13	4.66E+13
4.00E-01	6.73E+13	9.97E+13	1.22E+14	1.32E+14	1.25E+14	1.04E+14	7.27E+13
9.00E-01	5.15E+13	7.52E+13	9.31E+13	1.00E+14	9.48E+13	7.87E+13	5.49E+13
1.40E+00	2.95E+13	4.28E+13	5.31E+13	5.84E+13	5.47E+13	4.52E+13	3.20E+13
1.85E+00	1.98E+13	2.76E+13	3.43E+13	3.79E+13	3.55E+13	2.93E+13	2.08E+13
2.35E+00	1.35E+13	1.96E+13	2.42E+13	2.66E+13	2.47E+13	2.04E+13	1.47E+13
2.48E+00	3.30E+12	4.66E+12	5.94E+12	6.29E+12	5.84E+12	4.69E+12	3.57E+12
3.00E+00	7.68E+12	1.14E+13	1.42E+13	1.52E+13	1.49E+13	1.26E+13	8.40E+12
4.80E+00	1.22E+13	1.72E+13	2.13E+13	2.30E+13	2.16E+13	1.80E+13	1.32E+13
6.43E+00	3.57E+12	4.89E+12	6.07E+12	6.76E+12	6.15E+12	4.99E+12	3.74E+12
8.19E+00	1.15E+12	1.67E+12	2.02E+12	2.11E+12	1.98E+12	1.81E+12	1.13E+12
2.00E+01	4.60E+11	6.16E+11	8.11E+11	8.66E+11	8.27E+11	6.24E+11	4.55E+11

C–6.4 7A Radial Flux Tallies

	Midplane			Bottom Row			Top Row		
Energy [MeV]	**Inner Column**	**Center Column**	**Outer Column**	**Inner Column**	**Center Column**	**Outer Column**	**Inner Column**	**Center Column**	**Outer Column**
3.00E-09	1.28E+12	1.14E+12	1.41E+12	6.00E+11	6.63E+11	8.46E+11	4.13E+11	5.62E+11	7.25E+11
7.50E-09	7.42E+12	7.02E+12	8.25E+12	3.31E+12	3.97E+12	4.86E+12	2.33E+12	3.16E+12	4.41E+12
1.00E-08	6.71E+12	6.31E+12	7.33E+12	3.06E+12	3.39E+12	4.20E+12	2.11E+12	2.87E+12	3.96E+12
2.53E-08	6.48E+13	6.30E+13	7.23E+13	2.92E+13	3.40E+13	4.31E+13	2.09E+13	2.80E+13	3.79E+13
3.00E-08	2.38E+13	2.34E+13	2.64E+13	1.05E+13	1.27E+13	1.55E+13	7.79E+12	1.00E+13	1.37E+13
4.00E-08	5.13E+13	4.99E+13	5.56E+13	2.29E+13	2.71E+13	3.28E+13	1.63E+13	2.24E+13	2.88E+13
5.00E-08	4.77E+13	4.72E+13	5.17E+13	2.10E+13	2.46E+13	2.99E+13	1.50E+13	2.06E+13	2.69E+13
7.00E-08	7.66E+13	7.63E+13	8.31E+13	3.40E+13	3.97E+13	4.70E+13	2.44E+13	3.29E+13	4.19E+13
1.00E-07	7.33E+13	7.24E+13	7.71E+13	3.16E+13	3.68E+13	4.34E+13	2.38E+13	3.09E+13	3.85E+13
1.50E-07	5.64E+13	5.48E+13	5.64E+13	2.33E+13	2.67E+13	3.05E+13	1.78E+13	2.29E+13	2.72E+13
2.00E-07	2.47E+13	2.33E+13	2.30E+13	9.84E+12	1.06E+13	1.16E+13	7.98E+12	9.54E+12	1.06E+13

2.25E-07	8.19E+12	7.42E+12	7.28E+12	3.26E+12	3.35E+12	3.45E+12	2.43E+12	3.01E+12	3.33E+12
2.50E-07	6.83E+12	6.21E+12	5.61E+12	2.63E+12	2.63E+12	2.79E+12	2.16E+12	2.49E+12	2.68E+12
2.75E-07	5.84E+12	5.53E+12	5.08E+12	2.23E+12	2.39E+12	2.37E+12	1.76E+12	2.25E+12	2.25E+12
3.35E-07	1.15E+13	1.05E+13	9.78E+12	4.42E+12	4.65E+12	4.72E+12	3.73E+12	4.36E+12	4.39E+12
3.50E-07	2.48E+12	2.35E+12	2.16E+12	9.75E+11	1.08E+12	1.03E+12	8.17E+11	9.00E+11	9.70E+11
3.75E-07	4.00E+12	3.70E+12	3.32E+12	1.45E+12	1.57E+12	1.54E+12	1.25E+12	1.44E+12	1.47E+12
4.00E-07	3.60E+12	3.36E+12	3.08E+12	1.34E+12	1.54E+12	1.48E+12	1.25E+12	1.26E+12	1.43E+12
6.25E-07	2.48E+13	2.29E+13	2.12E+13	9.39E+12	1.01E+13	9.99E+12	8.39E+12	9.40E+12	9.84E+12
1.00E-06	2.54E+13	2.37E+13	2.18E+13	1.04E+13	1.04E+13	1.04E+13	9.49E+12	9.79E+12	1.03E+13
1.77E-06	3.05E+13	2.78E+13	2.54E+13	1.27E+13	1.30E+13	1.27E+13	1.17E+13	1.21E+13	1.26E+13
3.00E-06	2.85E+13	2.53E+13	2.39E+13	1.18E+13	1.19E+13	1.17E+13	1.08E+13	1.17E+13	1.14E+13
4.75E-06	2.34E+13	2.13E+13	1.98E+13	1.02E+13	1.02E+13	9.57E+12	9.55E+12	1.00E+13	9.70E+12
6.00E-06	1.32E+13	1.17E+13	1.03E+13	5.51E+12	5.42E+12	5.42E+12	5.57E+12	5.36E+12	5.29E+12
8.10E-06	1.69E+13	1.47E+13	1.34E+13	7.54E+12	7.08E+12	6.75E+12	7.14E+12	6.92E+12	6.92E+12
1.00E-05	1.15E+13	1.02E+13	9.53E+12	5.58E+12	5.02E+12	4.84E+12	5.12E+12	5.07E+12	4.86E+12
3.00E-05	5.95E+13	5.34E+13	4.79E+13	2.69E+13	2.58E+13	2.46E+13	2.65E+13	2.58E+13	2.53E+13
1.00E-04	6.93E+13	6.26E+13	5.60E+13	3.28E+13	3.08E+13	2.85E+13	3.19E+13	3.15E+13	2.92E+13
5.50E-04	1.00E+14	9.02E+13	7.91E+13	4.91E+13	4.53E+13	4.10E+13	5.03E+13	4.70E+13	4.30E+13
3.00E-03	1.05E+14	9.21E+13	8.01E+13	5.29E+13	4.73E+13	4.14E+13	5.56E+13	5.00E+13	4.41E+13
1.70E-02	1.07E+14	8.90E+13	7.63E+13	5.42E+13	4.44E+13	3.98E+13	5.85E+13	4.93E+13	4.22E+13
2.50E-02	2.54E+13	2.16E+13	1.92E+13	1.31E+13	1.07E+13	9.96E+12	1.38E+13	1.16E+13	1.02E+13
1.00E-01	1.02E+14	8.60E+13	7.67E+13	5.12E+13	4.36E+13	3.84E+13	5.44E+13	4.66E+13	4.16E+13
4.00E-01	1.58E+14	1.32E+14	1.13E+14	7.98E+13	6.73E+13	5.79E+13	8.64E+13	7.27E+13	6.25E+13
9.00E-01	1.24E+14	1.00E+14	8.21E+13	6.28E+13	5.15E+13	4.26E+13	6.78E+13	5.49E+13	4.53E+13
1.40E+00	7.32E+13	5.84E+13	4.62E+13	3.67E+13	2.95E+13	2.42E+13	3.97E+13	3.20E+13	2.59E+13
1.85E+00	4.83E+13	3.79E+13	3.03E+13	2.44E+13	1.98E+13	1.56E+13	2.60E+13	2.08E+13	1.65E+13
2.35E+00	3.44E+13	2.66E+13	2.04E+13	1.74E+13	1.35E+13	1.05E+13	1.90E+13	1.47E+13	1.15E+13
2.48E+00	8.36E+12	6.29E+12	4.61E+12	4.25E+12	3.30E+12	2.64E+12	4.65E+12	3.57E+12	2.77E+12
3.00E+00	2.11E+13	1.52E+13	1.14E+13	1.07E+13	7.68E+12	6.09E+12	1.15E+13	8.40E+12	6.36E+12
4.80E+00	3.14E+13	2.30E+13	1.71E+13	1.60E+13	1.22E+13	9.02E+12	1.71E+13	1.32E+13	9.72E+12
6.43E+00	9.09E+12	6.76E+12	5.19E+12	4.71E+12	3.57E+12	2.69E+12	4.97E+12	3.74E+12	2.89E+12
8.19E+00	3.03E+12	2.11E+12	1.58E+12	1.59E+12	1.15E+12	8.60E+11	1.69E+12	1.13E+12	8.86E+11
2.00E+01	1.14E+12	8.66E+11	7.31E+11	6.62E+11	4.60E+11	3.11E+11	6.22E+11	4.55E+11	3.82E+11

C–7 STEEL SAMPLES, BEGINNING OF CYCLE – THREE-CHANNEL ASSEMBLY

C–7.1 Channel 12 Flux Tallies

Energy [MeV]	-20.0025 cm	-13.335 cm	-6.6675 cm	Midplane	+6.6675 cm	+13.335 cm	+20.0025 cm
3.00E-09	8.57E+11	1.18E+12	1.64E+12	1.68E+12	1.41E+12	1.05E+12	6.83E+11
7.50E-09	4.87E+12	7.20E+12	9.15E+12	9.93E+12	8.65E+12	6.08E+12	3.92E+12
1.00E-08	4.31E+12	6.35E+12	8.11E+12	8.74E+12	7.38E+12	5.30E+12	3.44E+12
2.53E-08	4.16E+13	6.17E+13	7.89E+13	8.58E+13	7.15E+13	5.25E+13	3.25E+13
3.00E-08	1.53E+13	2.23E+13	2.91E+13	3.14E+13	2.60E+13	1.93E+13	1.21E+13
4.00E-08	3.19E+13	4.74E+13	6.13E+13	6.65E+13	5.53E+13	4.06E+13	2.53E+13
5.00E-08	2.94E+13	4.33E+13	5.65E+13	6.03E+13	5.23E+13	3.82E+13	2.33E+13
7.00E-08	4.60E+13	6.90E+13	8.95E+13	9.69E+13	8.24E+13	6.00E+13	3.67E+13
1.00E-07	4.21E+13	6.30E+13	8.25E+13	9.02E+13	7.67E+13	5.61E+13	3.38E+13
1.50E-07	2.96E+13	4.60E+13	6.00E+13	6.61E+13	5.76E+13	4.24E+13	2.44E+13
2.00E-07	1.15E+13	1.86E+13	2.41E+13	2.75E+13	2.41E+13	1.79E+13	9.73E+12
2.25E-07	3.43E+12	5.90E+12	7.65E+12	8.63E+12	7.56E+12	5.60E+12	2.87E+12
2.50E-07	2.77E+12	4.63E+12	6.36E+12	7.07E+12	6.09E+12	4.50E+12	2.35E+12
2.75E-07	2.40E+12	3.89E+12	5.25E+12	5.98E+12	5.44E+12	3.81E+12	2.02E+12
3.35E-07	4.78E+12	7.97E+12	1.09E+13	1.17E+13	1.06E+13	7.85E+12	4.15E+12
3.50E-07	1.02E+12	1.83E+12	2.33E+12	2.58E+12	2.25E+12	1.64E+12	9.60E+11
3.75E-07	1.65E+12	2.74E+12	3.66E+12	3.89E+12	3.77E+12	2.67E+12	1.41E+12
4.00E-07	1.45E+12	2.47E+12	3.35E+12	3.76E+12	3.40E+12	2.49E+12	1.43E+12
6.25E-07	1.07E+13	1.73E+13	2.23E+13	2.49E+13	2.25E+13	1.67E+13	9.25E+12
1.00E-06	1.09E+13	1.79E+13	2.27E+13	2.55E+13	2.27E+13	1.71E+13	1.00E+13
1.77E-06	1.34E+13	2.13E+13	2.73E+13	3.04E+13	2.75E+13	2.06E+13	1.26E+13
3.00E-06	1.21E+13	1.92E+13	2.48E+13	2.74E+13	2.48E+13	1.92E+13	1.17E+13
4.75E-06	1.08E+13	1.63E+13	2.11E+13	2.33E+13	1.96E+13	1.54E+13	1.03E+13
6.00E-06	5.77E+12	9.25E+12	1.14E+13	1.24E+13	1.17E+13	9.04E+12	5.96E+12
8.10E-06	7.44E+12	1.17E+13	1.45E+13	1.67E+13	1.49E+13	1.15E+13	7.63E+12
1.00E-05	5.27E+12	8.13E+12	1.05E+13	1.16E+13	1.03E+13	8.27E+12	5.40E+12
3.00E-05	2.83E+13	4.20E+13	5.33E+13	5.96E+13	5.36E+13	4.31E+13	2.72E+13
1.00E-04	3.39E+13	5.04E+13	6.31E+13	6.89E+13	6.18E+13	4.97E+13	3.37E+13
5.50E-04	5.08E+13	7.33E+13	9.21E+13	1.01E+14	9.06E+13	7.42E+13	5.19E+13
3.00E-03	5.39E+13	7.79E+13	9.64E+13	1.05E+14	9.73E+13	8.00E+13	5.69E+13
1.70E-02	5.56E+13	8.18E+13	1.01E+14	1.09E+14	1.02E+14	8.45E+13	6.00E+13
2.50E-02	1.37E+13	1.98E+13	2.47E+13	2.61E+13	2.50E+13	2.08E+13	1.46E+13
1.00E-01	5.46E+13	7.86E+13	9.68E+13	1.06E+14	9.89E+13	8.08E+13	5.69E+13
4.00E-01	8.12E+13	1.20E+14	1.48E+14	1.59E+14	1.51E+14	1.25E+14	8.72E+13
9.00E-01	6.10E+13	8.83E+13	1.10E+14	1.20E+14	1.12E+14	9.28E+13	6.51E+13
1.40E+00	3.55E+13	5.14E+13	6.37E+13	6.93E+13	6.44E+13	5.35E+13	3.79E+13

1.85E+00	2.28E+13	3.36E+13	4.19E+13	4.52E+13	4.23E+13	3.48E+13	2.48E+13
2.35E+00	1.56E+13	2.34E+13	2.84E+13	3.11E+13	2.92E+13	2.38E+13	1.71E+13
2.48E+00	3.90E+12	5.40E+12	7.09E+12	7.60E+12	6.92E+12	5.84E+12	3.90E+12
3.00E+00	9.14E+12	1.29E+13	1.66E+13	1.82E+13	1.68E+13	1.40E+13	1.01E+13
4.80E+00	1.40E+13	2.00E+13	2.49E+13	2.80E+13	2.55E+13	2.14E+13	1.49E+13
6.43E+00	4.02E+12	5.71E+12	7.23E+12	7.72E+12	7.38E+12	5.93E+12	4.30E+12
8.19E+00	1.31E+12	1.72E+12	2.24E+12	2.46E+12	2.30E+12	1.97E+12	1.42E+12
2.00E+01	4.78E+11	6.74E+11	9.19E+11	1.05E+12	1.02E+12	7.66E+11	5.91E+11

C–7.2 Channel 14 Flux Tallies

Energy [MeV]	-20.0025 cm	-13.335 cm	-6.6675 cm	Midplane	+6.6675 cm	+13.335 cm	+20.0025 cm
3.00E-09	8.33E+11	1.23E+12	1.67E+12	1.65E+12	1.46E+12	1.09E+12	6.39E+11
7.50E-09	5.16E+12	7.25E+12	9.61E+12	1.01E+13	8.51E+12	6.31E+12	3.94E+12
1.00E-08	4.44E+12	6.30E+12	8.33E+12	8.86E+12	7.52E+12	5.38E+12	3.37E+12
2.53E-08	4.24E+13	6.24E+13	8.06E+13	8.71E+13	7.29E+13	5.39E+13	3.31E+13
3.00E-08	1.53E+13	2.24E+13	2.91E+13	3.20E+13	2.69E+13	1.94E+13	1.23E+13
4.00E-08	3.23E+13	4.79E+13	6.18E+13	6.72E+13	5.67E+13	4.15E+13	2.51E+13
5.00E-08	2.98E+13	4.39E+13	5.73E+13	6.15E+13	5.25E+13	3.84E+13	2.33E+13
7.00E-08	4.70E+13	6.98E+13	9.01E+13	9.88E+13	8.33E+13	6.11E+13	3.69E+13
1.00E-07	4.29E+13	6.39E+13	8.38E+13	9.15E+13	7.80E+13	5.70E+13	3.39E+13
1.50E-07	2.96E+13	4.68E+13	6.16E+13	6.68E+13	5.82E+13	4.21E+13	2.43E+13
2.00E-07	1.17E+13	1.84E+13	2.47E+13	2.71E+13	2.41E+13	1.78E+13	9.69E+12
2.25E-07	3.50E+12	5.87E+12	7.68E+12	8.49E+12	7.60E+12	5.70E+12	2.94E+12
2.50E-07	2.96E+12	4.76E+12	6.36E+12	6.78E+12	6.20E+12	4.54E+12	2.36E+12
2.75E-07	2.36E+12	4.23E+12	5.53E+12	6.01E+12	5.36E+12	3.87E+12	2.02E+12
3.35E-07	4.71E+12	7.93E+12	1.09E+13	1.17E+13	1.05E+13	7.73E+12	4.06E+12
3.50E-07	9.54E+11	1.79E+12	2.39E+12	2.49E+12	2.25E+12	1.74E+12	9.23E+11
3.75E-07	1.56E+12	2.62E+12	3.50E+12	4.05E+12	3.47E+12	2.69E+12	1.46E+12
4.00E-07	1.56E+12	2.42E+12	3.43E+12	3.78E+12	3.35E+12	2.69E+12	1.37E+12
6.25E-07	1.03E+13	1.69E+13	2.24E+13	2.53E+13	2.24E+13	1.70E+13	9.50E+12
1.00E-06	1.07E+13	1.76E+13	2.29E+13	2.56E+13	2.30E+13	1.68E+13	1.02E+13
1.77E-06	1.36E+13	2.15E+13	2.77E+13	3.02E+13	2.71E+13	2.08E+13	1.23E+13
3.00E-06	1.25E+13	1.96E+13	2.51E+13	2.73E+13	2.50E+13	1.94E+13	1.19E+13
4.75E-06	1.08E+13	1.64E+13	2.09E+13	2.33E+13	1.98E+13	1.57E+13	1.01E+13
6.00E-06	5.95E+12	9.01E+12	1.16E+13	1.31E+13	1.12E+13	9.27E+12	5.90E+12
8.10E-06	7.53E+12	1.17E+13	1.47E+13	1.64E+13	1.49E+13	1.14E+13	7.28E+12
1.00E-05	5.46E+12	7.94E+12	1.07E+13	1.14E+13	1.05E+13	8.16E+12	5.34E+12
3.00E-05	2.85E+13	4.24E+13	5.43E+13	5.97E+13	5.24E+13	4.32E+13	2.78E+13
1.00E-04	3.41E+13	5.02E+13	6.32E+13	6.97E+13	6.30E+13	5.10E+13	3.37E+13

5.50E-04	5.03E+13	7.28E+13	9.15E+13	1.00E+14	9.16E+13	7.42E+13	5.14E+13
3.00E-03	5.45E+13	7.88E+13	9.73E+13	1.05E+14	9.69E+13	8.09E+13	5.70E+13
1.70E-02	5.56E+13	8.24E+13	1.01E+14	1.09E+14	1.03E+14	8.66E+13	6.00E+13
2.50E-02	1.35E+13	1.98E+13	2.46E+13	2.68E+13	2.51E+13	2.07E+13	1.45E+13
1.00E-01	5.43E+13	7.90E+13	9.67E+13	1.06E+14	9.88E+13	8.25E+13	5.76E+13
4.00E-01	8.19E+13	1.19E+14	1.49E+14	1.60E+14	1.52E+14	1.25E+14	8.79E+13
9.00E-01	6.04E+13	8.81E+13	1.12E+14	1.20E+14	1.13E+14	9.34E+13	6.49E+13
1.40E+00	3.49E+13	5.02E+13	6.33E+13	6.95E+13	6.41E+13	5.44E+13	3.76E+13
1.85E+00	2.31E+13	3.33E+13	4.11E+13	4.49E+13	4.22E+13	3.56E+13	2.48E+13
2.35E+00	1.60E+13	2.33E+13	2.84E+13	3.12E+13	2.96E+13	2.41E+13	1.72E+13
2.48E+00	3.79E+12	5.47E+12	6.61E+12	7.49E+12	6.82E+12	5.76E+12	3.96E+12
3.00E+00	9.32E+12	1.33E+13	1.64E+13	1.80E+13	1.67E+13	1.38E+13	9.91E+12
4.80E+00	1.40E+13	2.03E+13	2.48E+13	2.66E+13	2.61E+13	2.17E+13	1.49E+13
6.43E+00	3.96E+12	5.82E+12	7.22E+12	8.04E+12	7.29E+12	6.14E+12	4.50E+12
8.19E+00	1.26E+12	1.87E+12	2.20E+12	2.61E+12	2.35E+12	1.98E+12	1.41E+12
2.00E+01	5.04E+11	6.84E+11	8.50E+11	9.46E+11	9.76E+11	8.37E+11	5.62E+11

C–7.3 Channel 16 Flux Tallies

Energy [MeV]	-20.0025 cm	-13.335 cm	-6.6675 cm	Midplane	+6.6675 cm	+13.335 cm	+20.0025 cm
3.00E-09	9.76E+11	1.39E+12	1.78E+12	1.78E+12	1.56E+12	1.20E+12	7.95E+11
7.50E-09	5.68E+12	7.82E+12	1.02E+13	1.07E+13	9.27E+12	6.93E+12	4.95E+12
1.00E-08	5.03E+12	6.85E+12	8.71E+12	9.20E+12	8.19E+12	6.10E+12	4.14E+12
2.53E-08	4.76E+13	6.73E+13	8.51E+13	9.01E+13	7.96E+13	6.08E+13	4.11E+13
3.00E-08	1.75E+13	2.44E+13	3.05E+13	3.27E+13	2.89E+13	2.19E+13	1.47E+13
4.00E-08	3.72E+13	5.17E+13	6.49E+13	6.99E+13	6.16E+13	4.66E+13	3.09E+13
5.00E-08	3.33E+13	4.74E+13	5.95E+13	6.37E+13	5.67E+13	4.29E+13	2.85E+13
7.00E-08	5.29E+13	7.49E+13	9.41E+13	1.01E+14	9.00E+13	6.77E+13	4.48E+13
1.00E-07	4.77E+13	6.86E+13	8.69E+13	9.36E+13	8.29E+13	6.25E+13	4.04E+13
1.50E-07	3.29E+13	4.82E+13	6.24E+13	6.66E+13	6.01E+13	4.52E+13	2.89E+13
2.00E-07	1.24E+13	1.89E+13	2.44E+13	2.67E+13	2.40E+13	1.77E+13	1.11E+13
2.25E-07	3.65E+12	5.64E+12	7.45E+12	7.99E+12	7.51E+12	5.55E+12	3.38E+12
2.50E-07	2.91E+12	4.56E+12	5.89E+12	6.43E+12	5.83E+12	4.43E+12	2.67E+12
2.75E-07	2.42E+12	3.88E+12	5.23E+12	5.52E+12	5.22E+12	3.80E+12	2.26E+12
3.35E-07	4.93E+12	7.53E+12	1.01E+13	1.05E+13	9.95E+12	7.36E+12	4.48E+12
3.50E-07	1.04E+12	1.79E+12	2.11E+12	2.38E+12	2.21E+12	1.73E+12	1.02E+12
3.75E-07	1.59E+12	2.63E+12	3.20E+12	3.57E+12	3.34E+12	2.55E+12	1.58E+12
4.00E-07	1.57E+12	2.32E+12	3.19E+12	3.40E+12	3.20E+12	2.49E+12	1.38E+12
6.25E-07	1.05E+13	1.58E+13	2.05E+13	2.28E+13	2.08E+13	1.61E+13	9.90E+12
1.00E-06	1.11E+13	1.66E+13	2.13E+13	2.32E+13	2.11E+13	1.65E+13	1.06E+13

1.77E-06	1.33E+13	1.99E+13	2.52E+13	2.71E+13	2.53E+13	2.01E+13	1.28E+13
3.00E-06	1.24E+13	1.84E+13	2.31E+13	2.53E+13	2.30E+13	1.84E+13	1.18E+13
4.75E-06	1.04E+13	1.57E+13	1.94E+13	2.19E+13	1.95E+13	1.51E+13	1.03E+13
6.00E-06	5.63E+12	8.32E+12	1.08E+13	1.17E+13	1.05E+13	8.30E+12	5.57E+12
8.10E-06	7.24E+12	1.10E+13	1.39E+13	1.54E+13	1.35E+13	1.10E+13	7.19E+12
1.00E-05	5.43E+12	7.40E+12	9.52E+12	1.05E+13	9.72E+12	7.66E+12	5.19E+12
3.00E-05	2.71E+13	3.90E+13	4.89E+13	5.39E+13	4.89E+13	3.93E+13	2.72E+13
1.00E-04	3.23E+13	4.61E+13	5.77E+13	6.27E+13	5.74E+13	4.68E+13	3.21E+13
5.50E-04	4.67E+13	6.66E+13	8.17E+13	8.93E+13	8.27E+13	6.81E+13	4.76E+13
3.00E-03	4.83E+13	7.03E+13	8.58E+13	9.14E+13	8.61E+13	7.20E+13	5.11E+13
1.70E-02	4.86E+13	7.06E+13	8.76E+13	9.38E+13	8.78E+13	7.37E+13	5.18E+13
2.50E-02	1.19E+13	1.68E+13	2.07E+13	2.28E+13	2.16E+13	1.82E+13	1.27E+13
1.00E-01	4.54E+13	6.56E+13	8.08E+13	8.76E+13	8.23E+13	6.92E+13	4.81E+13
4.00E-01	6.58E+13	9.50E+13	1.18E+14	1.28E+14	1.21E+14	9.96E+13	7.06E+13
9.00E-01	4.63E+13	6.72E+13	8.23E+13	8.94E+13	8.50E+13	7.06E+13	4.95E+13
1.40E+00	2.62E+13	3.85E+13	4.77E+13	5.15E+13	4.83E+13	4.00E+13	2.85E+13
1.85E+00	1.72E+13	2.45E+13	2.98E+13	3.29E+13	3.09E+13	2.55E+13	1.86E+13
2.35E+00	1.15E+13	1.63E+13	2.02E+13	2.16E+13	2.10E+13	1.74E+13	1.26E+13
2.48E+00	2.57E+12	3.72E+12	4.62E+12	5.14E+12	4.90E+12	4.15E+12	3.00E+12
3.00E+00	6.38E+12	9.40E+12	1.11E+13	1.21E+13	1.12E+13	9.49E+12	6.68E+12
4.80E+00	9.75E+12	1.40E+13	1.70E+13	1.86E+13	1.73E+13	1.44E+13	1.07E+13
6.43E+00	2.86E+12	3.90E+12	4.98E+12	5.33E+12	4.89E+12	4.36E+12	3.13E+12
8.19E+00	9.57E+11	1.33E+12	1.62E+12	1.54E+12	1.58E+12	1.31E+12	9.78E+11
2.00E+01	3.71E+11	4.42E+11	6.86E+11	6.46E+11	6.41E+11	5.51E+11	3.80E+11